SYNTHESIS OF ACTIVATED CARBONS FROM BIOWASTE MATERIALS AND STUDIES ON THEIR CHARACTERIZATION AND APPLICATIONS

By

CHUBAAKUM PONGENER

DEPARTMENT OF CHEMISTRY
SCHOOL OF SCIENCES

Submitted

in Partial Fulfillment of the Requirements

for award of the Degree

of

Doctor of Philosophy in Chemistry

of

NAGALAND UNIVERSITY
LUMAMI-798627
INDIA

Dedicated

To

My Parents,

My brothers and sisters

NAGALAND UNIVERSITY
(A Central University Estd. By the Act of Parliament No. 35 of 1989)
Headquarters: Lumami – 798627

Department of Chemistry.

DECLARATION

I, Mr. Chubaakum Pongener, bearing registration No. 522/2013, hereby declare that the subject matter of the thesis entitled "Synthesis of activated carbons from biowaste materials and studies on their characterization and applications" is the record of work done by me, that the contents of this thesis did not form basis of the award of any previous degree to me or to the best of my knowledge to anybody else, and that the thesis has not been submitted by me for any research degree in any other university/institute.

This is being submitted to the Nagaland University for the degree of Doctor of Philosophy in Chemistry.

(Chubaakum Pongener)
Candidate

(Prof. Dipak Sinha)	(Prof. Dipak Sinha)	(Dr. Rajib Locham Goswamee)
Head, Dept. of Chemistry	Supervisor	Co-Supervisor CSIR-NEIST

NAGALAND UNIVERSITY
(A Central University Estd. By the Act of Parliament No. 35 of 1989)
Headquarters : Lumami – 798627

Department of Chemistry.

CERTIFICATE

This is to certify that Mr. Chubaakum Pongener was registered as a Research Scholar for Ph.D. (Sci.) degree in Chemistry in Nagaland University and has been working under our supervisions. His thesis entitled "Synthesis of activated carbons from biowaste materials and studies on their characterization and applications" is being forwarded for submission for the Ph.D. (Science) degree of this University. It is certified that he has fulfilled all the requirements according to the rules of this University regarding investigations embodied in his thesis and the work described in this thesis is original and has not been submitted for any other degree or diploma in this or any other University.

(Prof. Dipak Sinha)
Supervisor

(Dr. Rajib Lochan Goswamee)
Co-supervisor
CSIR-NEIST

NAGALAND UNIVERSITY
(A Central University Estd. By the Act of Parliament No. 35 of 1989)
Headquarters: Lumami – 798627

Department of Chemistry.

Course Completion Certificate

This is to certify that Mr. Chubaakum Pongener has satisfactorily completed the course offered in the PhD Course Work Programme in Chemistry.

The Courses include:

CHEM-601 Research Methodology

CHEM-602 Advances in Chemistry

CHEM-603 Literature review, Report writing and Presentation

(Prof. Dipak Sinha)
Head
Department of Chemistry
Nagaland University

Acknowledgement

I take this glorious opportunity to thank everyone who has moulded and shaped my life, personality, character and help me during my research. I find joy in sharing my hearties gratitude to my respected sir, Prof. Dipak Sinha, for being my mentor. His vast knowledge, experience, wisdom and undying enthusiasm to explore new ideas have made my research interesting. I thank him for guiding me with his constant encouragement and support. The time I spent working with him are all worthwhile.

I would like to mention a special person, Dr. Rajib Lochan Goswamee, My co-supervisor, who always with a smiling and happy face has made my working atmosphere enjoyable and interesting. He is one of a great teacher I ever met. His vast knowledge and wisdom has inspired me deeply. I cherish every moment spent under his great mentorship.

I am grateful to Prof. K. S. Rao, for always pointing me in the right direction and for motivating me in my research work. He has been and always will be a great inspiration to me.

I express my sincere gratitude to Dr. Upasana Bora Sinha, for willingly giving her precious time generously and proof reading my thesis. She has been a great source of inspiration.

I would like to thank Prof. Indira Devi, Dr. Tovishe, Dr. Prabhakar, Dr. Nurul and Dr. Dushila for their constructive suggestion and advices.

I am grateful to all the technical staffs specially, Sunepjungla, Bendangtemsu and Temsuienla for their valuable assistance that kept my progress on schedule.

I extend my acknowledgement to CSIR-NEIST, Jorhat, ISSAT, Guwhati, Tezpur University, Tezpur and Delta Institue, Andhra University, for providing their valuable technical assistance for different analysis.

My heartfelt gratitude goes to my entire lab. mates for sharing their ideas, knowledge and skill. I specially thank Dr. Daniel Kibami, Parimal and Aola Supong for their great support and encouragement.

And my parents, my brothers and sisters. Yanger, Tia, Aren and Meren. They are the true source of all my joy, love and strength. I sincerely acknowledge their great sacrifices, support and love. I thank them humbly for making me the person I am today.

Above all I thank God for his abundance love, grace and blessings.

Chubaakum Pongener

CONTENTS

CHAPTER-1

INTRODUCTION

In this chapter, a brief introduction about activated carbon, its structure, properties and applications are discussed. The different methods of synthesis from variety of carbonaceous materials using different activating agents are reported in this chapter. Classification of activated carbon based on their properties and applications are also presented here.

1.1. Introduction

The useful properties of activated carbon have been known since ancient times. This traces back to 1500 BC when Egyptians used charcoal as an adsorbent for medicinal purposes and as purifying agent (Bandosz, 2006). Around 420 BC it was observed that Hippocrates dusted wounds with powdered charcoal to remove their odour. Ancient Hindu societies purified their water by filtration through charcoal (Bansal and Goyal 2005). In 1773, the Swedish chemist Karl Wilhelm Scheele was the first to observe adsorption of gases on charcoal. A few years later activated carbons began to find its application in the sugar industry as a decolorizing agent for syrup.

In the early 20th century the first plant to produce activated carbon industrially was built for use in sugar refining industry in Germany. Many other plants emerged in the early 1900's to make activated carbons primarily for decolorisation. During World War I, activated carbon was used in gas masks for protection against hazardous gases and vapours. Today, activated carbons are used to remove colour from pharmaceutical and food products, as air pollution control devices for industrial and automobile exhaust, for chemical purification, and as electrodes in batteries. 500,000 tons per year of activated carbon are produced globally (Jankowska et al., 1991). 80% of this is used for liquid phase applications, and 20% is used for solid phase applications (Bansal and Goyal 2005).

Activated carbon is defined as a carbonaceous material with a large internal surface area and highly developed porous structure resulting from the processing of raw materials under high temperature reactions. It is composed of 87% to 97% carbon but also contains other elements depending on the processing method used and raw material it is derived from. Activated carbon's porous structure allows it to adsorb materials from the liquid and gas phase (Jankowska et al., 1991). Its pore volume typically ranges from 0.20 to 0.60 $cm^3\ g^{-1}$, and has been found to be as large as 1 $cm^3\ g^{-1}$. Its surface area ranges typically from 800 to 1500 $m^2\ g^{-1}$ (Biscoe and Warren 1942) but has been found to be in excess of 3,000 $m^2\ g^{-1}$. The surface area mostly contains micropores with pore diameters smaller than 2 nm (Bokros 1969). These favourable properties make activated carbon a popular adsorbent for many applications. Carbon-oxygen surface groups are by far the most important surface groups that influence the surface characteristics such as wettability, polarity, and acidity, and physico-chemical properties such as catalytic, electrical, and chemical

reactivity of these materials. In fact, the combined oxygen has often been found to be the source of the property by which a carbon becomes useful or effective in certain respects.

According to Kipling, the atoms of oxygen and hydrogen are essential components of an active carbon with good adsorptive properties, and the surface of such materials is to be considered as a hydrocarbon surface modified at some points by oxygen atoms (Kipling 1956). Carbons have great tendency to extend this layer of chemisorbed oxygen, and many of their reactions arise because of this tendency. They also decompose aqueous solutions of silver salts, halogens, ferric chloride, potassium and ammonium persulphate, sodium hypochlorite, potassium permanganate, potassium dichromate, sodium thiosulphate, hydrogen peroxide and nitric acid (Bansal and Goyal 2005). In each case, there is chemisorption of oxygen and the formation of carbon-oxygen surface compounds. It is possible to oxidize carbon by heat treatment in air, CO_2 or oxygen. The formation of surface oxygen group and the nature of the carbon are depended upon the different oxidative treatment, history of its formation, its surface area and its temperature. The formation of carbon-oxygen surface compounds using different active carbons and using various oxidative treatment in gaseous and solution phase, has been studied by a large number of investigators and has been very well reviewed (Fanning and Vannice 1997; Tesssmer et al., 1997, Suhas and Ribeiro, 2007; Shafeeyan et al., 2010). Thus, it can be pointed out that carbons have a tendency to pick upon oxygen, at least to some extent under all conditions. Carbons also have an acid-base character. This fact has encouraged many investigators to devote their research effort to understand the cause and mechanism by which a carbon acquires an acidic or a basic character where three types of carbon-oxygen surface groups (acidic, basic, and neutral) have been recognized (Fig 1.1). The acidic surface groups are very well characterized and are formed when carbon is treated with oxygen at temperatures up to 400°C or by reaction with oxidizing solutions at room temperature (Lopez-Ramon et al., 1999). These surface groups are thermally less stable and decompose on heat treatment in vacuum or in an inert atmosphere in the temperature range of 350 to 750°C evolving CO_2. These acidic surface groups render the carbon surface hydrophilic and polar in character and have been postulated to be carboxylic, lactone, and phenolic groups (Viswanathan et al., 2009) (Fig.1.2). The structure of activated carbons is formed by imperfect sections of graphene layers which are bonded together to build a 3-dimensional structure, as shown in Fig 1.3.

This structure includes many defects and spaces between different layers which are the source of activated carbon porosity.

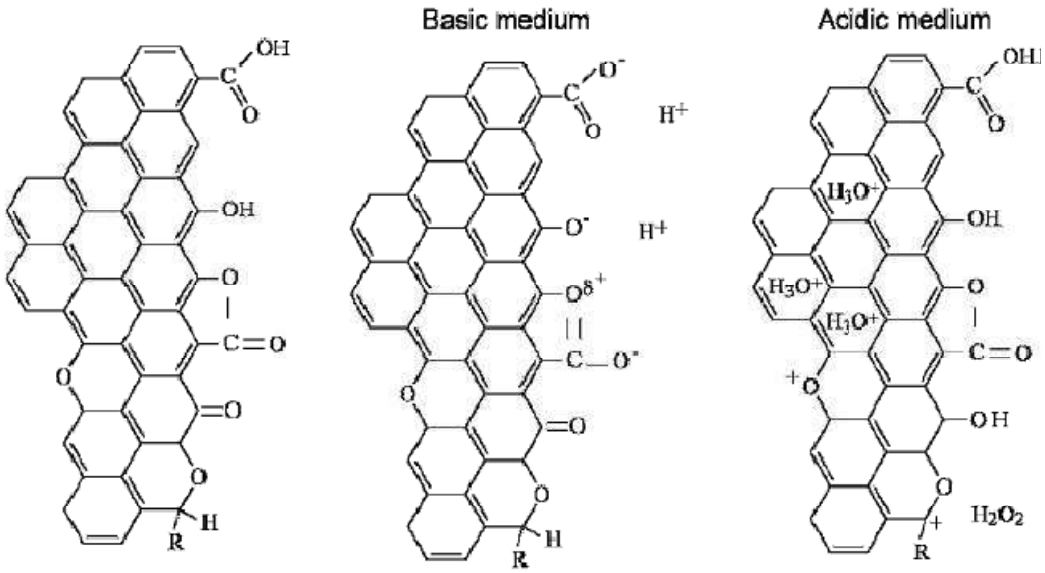

Fig.1.1. Schematic representation of the acidic and basic behaviour of the oxygen-containing surface groups and delocalized π-electrons of the basal plane (Bandosz 2006)

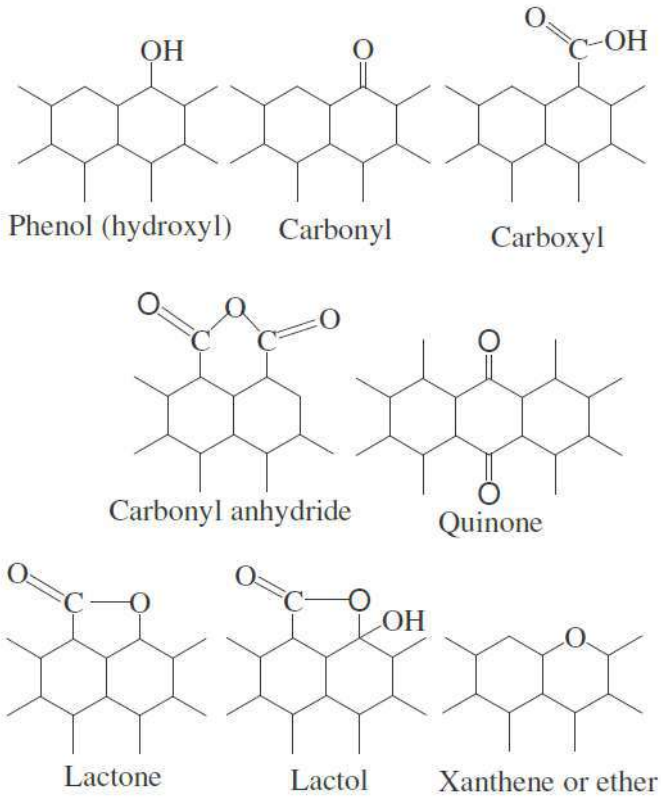

Fig 1.2. Common oxygen surface functional groups present on the surface of carbon materials (Viswanathan et al., 2009)

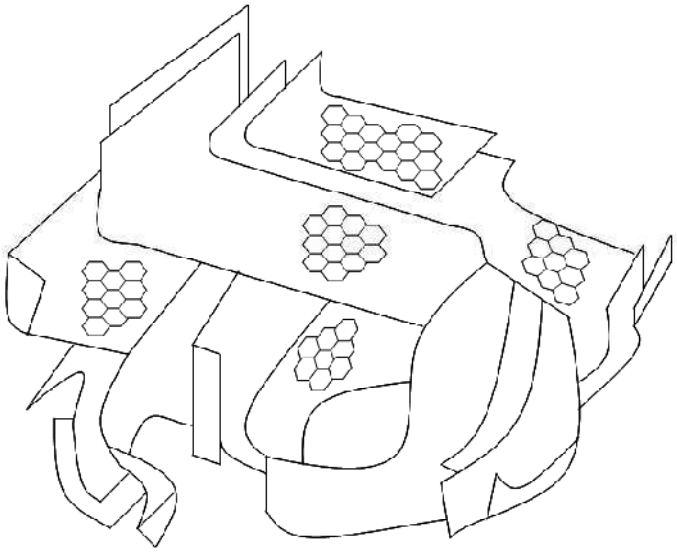

Fig.1.3. Schematic representation of the structure of activated carbon (Stoeckli 1990)

Carbon materials are unique and versatile in their performance, and therefore they have major industrial significance. Activated carbon is a material with high porosity consisting of hydrophobic graphene layer as well as hydrophilic surface functional groups, thus making them beneficial for sorption and catalytic applications. Specific industrial applications include areas such as oil and natural gas, food, pharmaceuticals, water treatment, hydro metallurgy, gold recovery and carbon-in-pulp process (Soleimani and Kaghazchi 2008), batteries (Endo et al., 2000), fuel cells (Dicks 2006), supercapacitors (Pandolfo and Hollenkamp 2006). Activated carbon materials are effective in removing pollutants both in gaseous and liquid phase. The advantage of activated carbon materials as adsorbents is that the treated effluent is of high quality; the design of the process is simple, operational procedure of the process developed or adopted is generally easy. In addition carbon materials are resistant to corrosive (acidic and basic) and toxic environments (Chen et al., 2002). Microporous carbon materials are highly disordered. In general, the structure comprises of aromatic sheets and strips (Fig. 1.4). Such sheets are often bent imitating crumpled papers and wood shavings. The voids and gaps of molecular dimensions, between such aromatic sheets are regarded as micropores (Dubinin and Polyakov, 1986). Again the microporosity is dependent on the carbon precursor as well as the method of preparation.

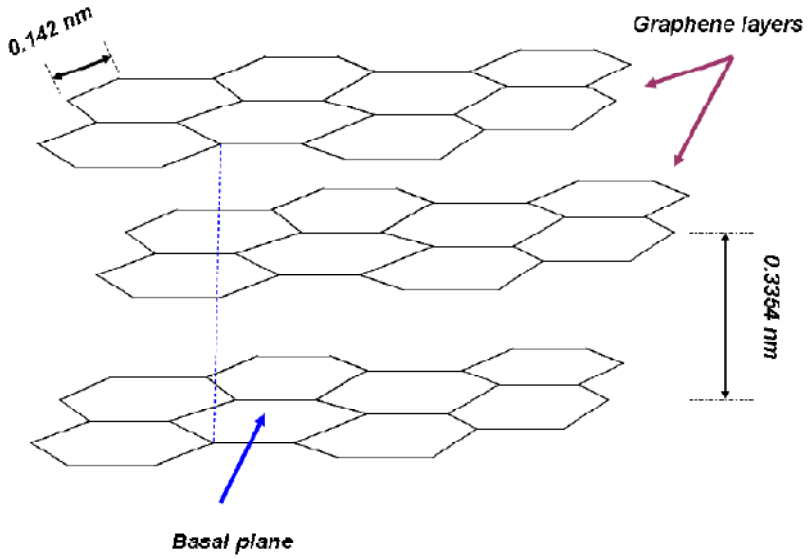

Fig.1.4. The structure of hexagonal graphite (Marsh and Rodriguez- Reinoso 2006).

In recent years, there has been a drastic rise in the demand for activated carbon owing to the increased utility of the carbon materials in pollution control. As a result, cost of activated carbon is also growing depending on the application. Designing ways for the production of activated carbon through economic ways has become the need of the hour. A range of low cost, easily available, carbon rich and low ash precursors and sources are being explored for the production of carbon materials.

1.2. Synthesis of activated carbon

Most of the commercial activated carbons are either coal based (Kruk et al., 2005; Ru and Zheng 2001) or petroleum pitch based (Hayashi et al., 2000) which are prone to exhaustion. Their global distribution is non uniform. As the applications of activated carbon are immense, the gap between demand and supply is ever widening. This may in due course result in scarcity of the material in addition to becoming expensive. This situation necessitates the need for the exploration of new sources of carbon materials with desired physico chemical properties namely, high specific surface area, micro or meso porosity or both, surface functionality, thermal stability, carbon purity, adsorptive capacity and chemical composition, depending on the end application. Bio-materials which are renewable and inexhaustible are supposed to be the only continuous source of carbon supply. In addition they are more evenly distributed throughout the globe relative to either coal or petroleum. Thus, bio-materials, which are renewal natural resources, appear as viable options for the generation of carbon materials rather than fossil fuels. The carbon precursors and the method of

preparations are the determining factors of the textural and surface properties of carbon materials (Olivares et al., 2006). Taking into consideration some specific properties like volatile matter, ash content and fixed carbon content as well as the derivable porosity, several researchers have studied the possibility of producing carbon materials from different bio-materials. For instance, Ganan et al., (Ganan et al., 2006) have used the bio-material almond tree pruning as precursor for producing activated carbon. Kazemipour et al., (Kazemipour et al., 2008) have also used almond *(Amygodolus)* shells, apricot *(Armeniaca bulgar)* stones, hazel nut *(Corylus avellana),* pistacio *(Pistaca) and* walnut *(Jouglans regia L.)* as precursors for producing activated carbon materials with specific surface area values of 1208, 861, 786, 635 and 941 m^2/g by the method of carbonization in inert atmosphere at 1073 K. Whereas (Onal et al., 2007) has used apricot stones to produced activated carbon with surface area 1060 $m^2\ g^{-1}$ by using $ZnCl_2$. The use of H_2SO_4 as activating agent has also been reported (Demirbas et al., 2008) where the specific surface area was found to be 560 m^2g^{-1} at an activation temperature of 523 K in air oven using. The use of Bamboo *(bambusoidae)* for producing activated carbon with specific surface area of 1896 $m^2g^{-1}$by adopting a physico chemical method of activation using KOH as well as CO_2 as activating agents at an activation temperature of 1123 K has been reported (Hameed et al., 2007). Kim and co-worker (Kim et al., 2006) have produced activated carbon from bamboo using KOH activation method at 1073 K in Ar atmosphere with specific surface area value of 894 m^2g^{-1}. Mohan and co-worker (Mohan et al., 2006) have employed coconut shell fiber using H_2SO_4 as well as thermal means to activate the material which produce activated carbon with specific surface area of 512 $m^2\ g^{-1}$. Jermias et al., (Jeremias et al., 2007) have employed coir pith, coir fiber and endocarp from coconut shell to generate activated carbon material using physicochemical activation process. Girgis et al., (Girgis et al., 2007) have employed Peach stone shells as precursor for producing activated carbon materials with specific surface area of 1053 – 1404 $m^2\ g^{-1}$ using H_3PO_4 as activating agent. Tseng et al., (Tseng et al., 2006) has produced activated carbon material from the cane pith of sugar cane *(Saccharum officinarum)* through activation with KOH at 1053 K in N_2 atm with specific surface area of 2300 $m^2\ g^{-1}$. Thus it can be understood that activation methods as well as precursor materials for producing activated carbon greatly influence the properties of the carbon.

In addition to the above mentioned bio-materials several other bio-materials materials, namely, *Canarium sublatum guillaumin* (Srisa-ard 2014), cane bagesse (Syna et al., 2003), *Cajanus cajan* Seed Husk (Ganvir and Syed 2014), Casuarina (Supriya et al., 2014), corn cob (Cao et al., 2006), coconut shell (Achaw and Afrane, 2008; Li et al., 2008; Peng et al., 2008), corn stalks (Zhang et al., 2008), date pits (Merzougui and Addoun, 2008; Mahmoudi et al., 2014), eucalyptus wood (Rocha et al., 2002), guava seeds (Rahman and Saad 2003), kenaf core fiber (Shamsuddin et al., 2016) Jatropha Seed Coat (Hirunpraditkoon et al., 2014), Mango leaves (Madhu et al., 2014), oat hulls (Fan et al., 2004), olive-stone (Rodrigue et al., 2008), Orange peel (Kulkarni and Mahdi 2014), Palm oil (Salman 2014), Palm oil shell (Hussaro 2014**),** pea nut hulls (Girgis et al., 2002), pine wood (Tseng et al., 2003) Pine cone (Özhan et al., 2014), rice husk (Guo et al., 2005; Kalderis et al., 2008), rice straw (Wang et al., 2007; Daifullah et al., 2007), rock rose (Villegas and Valle 2002), saw dust (Ismadji et al., 2005) *Typha orientalis* (Anisuzzaman et al., 2015), walnut wood (Sarrano et al., 2005), walnut shell (Jahangiri et al., 2012), *Sindora siamensis* Seed (Srisa-ard 2014), have also been exploited by researchers for producing activating carbon materials.

Activation of carbon

The procedure for processing activated carbon typically consists of a carbonisation followed by an activation of the carbonaceous material. Carbonisation is a heat treatment at 400-800°C which converts raw materials to carbon by minimizing the content of volatile matter and increasing the carbon content of the material. This increases the materials strength and creates an initial porous structure which is necessary if the carbon is to be activated. Adjusting the conditions of carbonisation can affect the final product significantly. An increased carbonisation temperature increases reactivity, but at the same time decreases the volume of pores present. This decreased volume of pores is due to an increase in the condensation of the material at higher temperatures of carbonisation which yields an increase in mechanical strength. Therefore, it becomes important to choose the correct process temperature based on the desired product of carbonisation (Bansal and Goyal 2005).

Preparation of activated carbon

Activated carbon is nothing but carbon produced from carbonaceous source materials like nutshells, peat, wood, coir, lignite, coal and petroleum pitch. It can be produced by any one of following described processes:

Physical activation

In this process precursor is developed into activated carbons using gases. This is generally done by using one or a combination of the following processes:

Carbonisation

Material having appreciable carbon content is pyrolysed at temperature ranging between 600–900°C, in the absence of oxygen (usually in inert atmosphere with gases like argon or nitrogen)

Activation/Oxidation

In this process raw material or carbonised material is exposed to oxidizing atmospheres (carbon monoxide, oxygen, or steam) at temperatures above 250°C, usually in the temperature range of 600–1200°C.

Chemical activation

Before carbonisation, the raw material can be impregnated with certain chemicals. The chemical needs to be typically an acid, strong base, or a salt (phosphoric acid, potassium hydroxide, sodium hydroxide, zinc chloride, respectively). After impregnation, the raw material needs to be carbonised at lower temperatures (450–900 °C). It is believed that the carbonisation/activation step proceeds simultaneously with the chemical activation. Chemical activation is preferred over physical activation owing to the lower temperatures and shorter time for activating the materials.

After the initial porous structure has been created by carbonisation, an oxidation, referred as activation, is carried out in order to create micropores (Beguin and Frackowiak 2010). Typically, these micropores have a width of less than 2 nanometers and where the majority of adsorption occurs. Activation can be carried out by oxidizing gases or a chemical activation. In activation by oxidizing gases, such as steam activation, carbon reacts with the oxidizing agent producing oxides of carbon. These oxides diffuse out of the carbon resulting in a partial gasification which opens pores that were previously closed and further develops the carbons internal porous structure.

In chemical activation, the carbon is reacted at high temperatures with a dehydrating agent that eliminates the majority of hydrogen and oxygen from the carbon structure. Chemical activation often combines the carbonisation and activation step, but these two steps may still occur separately depending on the process (Jankowska et al., 1991). A significant amount of carbon mass loss occurs during the activation which generally correlates to an increase in porosity. Therefore, quick estimates of porosity

can be made by a gravimetric measurement. These gravimetric measurements can be used to compare carbons synthesised by using different process, parameters and raw materials.

Classification of activated carbon

Activated carbons are complex products which are difficult to classify on the basis of their behaviour, surface characteristics and preparation methods. However, some broad classification is made for general purpose based on their physical characteristics.

Powdered activated carbon (PAC)

Traditionally, active carbons are made in particulate form as powders or fine granules less than 1.0 mm in size with an average diameter between 0.15 and 0.25 mm. Thus they present a large surface to volume ratio with a small diffusion distance. PAC is made up of crushed or ground carbon particles. Granular activated carbon is defined as the activated carbon being retained on a 50-mesh sieve (0.297 mm) and PAC material as finer material, while ASTM classifies particle sizes corresponding to an 80-mesh sieve (0.177 mm) and smaller as PAC. PAC is generally added directly to other process units, such as raw water intakes, rapid mix basins, clarifiers, and gravity filters (Marsh and Reinoso, 2006).

Granular activated carbon (GAC)

Granular activated carbon has a relatively larger particle size compared to powdered activated carbon and consequently, presents a smaller external surface. Diffusion of the adsorbate is thus an important factor. These carbons are therefore preferred for all adsorption of gases and vapours as their rates of diffusion are faster. Granulated carbons are used for water treatment, deodorisation and separation of components of flow system. GAC can be either in the granular form or extruded (Marsh and Reinoso, 2006).

Extruded activated carbon (EAC)

Extruded activated carbon combines powdered activated carbon with a binder, which are then fused together and extruded into a cylindrical shaped activated carbon block with diameters from 0.8 to 130 mm. These are mainly used for gas phase applications because of their low pressure drop, high mechanical strength and low dust content (Marsh and Reinoso, 2006).

Impregnated carbon

Porous carbons containing several types of inorganic impregnants such as iodine, silver, as well as cations such as Al, Mn, Zn, Fe, Li, Ca have also been prepared for specific application in air pollution control especially in museums and galleries. Due to antimicrobial/antiseptic properties, silver loaded activated carbon is used as an adsorbent for purification of domestic water. Drinking water can be obtained from natural water by treating the natural water with a mixture of activated carbon and $Al(OH)_3$, a flocculating agent. Impregnated carbons are also used for the adsorption of H_2S and thiols. Adsorption rates for H_2S as high as 50% by weight have been reported (Marsh and Reinoso, 2006).

Polymer coated carbon

This is a process by which a porous carbon can be coated with a biocompatible polymer to give a smooth and permeable coat without blocking the pores. The resulting carbon is useful for hemoperfusion. Hemoperfusion is a treatment technique in which large volumes of the patient's blood are passed over an adsorbent substance in order to remove toxic substances from the blood (Marsh and Reinoso, 2006).

Activated carbon is also available in special forms such as cloths and fibres. The "carbon cloth" for instance is used in personnel protection for the military.

Properties of activated carbon

A gram of activated carbon can have a surface area in excess of 500 m^2, with 1500 m^2 being readily achievable (McElroy 2010). Under an electron microscope, the high surface-area structures of activated carbon are revealed displaying various kinds of porosity. These micropores provide superb conditions for adsorption to occur, since adsorbing material can interact with many surfaces simultaneously. Tests of adsorption behaviour are usually done with nitrogen gas at 77 K under high vacuum. Physically, activated carbon binds materials by Van der Waals force or London dispersion force (McElroy 2010).

Applications of activated carbon

Activated carbon is used in gas purification, gold purification, metal extraction, water purification, medicine, sewage treatment, air filters in gas masks and respirators, filters in compressed air and many other applications (Aksu 2005; Yen et al., 2007; Chen et al., 2011). Recently activated carbon filters have gained popularity among recreational users of Cannabis, and other smoking herbs for their use in effectively filtering out "Tar" from the smoke. One major industrial application involves use of

activated carbon in the metal finishing field. It is very widely employed for purification of electroplating solutions. Activated carbon, in 50% w/w combination with celite, is used as stationary phase in low pressure chromatographic separation of carbohydrates (mono-, di-trisacchardes) using ethanol solutions (5–50%) as mobile phase in analytical or preparative protocols (Gumus and Okpeku, 2015). In environmental field, activated carbon adsorption has numerous applications in removing pollutants from air or water streams both in the field and in industrial processes such as spill cleanup, groundwater remediation, drinking water filtration, air purification, volatile organic compounds capture during painting, dry cleaning, gasoline dispensing operations, and other processes. In medical applications, activated carbon is used to treat poisonings and overdoses following oral ingestion. It is thought to bind to poison and prevent its absorption by the gastrointestinal tract. In cases of suspected poisoning, medical personnel administer activated charcoal on the scene or at a hospital's emergency department. Thus, activated carbons show excellent adsorptive properties because of their high porosity, surface area and numerous oxygen functional groups which readily interact with other compounds through adsorption processes.

1.3. Adsorption phenomena

An understanding of the processes involved in adsorption is vital to gain an insight of the mechanisms involved. The principles of adsorption on to porous adsorbents, in particular activated carbons, are considered with reference to vapour and liquid adsorption processes. Adsorption is a physical process in which dissolved molecules or small particles (the adsorbate) are attracted and become attached to the surface of something larger (the adsorbent). The attraction is similar to that of a magnet on a refrigerator, but on an atomic or molecular scale. The energy differences and electrical attractive forces are known as Van der Waals forces, and cause molecules of the adsorbate to physically fasten and stick onto the adsorbent. Common in nature, the laboratory and industry, adsorption often occurs between solids and liquids or gases. Adsorption should not be confused with the completely different process of absorption, in which liquids and particles penetrate into another substance, such as a sponge that soaks in liquids. The amount of material adsorbed depends on a number of factors including the degree of attraction, the surface area exposed to mobile particles, the concentration of the contaminants, pH and temperature of the liquid.

Typically, the strongest adsorbents are micro porous or finely divided solids (clays, charcoal, powdered materials) and liquids (fine droplets like aerosols and sprays). As such adsorption is one of the most preferred techniques for pollutants removal from aqueous solutions and is frequently applied on large scale, as it can handle fairly large flow rates, producing a high quality of water without producing notorious sludge, residual contaminants, etc. Moreover, adsorption is universal, inexpensive and fast in nature, does not result in the formation of harmful substances (Gayatri and Ahmaruzzaman, 2010) and applicable for the removal of pollutants even at low concentration.

Principles of adsorption

The term adsorption is said to have been first used by Kayser in 1881 in order to explain the condensation of gases on surfaces, in contrast to gas adsorption in which gas molecules penetrate the bulk phase of the adsorbing solid. The term 'sorption' was proposed by McBain as a complete description of mass transport into a solid, encompassing surface adsorption, absorption by penetration into the solid and condensation within the pores. Adsorption is described as the enrichment of one or more components in the interfacial layer, which is an excess of molecules exists at the adsorbate/adsorbent interface upon exposure of an adsorbing solid to a gas or vapour (Fig. 1.6). It is the selective collection and concentration onto solid surfaces of certain molecules contained in a vapour or gas stream. Hence gases or vapours referred to as adsorbates when adsorbed, even of mixed systems and at low concentrations, may be captured, often selectively, and removed from the effluent stream using a material of the category of adsorbents.

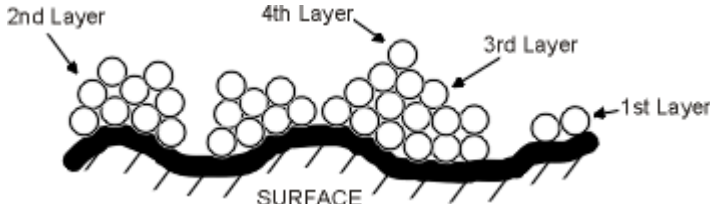

Fig.1.6. Schematic representation of adsorption

Classification of adsorption phenomenon

Depending upon the nature of the forces involved, the adsorption is of two types: physical adsorption and chemisorption. In the case of physical adsorption, the adsorbate is bound to the surface by relatively weak Van der Waals forces, which are

similar to the molecular forces of cohesion and are involved in the condensation of vapours into liquids. Chemisorption, on the other hand, involves exchange or sharing of electrons between the adsorbate molecules and the surface of the adsorbent resulting in a chemical reaction. The bond formed between the adsorbate and the adsorbent is essentially a chemical bond and is thus much stronger than in the physisorption (Bansal and Goyal, 2006).

Adsorbents

Any solid has some tendency to adsorb fluid medium onto its surface, however only some solid materials have the selective adsorption capacity towards adsorbate molecules. The adsorbate may be organic compound, colour, odour, moisture etc. The four most common adsorption processes in terms of their estimated annual sales, along with their characteristics, applications and disadvantages are listed in Table 1.

Table 1. Characteristics of Different Adsorbents

Type	Characteristics	Use	Disadvantages
Activated Carbon	Hydrophobic, favours organics over water	Removal of organic pollutants	Difficult to regenerate
Zeolites	Hydrophillic, polar, regular channels	Air separation, Dehydration	Low total capacity
Silica gel	High capacity, Hydrophilic	Drying gas streams	Trace removal not Effective
Activated alumina	High capacity, Hydrophilic	Drying gas streams	Trace removal not Effective

1.4. Adsorption isotherms

An adsorption isotherm is the presentation of the amount of solute adsorbed per unit weight of adsorbent as a function of the equilibrium concentration in the bulk solution at constant temperature. In order to help understand the adsorption of adsorbate onto the activated carbon by different models have been used to determine the effectiveness of the chemically modified activated carbon in adsorbing targeted. The adsorption data are analysed with the help of the following linear forms of Langmuir, Freundlich and Temkin isotherms.

Langmuir isotherm

In 1916, Irving Langmuir proposed adsorption Isotherm which explained the variation of adsorption with pressure. Based on his theory, he derived the Langmuir Equation which depicts a relationship between the number of active sites of any surface undergoing adsorption and pressure. Langmuir developed a theoretical isotherm to

describe the reaction between adsorbed gases above a solid surface at a fixed temperature; he was awarded Nobel Prize in chemistry for his work. The Langmuir isotherm, originally derived for the adsorption of gas molecules on solid surfaces, was modified to fit the adsorption isotherm of solutes onto solid surfaces in solution systems.

Assumptions of Langmuir isotherm

Langmuir proposed his theory by making following assumptions.

1. Fixed number of vacant or adsorption sites are available on the surface of solid.
2. All the vacant sites are of equal size and shape on the surface of adsorbent.
3. Each site can hold maximum of one gaseous molecule and a constant amount of heat energy is released during this process.
4. Dynamic equilibrium exists between adsorbed gaseous molecules and the free gaseous molecules.

$$A(g) + B(S) \underset{\text{Desorption}}{\overset{\text{Adsorption}}{\rightleftharpoons}} AB$$

Where A (g) is unadsorbed gaseous molecule, B(s) is unoccupied metal surface and AB is Adsorbed gaseous molecule.

5. Adsorption is monolayer or unilayer.

The general equation of Langmuir isotherm is given below,

$$q_e = \frac{k_L C_e}{1 + a_L C_e} \qquad \text{.....(1)}$$

A linear form of this expression is written as,

$$\frac{C_e}{q_e} = \frac{1}{k_L} + \frac{a_L}{k_L} C_e \qquad \text{.....(2)}$$

Where q_e (mg g^{-1}) is the amount of fluoride ion adsorbed per unit weight of adsorbent. C_e is the equilibrium fluoride concentration in the solution (mg L^{-1}). k_L (g L^{-1}) is the Langmuir adsorption constant, a_L/k_L gives the theoretical monolayer saturation capacity q_m (Aziz et al., 2011; Chinniagounder et al., 2011). Langmuir isotherm can

be expressed in terms of dimensionless constant called separation factor $R_{L,}$ which is given by the equation.

$$R_L = \frac{1}{1 + a_L C_i} \qquad \text{.....(3)}$$

The R_L values between 0 and 1 indicate a favourable adsorption process (Mckay et al., 1982), R_L =1 indicates a linear adsorption, R_L =0 indicates irreversible adsorption, while an R_L value greater than 1 signifies an unfavourable adsorption process.

Freundlich isotherm

In 1914, Freundlich popularized and justified theoretically another adsorption isotherm model, which is commonly used to describe the adsorption characteristics for the heterogeneous surface (Dada et al., 2012). These data often fit the empirical equation proposed by Freundlich. General form of Freundlich isotherm is given as,

$$\log\left(\frac{X}{M}\right) = \frac{1}{n}\ (\log Ce) + \log K \qquad \text{..... (4)}$$

Where *k* is a constant which indicates relative adsorption capacity and *1/n* is a constant which is considered to be relative indicator of adsorption capacity and adsorption intensity respectively (Goswamee et al., 1998). If n = 1 then the partition between the two phases are independent of the concentration. If value of *1/n* is below one it indicates a normal adsorption. On the other hand, *1/n* being above one indicates cooperative adsorption (Mohan and Karthikeyan, 1997). However, *K* and *n* are parameters characteristic of the sorbent-sorbate system, which must be determined by data fitting and whereas linear regression is generally used to determine the parameters of kinetic and isotherm models. Specifically, the linear least-squares method and the linearly transformed equations have been widely applied to correlate sorption data where *1/n* is a heterogeneity parameter, the smaller *1/n,* the greater the expected heterogeneity (Hui et al., 2009). This expression reduces to a linear adsorption isotherm when *1/n* = 1. If n lies between one and ten, this indicates a favourable sorption process (Dada et al., 2012) C_e is the equilibrium adsorbate concentration (mg g^{-1}) and *X* is the amount of adsorbate adsorbed (mg g^{-1}), *M* is the amount of adsorbent (g L^{-1}) used.

Temkin Isotherm

The behaviour of adsorption systems on heterogeneous surfaces has been described by the Temkin isotherm. This isotherm contains a factor that explicitly taking into the account of adsorbent–adsorbate interactions. By ignoring the extremely low and large value of concentrations, the model assumes that heat of adsorption (function of temperature) of all molecules in the layer would decrease linearly rather than logarithmic with coverage (Tempkin and Pyzhev, 1940; Aharoni and Ungarish, 1977). As implied in the equation, its derivation is characterised by a uniform distribution of binding energies (up to some maximum binding energy) was carried out by plotting the quantity sorbed q_e vs lnC_e and the constants were determined from the slope and intercept. The model is generally been expressed as (Tempkin and Pyzhev, 1940),

$$q_e = \frac{RT}{b} \ ln(AC_e) \qquad \text{.....(5)}$$

The linear form of the Temkin isotherm model equation is given as,

$$q_e = \frac{RT}{b} \ lnA + \frac{RT}{b} lnC_e \qquad \text{.....(6)}$$

Where B= [RT/b] corresponding to the heat of adsorption, R is the ideal gas constant, T(K) is the absolute temperature, b is the Temkins isotherm constant and A (Lg^{-1}) is the equilibrium binding constant corresponding to the maximum binding energy. Therefore, the constant A can be determined from a plot of q_e vs lnC_e.

Chi-square analysis

A chi-square analysis (χ^2) test is a statistical hypothesis in which the sampling distribution of the test is a χ^2 distribution is true (Bagdonavivius and Nikulin, 2011). The χ^2 test is used to determine whether there is a significant difference between the expected frequencies and the observed frequencies. Thus to determine suitable isotherm for sorption of adsorbate onto carbon adsorbents, the chi-square analysis has been used. The mathematical statement for chi-square analysis is,

$$\chi^2 = \sum \frac{(q_{e(exp)} - q_{e(cal)})^2}{q_{e(exp)}} \qquad \text{.....(7)}$$

where $q_{e(exp)}$ and $q_{e(cal)}$ are the experimental sorption capacity of fluoride (mg g^{-1}) at equilibrium time and the corresponding value that is obtained from the sorption model. If data from the model are similar to the experimental data, $\chi 2$ will be a small number, while if they differ; χ^2 will be a bigger number (Meeenakshi and Viswanathan, 2007).

1.5. Adsorption kinetics modelling

Adsorption kinetics studies are important, since they give information about the adsorption system behaviour and the rate at which specific constituents are removed using certain adsorbents. In addition, they provide information about whether the adsorption process is chemical or physical and which specifically is the rate limiting step. In adsorption the relationship between the adsorbent, its configuration and the attainment of equilibrium are indicative of the rate limiting process. Therefore, it is important to predict the rate at which the adsorptions take place in an adsorption system. The establishment of rate limiting step will greatly assist in maintaining the time of contact between the interacting molecules. Thus, determining the rate-limiting step for the adsorption process is of great importance which governs the overall removal rate and mechanisms of sorption and thereby help to interpret the experimental data appropriately. There are several kinetics models that describe the adsorption process namely pseudo first-order, pseudo second-order, Weber and Morris intraparticle diffusion model and Elovich equations.

Pseudo first-order model

A pseudo-first order kinetic model is considered as the earliest model developed to the kinetic process of adsorption. The Lagergren's rate equation is one of the most widely used rate equation to describe the adsorption of adsorbate from the liquid phase (Lagergren 1898; Weber and Morris, 1963). The final integrated form equation of this model as follows,

$$log(q_e\text{-}q_t) = logq_e - \frac{k_1}{2.303}\ t \quad \text{.....(8)}$$

where, q_e and q_t are the amounts of adsorbate adsorbed on adsorbent (mg g^{-1}) at equilibrium and at time t (min), respectively, and k_1 is the rate constant of pseudo first-order kinetics.

Pseudo-second order kinetic models

This model is commonly employed to describe the adsorption of metal ions and polar functional group such as, ketones, aldehydes, dyes, herbicides, and phenolic compounds from aqueous solution assuming that Langmuir equation applies. The linearsed integral form of the model is,

$$\frac{t}{q_t} = \frac{1}{k_2 q_e^2} + \frac{1}{q_e} t \qquad \text{.....(9)}$$

Where q_e and q_t (mg g^{-1}) are the adsorption capacity at equilibrium and at time t (min), respectively. K_2 is the rate constant (g mg^{-1} min)) (Mckay 1988). If the pseudo second-order kinetic equation is applicable, the plot of t/q_t against t should give a linear relationship, from which q_e and k_2 can be determined from the slope and intercept of the plot, and there is no need to know any parameter beforehand.

Weber and Morris intraparticle diffusion

In a liquid-solid system, the theory proposed by Weber and Morris to link the fractional uptake of solute on particles varies proportionally here with $t^{1/2}$. This model has been widely used by the researcher to establish a rate of sorption which controls the rate-limiting step. The Weber and Morris equation is,

$$q_t = (k_b t^{1/2}) + A \qquad \text{.....(10)}$$

q_t (mg g^{-1}), k_b (mg g^{-1} $min^{1/2}$) is the rate constant of intra-particle diffusion and (A) gives an idea about the thickness of the boundary layer. The value of k_b will be calculated from the slope of the resulting curve (Hinz et al., 2005).

Elovich equation

This equation was firstly used in the kinetics of chemisorption of gases on solids, the adsorption of solutes from a liquid solution has also been applied successfully a (Gerente, et al., 2007) The Elovich equation is given as follows,

$$q_t = \frac{1}{\beta} ln(\alpha\beta t) = \frac{1}{\beta} ln(\alpha\beta t) + \frac{1}{\beta} ln(t) \qquad \text{.....(11)}$$

Where, α (mg g^{-1} min^{-1}) is the initial sorption rate and the parameter β (g mg^{-1}) is related to the extent of surface coverage and activation energy for chemisorption. The kinetic results will be linear on a q_t vs $ln(t)$ plot, if the results follow an Elovich equation (Chakrapani et al., 2010).

Fitness of the kinetic models

The best-fit among the kinetic models was assessed by the squared sum of errors (*SSE*) values whereby the best model is obtained from the lowest *SSE* value for that particular system (Ho et al., 2000). The given equation was used to calculate the *SSE* values,

$$SSE = \sum \frac{(q_{e(exp)} - q_{e(cal)})^2}{q_e^{\,2}{}_{(exp)}} \quad \text{..... (12)}$$

Where, $q_{e(exp)}$ and $q_{e(cal)}$ are the experimental sorption capacity of fluoride (mg g^{-1}) at equilibrium time and the corresponding value that is obtained from the kinetic models.

Coefficient of determination (R^2)

R^2(*R-square*) is called the coefficient of determination, and it is given as the square of a correlation coefficient. It explains the amounts of variance accounted for in the relationship between two or more variables. Some of the features of R^2 are,

a) The coefficient of determination is a number between 0 and 1 inclusive (i.e. $0 \leq R^2 \leq 1$)
b) If $R^2=0$, the line has no explanatory value
c) If $R^2=1$, the line variable explains 100% of the variation in the response variable.

1.6. Thermodynamic studies

Thermodynamic studies of the adsorbate-adsorbent system provide information various parameters involved during the adsorption of adsorbate from aqueous solution by the adsorbent. The thermodynamic parameters were obtained by using the equation (Xu et al., 2008).

$$\Delta G^o = -RT\ln K_d \quad \text{.....(13)}$$

$$K_d = \frac{q_e}{C_e} \quad \text{.....(14)}$$

$$\ln K_d = \frac{\Delta S^o}{R} - \frac{\Delta H^o}{RT} \quad \text{.....(15)}$$

Where, K_d is the distribution coefficient for the adsorption, q_e is the amount of adsorbate adsorbed on the adsorbent per litre of solution at equilibrium, C_e is the equilibrium concentration of the adsorbate in solution, T is the absolute temperature,

R is gas constant (8.31445 $JK^{-1}mol^{-1}$), ΔG^0, ΔH^0 and $\Delta S^0$are Gibbs free energy change, enthalpy change and entropy change, respectively. The values of enthalpy change (ΔH^0) and entropy change (ΔS^0) are obtained from the slope and intercept of lnK_d versus $1/T$ plots of Vant Hoff, which are calculated by a curve fitting program. Finally, the ΔG^0 value is calculated by the following equation,

$$\Delta G^o = \Delta H^o - T\,\Delta S^o \qquad \text{.....(16)}$$

1.7. Importance of the study

The application of porous materials has been widely used for treatment of various effluents, to control the concentration of different solute, as catalyst, etc. but their uses are limited by various factors like unavailability of raw materials, high maintenance cost, expensive, etc. Thus in this piece of work, carbonaceous biowaste materials which are available almost throughout the year were selected for production of activated carbon which was then used as a cheap source of water treatment materials, keeping in mind that the process involved in the production of activated carbon and its application in removal of various organic, inorganic and biological pollutants should be simple, user-friendly and low-cost.

1.8. Aim and objectives of the work

The main objectives that were proposed under this research work include:

a). To synthesize activated carbon from the biowaste materials which are readily available

b). Activation of the prepared carbons by using oxidising agents such as HNO_3 and H_3PO_4

c). Studies on the utilization of activated carbon for defluoridation and decolorization.

d). To study the suitability of adsorption isotherms and adsorption kinetics.

e). Application of activation carbon for removal of coliform and *E.coli* bacteria from water

Scheme 1 presents an overall view of the Ph.D. research work that was carried out under this thesis.

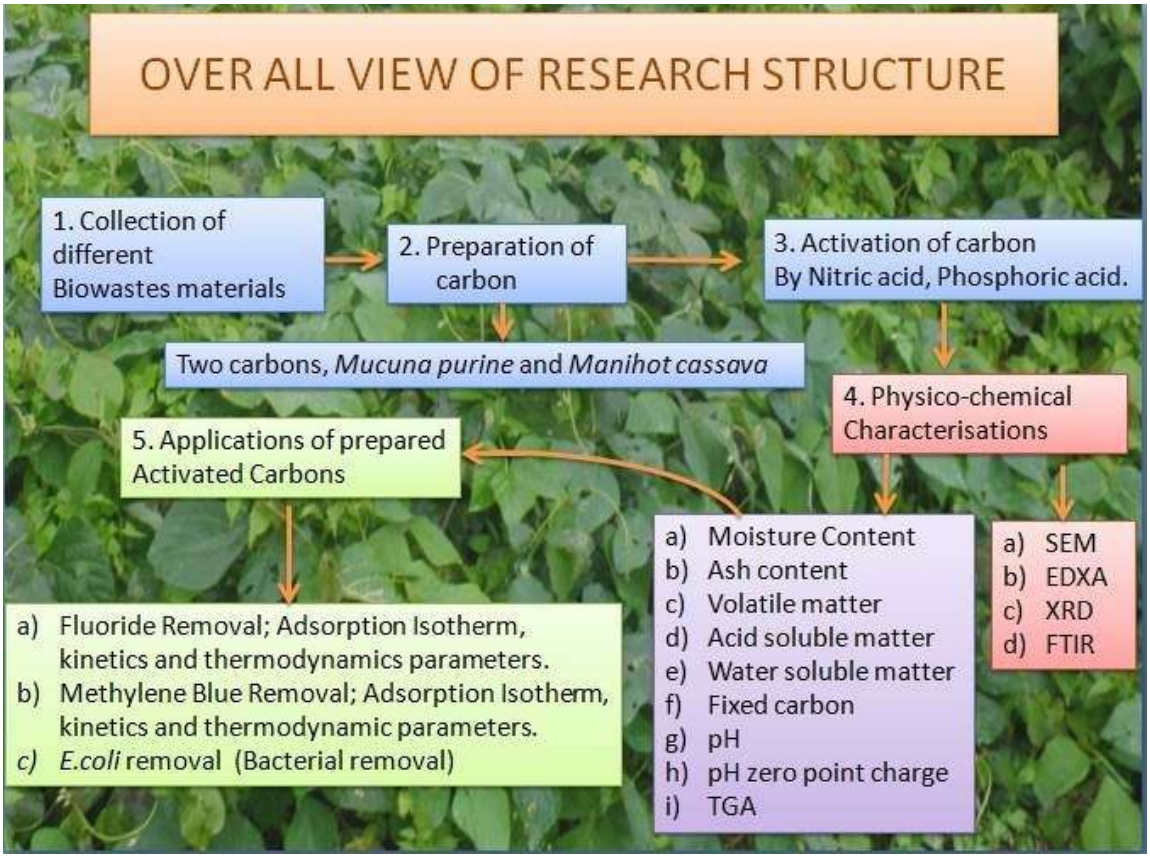

Scheme 1. Over all view of the Ph.D. research structure under the present thesis

References

Achaw, O.W., Afrane, G. (2008). The evolution of the pore structure of coconut shells during the preparation of coconut shell-based activated carbons. *Microporous Mesoporous Mater*, 112(1-3):284-290.

Aharoni, C., Ungarish, M. (1977). Kinetics of activated chemisorption. Part-2. Theoretical models. *J Chem Soc Faraday Trans 1: Phys Chem Condens Phases,* 73(3):456–464.

Aksu, Z. (2005). Application of biosorption for the removal of organic pollutants: a review. *Process Biochem,* 40(3–4):997–1026.

Anisuzzaman, S. M.,Joseph, C.G., Wan Daud, W.M.A.B., Krishnaiah, D., Yee, H.S. (2015). Preparation and characterization of activated carbon from typha orientalis leaves. *Int J Industrial Chem*, 6(1):9-21.

Aziz, H.A. (2011). Removal of high –strength color from semi – aerobic stabilized landfill leachate via adsorption on limestone and activate carbon mixture. *Res J ChemSci*, 1(6):1-7.

Bagdonavivius, S., Nikulin, M.S. (2011). Chi-square goodness-of-fit test for right censored data. *Int J Appl Math Stat*, 24:30-50.

Bandosz, T.J. (2006). Activated carbon surfaces in environmental redemption. *Interface Sci Technol,*7:3.

Bansal, R.C., Goyal, M. (2005). Activated Carbon Adsorption. Boca Raton, FL: CRC Press.

Beguin, F., Frackowiak, E. (2010). Carbons for electrochemical energy storage and conversion systems. CRC Press.

Byrne, J. F., Marsh H. (1995). In: Porosity in carbons: Characterization and applications; Patrick, Jr W. (Ed.) Edward Arnold: 1st ed., London, UK, chapter 1.

Cao, Q., Chang, K., Lv, Y.K., Bao, W.R. (2006). Process effects on activated carbon with large specific surface area from corn cob. *Bioresour Technol*, 97:110-115.

Chakrapani, C., Babu, C. S., Vani K.N.K., Rao, K.S. (2010). Adsorption kinetics for the removal of fluoride from aqueous solution by activated carbon adsorbents derived from the peels of selected citrus fruits. *E-J Chem,* 7:149-427.

Chen, Y., Zhu, Y., Wang, Y., Li, Y., Wang, L., Ding, L., Gao, X., Ma, Y., Guo, Y. (2011). Application studies of activated carbon derived from rice husks produced by chemical thermal process—A review. *Adv Colloid Interface Sci,* 163(1):39-52.

Chen, X., Jeyaseelan, S., Graham, N. (2002). Physical and chemical properties study of the activated carbon made from sewage sludge. *Waste Manag,* 22:755-760.

Chinniagounder, T., Shanker. M., Nageswaram, S. (2011). Adsorptive removal of crystal violet dye using agricultural waste cocoa (theobroma cacao). *Res J Chem Sci*,1(7):38-45.

Dada, A.O., Olalekan, A.P., Olatunya, A.M., Dada, O. (2012). Langmuir, Freundlich, Temki and Dubinin–Radushkevich Isotherms studies of equilibrium sorption of Zn^{2+} unto phosphoric acid modified rice husk. *J Appl Chem,* 3(1):38-45.

Daifullah, A. A. M., Yakout, S. M., Elreefy, S. A. (2007). Adsorption of fluoride in aqueous solutions using $KMnO_4$-modified activated carbon derived from steam pyrolysis of rice straw. *J Hazard Mater,* 147:633-643.

Demirbas, E., Kobya M., Sulak, M. T. (2008). Adsorption kinetics of a basic dye from aqueous solutions onto apricot stone activated carbon. *Bioresour Technol*, 99(13):5368-5373.

Dicks, A.L. (2006). The role of carbon in fuel cells. *J Power Sources*, 156:128-141.

Dubinin, M. M., Polyakov, N. S. (1986). Heterogeneous microporous structures and adsorption properties of carbonaceous adsorbents. *Russ Chem Bulletin,*35(9):1755-1762.

Endo, M., Kim, C., Nishimura, K., Fujino, T., Miyashita, K. (2000). Recent development of carbon materials for Li ion batteries. *Carbon*, 38:183-197.

Fan, M., Marshall, W., Daugaard, D., Brown, R. C. (2004). Steam activation of chars produced from oat hulls and corn stover. *Bioresour Technol*, 93:103-107.

Fanning, P.E., Vannice, M.A. (1993). A DRIFTS study of the formation of surface groups oncarbon by oxidation. *Carbon,* 31(5):721-730.

Ganan, J. F., Gonzalez, C. M., Gonzalez-Garcia, A., Ramiro, E., Roman, S. (2006). Carbon dioxide-activated carbons from almond tree pruning: Preparation and characterization. *Appl Surf Sci*, 252(17):5993-5998.

Ganvir, V. N., Syed, T. A. (2014). Synthesis of activated carbon from toor dall husk (*cajanus cajan* seed husk) by chemical activation. *Int J Chemtech Res*. 6(5):2750-2754.

Gayatri, S. L., Ahmaruzzaman, Md. (2010). Adsorption technique for the removal of phenolic compounds from waste water using low-costnatural removal adsorbents. *J Sci Techno,* 5:156-166.

Gerente, C., Lee, V.K.C., Le Clorec, P., McKay, G. (2007). Application of chitosan for the removal of metals from wastewaters by adsorption—mechanisms and models review. *Crit Rev Environ Sci Technol*, 37: 41–127.

Girgis, B.S., El-Hendawy, A.N.A. (2002). Porosity development in activated carbons obtained from date pits under chemical activation with phosphoric acid. *Microporous Mesoporous Mater*, 52:105-117.

Girgis, B.S., Yunis, S.S., Soliman, A.M. (2002). Characteristics of activated carbon from peanut hulls in relation to conditions of preparation. *Mater Lett*, 57:164-172.

Girgis, B.S., Attia, A.A., Fathy, N.A. (2007). Modification in adsorption characteristics of activated carbon produced by H_3PO_4 under flowing gases. *Colloids and Surfaces A: Physico Chem Eng Aspects,* 299:79-87.

Goswamee, R.L., Sengupta, P., Bhattacharyya, K. G., Dutta, D. K. (1998). Adsorption of Cr (VI) in layered double hydroxides. *Appl Clay Sci,* 13:21-34.

Gumus, R.H., Okpeku, I. (2015). Production of activated carbon and characterization from snail shell waste (Helix pomatia). *Adv Chem Eng Sci,* 5:51-61.

Guo, Y., Zhao, J., Zhang, H., Yang, S., Qi, J., Wang, Z., Xu, H. (2005). Use of rice husk-based porous carbon for adsorption of Rhodamine B from aqueous solutions. *Dyes Pigments,* 66:123-128.

Hameed, B. H., Din, A. T. M., Ahmed, A. L. (2007). Adsorption of methylene blue onto bamboo-based activated carbon: Kinetics and equilibrium studies. *J Hazard Mater,* 141:819-825.

Hayashi, J., Kazehaya, A., Muroyama, K., Watkinson, A.P. (2000). Preparation of activated carbon *from lignin by chemical activation. Carbon,* 28:1873-1878.

Hinz, B., Chevts, J., Renner, B.(2005). Bioavailability of diclofenacpotassium at low doses. *Brit J Clinic Pharma*,59(1):80-84.

Hirunpraditkoon, S., Srinophakun, P., Sombun, Moore, N.E. J. (2015). Synthesis of activated carbon from jatropha seed coat and application to adsorption of iodine and methylene blue. *Chem Eng Comm,* 202(1):32-47.

Ho, Y.S., Ng, J.C.Y., McKay, G.(2000*).* Kinetics of pollutant sorption by biosorbents: review. *Sep Purif Methods*, 29:189–232.

Hui Qiu, Lu, L.V., Bing-cai P.A., Qing-jian, Wei-ming, Quan-xing. (2009). Critical review in adsorption kinetic models. *J Zhejiang-Unv Sci A*,716-724.

Hussaro, K. (2014). Preparation of activated carbon from palm oil shell by chemical activation with Na_2CO_3 and $ZnCl_2$ as imprenated agents for H_2S adsorption. *Am J Environ Sci,* 10 (4):336-346.

Ismadji, S., Sudaryanto, Y., Hartono, S.B., Setiawan, L.E.K., Ayucitra, A. (2005). Activated carbon from char obtained from vacuum pyrolysis of teak sawdust: pore structure development and characterization.*Bioresour Technol,* 96(12):1364-1369.

Jankowska, H., Swiatkowski, A., Choma, J. (1991). Active Carbon. Ellis Horwood Limited.

Jahangiri, M., Shahtaheri, S.J., Adl, J., Rashidi, A., Kakooei, H., Forushani, A.R., Nasiri, G., Ghorbanali, A., Ganjali, M.R. (2012.) Preparation of activated carbon from walnut shell and its utilization for manufacturing organic-vapour respirator cartridge.

Fres Env Bulletin, 21(6):1508-1514.

Kalderis,D., Koutoulaskis, D., Paraskeva, P., Diamadopoulos, E., Otal, E., Valle, J.O.D., Pereira, C.F. (2008). Adsorption of polluting substances on activated carbons prepared from rice husk and sugarcane bagasse. *Chem Eng J*, 144:42-50.

Kazemipour, M., Ansari, M., Tajrobehkar, S., Majdzadeh, M., Kermani, H.R. (2008). Removal of lead, cadmium, zinc, and copper from industrial wastewater by carbon developed from walnut, hazelnut, almond, pistachio shell, and apricot stone. *J HazdMater*, 150:322-327.

Kim, Y.J., Lee, B.J., Suezaki, H., Chino, T., Abe, Y., Yanagiura, T., Park, K., Endo, M. (2006). Preparation and characterization of bamboo-based activated carbons as electrode materials for electric double layer capacitors. *Carbon,* 44:1592-1595.

Kruk, M., Dufour, B., Celer, E.B., Kowalewski, T., Mietek Jaroniec, M., Matyjaszewski, K. (2005). Synthesis of mesoporous carbons using ordered and disordered mesoporous silica templates and polyacrylonitrile as carbon precursor. *J Phys Chem*, 109:9216- 9225.

Kulkarni, H., Mahdi, H. (2014). Adsorption of carbon dioxide on orange peel and carbon synthesized from orange peel kavita. *Int J Chem Sci*, 12(3):773-784.

Lagergren, S. (1898). About the theory of so-called adsorption of soluble substances. *K Svenska Vetenskapsakad Handl,* 24:1–39.

Li, W. Yang, K., Peng, J., Zhang, L., Guo, S., Xia, H. (2008). Effects of carbonization temperatures on characteristics of porosity in coconut shell chars and activated carbons derived from carbonized coconut shell chars. *Indus Crops and Prod,* 28:190-198.

Lopez-Ramon, M.V., Stoeckli, F., Moreno-Castilla, C., Carrasco-Marin. F. (1999). On the characterization of acidic and basic surface sites on carbons by various techniques. *Carbon,* 37:1215–1221

Madhu, R., Sankar, K.V., Chen, S.M., Selvan, R.K. (2014). Eco-Friendly synthesis of activated carbon from dead mango leaves for the ultrahigh sensitive detection of toxic heavy metal ions and energy storage applications. *RSC Advances,* 4:1225-1233.

Mahmoudi, K., Hamdi, N., Srasra, E. (2014). Preparation and characterization of activated carbon from date pits by chemical activation with zinc chloride for methyl orange adsorption. *J Mater Environ Sci,* 5(6):1758-1769.

Marsh, H., Rodriguez-Reinoso, F. (2006). Activated carbon. Publisher: Elsevier Science & Technology Books.

McElroy, M. (2010). Energy Perspectives, Problems, & Prospects. New York: Oxford University Press.

Mckay, G., Blair, H. S., Gardener, J. K.(1982). Adsorption of dye on Chitin-I: equilibrium studies. *J Appl Poly Sci,*27:3043-3057.

Mckay, G. (1988). The kinetics of sorption of basic dyes from aqueous solution by sphagnum moss peat. *Canad J Chem Eng,* 76(4):822-827.

Meeenakshi, S., Viswanathan, N. (2007). Identification of selective ion exchange resin for fluoride sorption. *J Colloid Interface Sci*, 308:438–450.

Merzougui, Z., Addoun, F. (2008). Effect of oxidant treatment of date pit activated carbons application to the treatment of waters. *Desalination*, 222:394-403.

Mohan, D., Singh, K. P., Singh, V.K. (2006). Trivalent chromium removal from wastewater using low cost activated carbon derived from agricultural waste material and activated carbon fabric cloth. *J Hazard Mater*,135:280-295.

Mohan, S., Karthikeyan, J. (1997). Removal of lignin and tannin color from aqueous solution by adsorption on to activated carbon solution by adsorption on to active charcoal. *Environ Pollut,* 97:183-187.

Morgan, P. (2005). Carbon fibers and their composites. CRC press: Boca raton, FL, USA, 1st ed.

Olivares –Marin, C.M., Gonzalez, A.F., Garcia, V.M., Serrano, G. (2006). Preparation of activated carbon from cherry stones by chemical activation with $ZnCl_2$. *Appl Surf Sci,* 252:5967-5971.

Onal, Y., Akmil-Basar, C., Sarici-Ozdemir, C. (2007). Elucidation of the naproxen sodium adsorption onto activated carbon prepared from waste apricot: Kinetic, equilibrium and thermodynamic characterization. *J Hazard Mater,* 148(3):727-734.

Özhan, A., Şahin, Ö., Küçük, M.M., Saka, C. (2014). Preparation and characterization of activated carbon from pine cone by microwave-induced $ZnCl_2$ activation and its effects on the adsorption of methylene blue. *Cellulose,* 21(4):2457-2467.

Pandolfo, A.G., Hollenkamp, A.F. (2006). Carbon properties and their role in supercapacitors. *J Power Sources,* 157:11-27.

Peng, J., Zhang, L., Yang, K., Xia, H., Zhang, S., Guo, S.H. (2008). Preparation of activated carbon from coconut shell chars in pilot-scale microwave heating equipment at 60 kW. *Waste Manag,* 29:756-760.

.

Rahman, I.A., Saad, B. (2003). Utilization of guava seeds as a source of activated carbon for removal of methylene blue from aqueous solution. *Malay J Chem*, 5(1):8-14.

Rouquerol F., Rouquerol, J., Sing, K. (1999). Adsorption by powders and porous solids: priciples, methodology and applications. Academic press: San Diego, USA, 1st ed.

Rocha, J. D., Coutinho, A. R., Luengo, C. A. (2002). Biopitch produced from eucalyptus wood pyrolysis liquids as a renewable binder for carbon electrode manufacture. *Braz J Chem Eng*, 19:127-132.

Rodriguez-Reinoso, F. (1998). The role of carbon materials in heterogeneous catalysis. *Carbon*, 36(3):159-175.

Ru, A.H., Zheng J. T. (2001). Study of microstructure of high-surface-area polyacrylonitrile activated carbon fibers. *J Colloid Interface Sci,* 236:369–374.

Salman, J.M. (2014). Optimization of preparation conditions for activated carbon from palm oil fronds using response surface methodology on removal of pesticides from aqueous solution. *Arabian J Chem.* 7(1):101-108.

Sarrano, V.G., Correa, E.M.C., Gonzalez, M.C.F., Franco, M.F.A., Garcia, A.M. (2005). Preparation of activated carbons from walnut wood: a study of microporosity and fractal dimension. *Smart Mater Struct*, 14:363-368.

Serrano, V.G., Villegas, J.P., Valle, C.J.D., Calahorro, C.V. (1996). Heat treatment of rockrose char in air. Effect on surface chemistry and porous texture. *Carbon,* 34:533-538.

Shamsuddin, M.S., Yusoff, N.R.N., Sulaiman, M.A. (2016). Synthesis and characterization of activated carbon produced from kenaf core fiber using H_3PO_4 activation. *Procedia Chem,* 19:558-565

Soleimani, M., Kaghazchi, T. (2008). Adsorption of gold ions from industrial wastewater using activated carbon derived from hard shell of apricot stones — An agricultural waste. *Biores Technol,* 99:5374–5383.

Stoeckli, H. F. (1990). Microporous carbons and their characterization: The present state of the art. *Carbon,* 28(1):1-6.

Suhas, P.J.M.C., Ribeiro, M.M.L.C. (2007). Lignin – from natural adsorbent to activated carbon: A review. *Bioresourc Technol,* 98(12):2301-2321.

Supriya, S., Palanisamy, P.N., Shanthi, P. (2014). Preparation and characterization of activated carbon from casuarina for the removal of dyes from textile wastewater. *Int J Chemtech Res,* 6(7):3635-3641.

Srisa-ard, S. (2014). Preparation of activated carbon from sindora siamensis seed and canarium sublatum guillaumin fruit for methylene blue adsorption. *Int Trans J Eng Manag Appl Sci Tech,* 5(4):235-245.

Syna, N., Valix, M. (2003). Assessing the Potential of activated bagasse as gold adsorbent for gold-thiourea, *Miner Eng,* 16:511-518.

Tessmer, C.H., Vidic, R.D., Uranowski, L.J. (1997). Impact of oxygen-containing surface functional groups on activated carbon adsorption of phenols. *Environ Sci Technol,* 31(7):1872-1878.

Tseng, R.L., Wu, F.C., Juang, R.S. (2003). Liquid-phase adsorption of dyes and phenols using pinewood-based activated carbons, *Carbon*. 41:487-495.

Tempkin, M.J., Pyzhev, V. (1940). Kinetics of ammonia synthesis on promoted iron catalysts. *Acta Physio Chem Urs,* 12:217-222.

Tseng, R.L., Tseng, S.K. (2006). Characterization and use of high surface area activated carbons prepared from cane pith for liquid-phase adsorption. *J Hazard Mater B*, 136:671-680.

Villegas, J.P., Valle, C.J.D. (2002). Pore structure of activated carbons prepared by carbon dioxide and steam activation at different temperatures from extracted rockrose. *Carbon,* 40:397-402.

Wang, S.L., Tzon, Y.M., Lu, Y.H., Sheng, G. (2007). Removal of 3-chlorophenol from water using rice-straw-based carbon. *J Hazard Mater,* 147:313-318.

Weber Jr., W.J., Morris J.C. (1963). Kinetics of adsorption on carbon from solution. *J Sanit Eng Div,* 89:31–59.

Xu, D., Tan, X.L., Chen, C.L., Wang, X.K. (2008). Adsorption of Pb(II) from aqueous solution to MX-80 bentonite: Effect of pH, ionic strength, foreign ions and temperature. *Appl Clay Sci*, 41: 37-46.

Yin, C.Y., Aroua, M.K., Daud, W.M.AW. (2007). Review of modifications of activated carbon for enhancing contaminant uptakes from aqueous solutions. *Sep Pur Technol*, 52(3):403–415

Zhang, F., Ma, H., Chen, J., Li, G.D., Zhang, Y., Chen, J.S. (2008). Preparation and gas storage of high surface area microporous carbon derived from biomass source cornstalks. *BioresourTechnol*, 99:4803-4808.

CHAPTER-2

SYNTHESIS AND CHARACTERIZATION OF ACTIVATED CARBONS

This chapter includes collection of bio-waste materials i.e., Mucuna pruriens and Manihot esculenta, followed by carbonization and chemical activation using Nitric acid and Phosphoric acid. Studies on various physico-chemical properties such as Moisture content, volatile matter, ash content, acid/water soluble matter, pH, pH_{ZPC}, FT-IR, TGA, SEM, EDX, XRD,BET surface analysis were studied to understand and appreciate the carbon properties for its future application.

2.1 Introduction

Activated carbon in its broadest sense includes a wide range of processed amorphous carbon-based materials. Activated carbons have a highly developed porosity and an extended interparticulate surface area. Their adsorptive properties are due to their high surface area, a microporous structure, and a high degree of surface reactivity. The unique properties of activated carbon have led to identification of applications in diverse areas such as, food processing, pharmaceutical, chemical, nuclear, petroleum industries (Bandosz 2006; Bansal and Goyal, 2005). However, activated carbon finds major use in the technologies that have been developed for water treatment. An increasing attention to the activated carbon adsorption for removal of pollutants from aqueous solutions was initiated by the pollution of the environment, which includes air and water, due to rapid industrialisation (Marsh and Rodriguez, 2006).

Activated carbon can be synthesized from any material that has reasonable elemental carbon content and the use of these materials has been reported by many researchers; (Cao et al., 2006; Daifullah et al., 2007; Hirunpraditkoon et al., 2014; Kulkarni and Mahdi, 2014; Madhu et al., 2014; Mahmoudi et al., 2014; Peng et al., 2008; Salman 2014; Sarrano et al., 2005; Shamsuddin et al., 2016; Srisa-ard 2014; Supriya et al., 2014). The preparation of activated carbon involves two main steps, first step is the (i) carbonisation of the carbonaceous raw material at temperatures below 800°C in an inert atmosphere and second step is the (ii) activation of the carbonised product.

The importance of the carbonisation process is that it leads to the elimination of the non-carbon elements such as oxygen, hydrogen, and nitrogen as volatile gaseous species. This is done by pyrolytic decomposition, and during this process, the residual elementary carbon atoms group themselves into stacks of flat, aromatic sheets cross-linked in a random manner. These aromatic sheets are irregularly arranged, thereby leaving free interstices. These interstices give rise to pores, which make activated carbons excellent adsorbents (Bandosz 2006). From literature reports it is known that the aromatic sheets in activated carbons also contain free radical structure or structure with unpaired electrons. These unpaired electrons are resonance stabilized and trapped during the carbonization process, due to the breaking of bonds at the edges of the aromatic sheets, and thus, they create edge carbon atoms. These edge carbon atoms have unsaturated valencies and can, therefore, interact with heteroatoms such

as oxygen, hydrogen, nitrogen, and sulfur, giving rise to different types of surface groups (Bandosz 2006).

During the activation process, the pore structure in carbonised raw materials is further developed and enhanced. During this process, the carbonised raw material is converted into a form that contains the greatest possible number of randomly distributed pores of various sizes and shapes, giving rise to an extended and extremely high surface area of the product. There are two types of activation, namely physical/thermal activation and chemical activation (Viswanathan et al., 2009). It is also possible to combine thermal and chemical activation processes to obtain a desired activated carbon (Marsh and Rodriguez, 2006).

It is understood that though activated carbon has been studied and used for different purposes, however, there is still scope for further work in this area. Some of the concerns are reduction of cost for synthesis so that the carbon absorbent can be synthesised in a large scale, which requires identification of practically and commercially viable material for synthesis of carbon absorbent. Also very relevant is the modification of carbon absorbent in terms of its surface area, pore sizes and also presence of functional groups. This is very significant as it directly affects the absorption efficiency of the absorbent, and therefore continuous efforts are on to synthesise different types of carbons by selecting different starting materials as well as activation processes.

In view of this, through the present work an attempt has been made to synthesis low cost activated carbon from two biowaste plants (*Mucuna pruriens* and *Manihot esculenta)* which are locally available in plenty and thereafter identify their potential for utility in various fields as an alternative to commercially available activated carbon.

This Chapter presents the details of synthesis of different activated carbons and discusses the characterization of these carbons by different analytical techniques.

2.2. Collection of raw materials for the synthesis of activated carbons

For this study, the raw materials for synthesising activated carbon were selected on the basis of their availability, abundance and ease of handling. Two locally available plants were selected, *viz*., *Mucuna pruriens* (Fig. 2.1) and *Manihot esculenta* (Fig. 2.2). The reason for selecting *Mucuna pruriens* plant is that, its vines can spread over a great length covering large areas, hence the local community treat this plant as weed and often burn and destroy the plant and hence it was selected to see if it could be

used for a noble application. The *Manihot esculenta* plant has an edible tuberous root. After the root is harvested, most of the stem and leaves are just dumped in an around the fields. Hence the stem and leaves were collected and used raw materials to synthesize activated carbon for application in various purification processes. Given below are some details about *Mucuna pruriens* and *Manihot esculenta* plants.

Mucuna pruriens

Fig. 2.1. *Mucuna pruriens* plant

Scientific classification

Kingdom:	Plantae
Order:	Fabales
Family:	Fabaceae
Subfamily:	Faboideae
Tribe:	Phaseoleae
Genus:	*Mucuna*
Species:	***M. pruriens***

Mucuna pruriens is a tropical legume native to Africa and tropical Asia and widely naturalized. English common names include velvet bean, Bengal velvet bean, Florida velvet bean, Mauritius velvet bean, Yokohama velvet bean, cowage, cowitch, lacuna bean, Lyon bean (Wilmot-Dear 1984). The plant is an annual climbing shrub with long vines that can reach over 15 m in length. When the plant is young, it is almost completely covered with fuzzy hairs, but after maturation, it is almost completely free of hairs (Howard 1989). The leaves are tripinnate, ovate, reverse ovate, rhombus-shaped or widely ovate. In many parts of the world, *Mucuna pruriens* is used as an

important forage, fallow and green manure crop (Keay et al., 1972). Since the plant is a legume, it fixes nitrogen and fertilizes soil.

Manihot esculenta

Fig. 2.2. *Manihot esculenta* plant

Scientific classification

Kingdom:	Plantae
Order:	Malpighiales
Family:	Euphorbiaceae
Subfamily:	Crotonoideae
Tribe:	Manihoteae
Genus:	*Manihot*
Species:	***M. esculenta***

Manihot esculenta, Brazilian arrowroot, manioc, and *tapioca*) of the spurge family, is a woody shrub native to South America Euphorbiaceae (Allem 1994). It is extensively cultivated as an annual crop in tropical and subtropical regions for its edible starchy tuberous root, a major source of carbohydrates. Cassava is the third largest source of food carbohydrates in the tropics, after rice and maize (Balakrishnan and Chakrabarty, 2007). Cassava is a major staple food in the developing world, providing a basic diet for over half a billion people. It is one of the most drought-tolerant crops, capable of growing on marginal soils. Nigeria is the world's largest producer of cassava, while Thailand is the largest exporter of dried cassava. Cassava is classified as either sweet or bitter. Like other roots and tubers, both bitter and sweet varieties of cassava contain antinutritional factors and toxins, with the bitter varieties containing much larger amounts (Rogers and Appan, 1973).

For this study, the leaves and the vines of *Mucuna pruriens* plant and stem and leaves of *Manihot esculenta* plant were collected washed and dried in the sun.

2.3. Preparation of activated carbons

Carbonisation of raw biowaste materials

The dried materials were crushed manually into small pieces and were packed in a clean stainless steel container and carbonisation was done using Muffle furnace (Narang Scientific-MSW-103) at around 900^{o}C for 4-6 hours under a uniform Nitrogen flow. After carbonisation, the carbon product was first crushed into fine powder with mortar and pestle after which it was washed with deionized water to remove adherent impurities and dried in the oven at 110^{o}C for 12 hours. The dried carbon was then grinded in a planetary Ball Mill (Fritsch-Pulver Isette -7) using zirconium ball at 600 rpm for 10 minutes to obtain uniform size carbon.

Chemical activation of carbons

In order to modify the surface properties of the carbon material, the carbonized product was activated with two different acids, *viz.,* 0.1N HNO_3 and 0.1 H_3PO_4 so that surface oxidation can take place in these carbon. For activation using nitric acid, 10 g of carbonized *Mucuna pruriens* was taken in a 250ml beaker and 0.1N HNO_3 solution was slowly poured until the carbon mass was submerged under the acid solution, after which it was magnetically stirred for 2-3 hours. It was then filtered using Whatman No. 42 filter paper and washed with 100 ml of double distilled water to remove the excess acid. Similar experimental procedure was followed for activation by using 0.1N H_3PO_4. For activation of carbonized *Manihot esculenta*, the above procedures were exactly followed.

Thereafter, the prepared adsorbents were dried in an oven at 110^{o}C for around 12 hours and stored in air tight containers. The activated carbons synthesized from *Mucuna pruriens* were labeled as MPAC-HNO_3 and MPAC-H_3PO_4, and *Manihot esculenta* activated carbons were labeled as MEAC-HNO_3 and MPAC-H_3PO_4.

2.4. Physico-chemical characterisation of activated carbon

Physico-chemical characterization of activated carbon is a fundamental requirement for its applications. Various parameters such as pH, conductivity, ash content, acid/water insoluble matters, bulk density, porosity, Iodine number and different functional groups present in the surface of the activated carbon reflects the properties of activated carbon.

The activated carbons, *viz.,* MPAC-HNO_3, MPAC-H_3PO_4, MEAC-HNO_3 and MPAC-H_3PO_4 were subject to different analytical techniques in order to fully characterize the compounds.

Moisture content

A silica crucible was pre-heated at 110 ^{o} C for 1 hour and allowed to cool at room temperature. Thereafter, 1g of carbon sample was weighed and placed in the pre-weighed silica crucible and dried in a drier continuously. The drying sample was constantly reweighed at 10 min. interval until a constant weight was obtained. The ratio of change in original weight expressed in percentage gives the moisture content (ASTM standards, 2004).

$$\text{Moisture content (\%)} = \frac{(C-D)}{(C-B)} \times 100 \quad \cdots\cdots\cdots\cdots (17)$$

Where, B = Mass of crucible (g), C = Mass of crucible with sample (g), D = Mass of crucible after weight loss (g).

Volatile matter

A silica crucible was preheated in an oven to 900^{o}C for 10 mins and cooled in a desiccator. 1g of carbon sample was taken in this pre heated silica crucible partially closed with a lid and heated at about 900^{o} C for 10 minutes in the oven. The crucible and its contents was collected and cooled in a desiccator. The loss in weight gives the volatile matter (ASTM standards, 2003).

$$\text{Volatile matter (\%)} = \frac{(C-D)}{(C-B)} \times 100 \quad \cdots\cdots\cdots\cdots (18)$$

Where, B = Mass of crucible (g), C = Mass of crucible with sample (g), D = Mass of crucible after weight loss (g).

Acid soluble matter

1 g of the adsorbent was placed in an evaporating dish and mixed with distilled water to form a thin slurry. This was followed by addition of 5-10 ml of Conc. HCl and the mixture was digested by warming until the sample was nearly dry. The digestion was repeated three times with 5 ml of the acid. Then it was diluted with 100 ml water. It was then filtered using a previously weighed sutured crucible; the weight of the insoluble matter was calculated after drying for a constant weight at 110^{o}C (Test method of activated carbon, 1989).

$$\text{Acid insoluble matter (\%)} = \frac{(C-D)}{(C-B)} \times 100 \quad \text{.....(19)}$$

Where B = Mass of crucible (g), C = Mass of crucible with sample (g), D = Mass of crucible after weight loss (g).

Water soluble matter

1 g of carbon sample was added to 100 ml of distilled water and shaken thoroughly for about 30 minutes and filtered. The residue i.e., adsorbent was dried, cooled and weighted. The loss in weight was calculated, which gives water soluble matter (ASTM standards, 2009).

$$\text{Water soluble matter (\%)} = \frac{(C-D)}{(C-B)} \times 100 \quad \text{.....(20)}$$

Where B = Mass of crucible (g), C = Mass of crucible with sample (g), D = Mass of crucible after weight loss (g).

Ash content

A silica crucible of known weight was preheated in an oven at 900^0 C for 1 hour. It was then allowed to cool in a desiccator and reweighed. 1 g of carbon sample was placed in the crucible and heated at 900^o C for 1 hour with lid on. The crucible and its content was then cooled in a desiccator and reweighed. The weight of the incombustible residue accounts for ash content (ASTM standards, 2009).

$$\text{Ash content (\%)} = \frac{(C-D)}{(C-B)} \times 100 \quad \text{.....(21)}$$

Where B = Weight of crucible (g), C = Weight of crucible with sample (g), D = Weight of crucible after weight loss (g).

Fixed carbon

The quantity of fixed carbon in percentage is obtained by subtracting the sum of percentage composition of volatile matter, moisture content, acid soluble, water soluble and ash content from 100 percent. Fixed carbon from the sample were obtained using the following relation:

$$\text{Fixed carbon (\%)} = 100 - (\text{Volatile matter} + \text{moisture content} + \text{acid soluble} + \text{water soluble} + \text{ash content}) \quad \text{.....(22)}$$

Apparent density, bulk density and porosity

A weighed amount of carbon was transferred into a pre-weighed silica crucible and dried in the oven at 105^oC until a constant weight was obtained, after which the

weight of the dried carbon was taken again. A pre-weighed well-corked density bottle was taken and the bottle was partially filled with known volume of water, corked and reweighed. Thereafter, small quantities of the dried carbon was added into the bottle and weighed again, and this was continued until the density bottle is filled up to mark. The bulk density, dry density and porosity were calculated using the following expressions (Ekpete and Horsfall 2011; Verla et al., 2012)

$$\text{Bulk density} = \frac{\text{Mass of wet sample}}{\text{mass of vol.}} \quad \text{..... (23)}$$

$$\text{Dry density} = \frac{\text{Mass of dry sample}}{\text{Vol. of cylinder}} \quad \text{..... (24)}$$

$$\text{Porosity } (\eta) = \frac{V_v}{V_t} \quad \text{..... (25)}$$

Where V_v = volume of void, V_t = total volume

The volume of void V_v was obtained by first determining the total volume of the cylinder

$$V_t = \pi r^2 h \quad \text{..... (26)}$$

used for the experiment and also determining the volume of solid *i.e*., the activated carbon used

$$V_s = M_s/G_s\rho_w \quad \text{..... (27)}$$

r = radius of cylinder, h = height of cylinder, M_s = mass of solid, G_s = specific gravity, ρ_w = density of water.

Then, volume of void (V_v) was obtained as (28)

$$V_v = V_t - V_s \quad \text{.....(28)}$$

Iodine number

A stock solution of 0.1N iodine was prepared by using 2.7g of iodine crystals and 4.1g of potassium iodide per litre. This prepared stock solution was standardized using 0.1N sodium thiosulphate solution, 0.5g of the activated carbon and 10ml of 5% v/v hydrochloric acid is taken in a 100 ml volumetric flask. The flask was stirred gently until the carbon was wetted. Then 100ml of 0.1N iodine solution was added and the flask was shaken using rotary shaker for 1 hour. The mixture was filtered

through a sintered glass crucible and an aliquot portion (20ml) was titrated with 0.1N sodium thiosulphate using starch as indicator. The concentration of iodine adsorbed by the activated carbon at room temperature was calculated as amount of iodine adsorbed in milligrams (Ekpete and Horsfall, 2011).

$$\frac{\text{I } mg}{g} = \frac{(B-S)}{B} x \frac{VM}{W} x\ 253.81 \quad \text{..... (29)}$$

In the above equation, *B* and *S* are the volumes of thiosulphate solution required for blank and sample titrations respectively. *W* is the mass of activated carbon sample, *M* is the concentration (mol) of the iodine solute, 253.81 is the atomic mass of iodine and *V* is 20ml aliquot.

pH and Conductivity

For this study, 1.0g of activated carbon in 100ml of distilled water was taken in a beaker and the mixture was stirred for one hour (ASTM standards, 2011). The sample was allowed to stabilize for some time and thereafter the pH and conductivity was measured using Thermo Scientific- Orion 4 star, ISE instrument.

Zero point charge (pH_{zpc})

Zero point charge is the pH at which the external surface charge becomes zero (Kosmulski, 2009). The zero point charge (pH_{zpc}) of the activated carbons were determined by adding 0.1g of activated carbons to different sets of 200ml solution of 0.1M NaCl taken in different conical flasks. The pH of the mixture was adjusted with 0.1 N HCl and/ or 0.1 N NaOH solution to make the solution acidic or basic as required. The flasks were sealed and placed on a shaker for 24hrs after which the final pH was measured. The pH_{zpc} occurred when there was no change in the pH after adsorption (Ekpete and Horsfall 2011). The pH_{zpc} is the point where the plot of pH_{final} *vs.* $pH_{initial}$ crosses the baseline in the graph.

Oxygen containing functional groups (Boehm's titration)

The Boehm titration method was used for the determination of oxygenated surface group (Boehm 1994). 1.0g of the activated carbons were kept in contact with 15ml solution of 0.1M $NaHCO_3$, 0.05M Na_2CO_3 and 0.1M NaOH for acidic groups and 0.1M HCl for basic groups /sites respectively at room temperature for more than 2 days. Subsequently, the aqueous solutions were back titrated with 0.1M HCl for acidic and 0.1M NaOH for basic groups. The numbers of acidic sites of various types

were calculated under the assumption that NaOH neutralizes carboxylic, phenolic, and lactonic groups and that Na_2CO_3-carboxylic and lactonic; and $NaHCO_3$ only carboxylic groups. The phenolic group content on the carbon sample was estimated by the amount of 0.1M $NaHCO_3$ uptake by the carbon sample. Lactonic group content $NaHCO_3$ uptake by the activated carbon sample. The difference between the amount of 0.1 M Na_2CO_3 and O.1 M NaOH uptake by the sample gives carboxylic group content. Neutralisation points were known using pH indicators of phenolphthalein solution for titration of strong base and strong acid, methyl red solution for weak base with strong acid and pH together.

Pore volume and surface area (BET method)

BET analysis provides precise specific surface area and porosity evaluation of materials by nitrogen multilayer adsorption measured as a function of relative pressure using a fully automated analyser. The technique encompasses external area and pore area evaluations to determine the total specific surface area in m^2g^{-1} yielding important information in studying the effects of surface porosity and particle size which finds use in many applications.

BET Surface area calculation was determined by employing BET equation, which is given as (Bansal and Goyal, 2005).

$$\frac{P}{V\,(P-P_o)} = \frac{1}{V_m C} + \frac{C-1}{V_m C}\,\frac{P}{P_o} \qquad \text{..... (30)}$$

The surface area is determined by the following equation

$$S_{BET} = \frac{N_A A_M V_m 10^{-20}}{m_s V_M} \qquad \text{.....(31)}$$

Where, S_{BET} is the surface area ($m^2\ g^{-1}$)

N_A is Avogadro's number (6.023 X 10^{23} molecules/mole)

A_M is the area occupied by an adsorbate molecule (16.2 $Å^2$ for Nitrogen)

V_m is the quantity of gas adsorbed for monolayer coverage of surface (cm^3)

M_s is the mass of the solid analyzed (g)

V_M is the molar volume of gas (22,414 cm^3mol^{-1})

For nitrogen as adsorptive gas, equation (30) becomes

$$S_{BET} = \frac{4.35V_M}{m_s} \quad \text{.....(32)}$$

For a porous material, or one that has an unsmooth surface, the BET surface area is generally appreciably larger than its non-porous material (Sing 2001).

Scanning Electron Microscopy (SEM) Study

The surface morphology of the activated carbon plays a vital role in the adsorption of different adsorbate and it also provides information about the random distribution of different pores of varying shape and sizes. Thus, in order to obtain the surface morphological information SEM techniques was studied at different magnification by using SEM-JEOL JMS 6390 LV.

Energy-Dispersive X-Ray (EDX) study

EDX analysis was carried out in conjunction with SEM to identify the presence of different elements on the surface of the activated carbon. This technique has the ability to characterize each element due to the fundamental principle that each element has a unique atomic structure thereby allowing x-rays that are characteristic of an element's atomic structure to be identified uniquely from each other.

FT-IR study

FT-IR is perhaps the most powerful tool for identifying types of chemical bonds (functional groups). This technique also allows measurements of lower concentrations of surface functional groups (Bansal and Goyal 2005). The wavelength of light absorbed is characteristic of the chemical bond as can be seen in this annotated spectrum. Thus, in order to identify the different functional group present in the activated carbon, the FTIR spectra were taken for the samples. The sample discs were prepared by mixing 1 mg of powdered carbon with 199 mg of KBr (Merck; for spectroscopy) followed by pressing under vacuum to obtain pellets. The spectra were measured in the range of 400-4000 cm^{-1}.

Thermo Gravimetric analysis (TGA) study

Thermo gravimetric analysis was carried out to understand the thermal properties of activated carbon in order to obtain information about decomposition patterns of activated carbon at different temperatures. Generally, the surface groups that liberate

CO_2 are less stable and decompose at temperatures as low as 350°C. The other chemical groups that liberate CO are more stable and decompose only above 500°C. Thus, TGA was done using TA instrument (SDT Q 600, M/S TA Instruments, USA) having alumina as a reference at a heating rate of 20^0C/ minute under argon atmosphere.

Powder *X-ray Diffraction* (PXRD) study

PXRD analysis was done using XRD (Model Rigaky-Ultima iv Japan) using CuKα radiation at the scanned rate of 0.2 degree per minute. Powder diffraction (XRD) is a technique used to characterise the crystallographic structure, crystallite size (grain size), and preferred orientation in polycrystalline or powdered solid samples. Powder diffraction is commonly used to identify unknown substances, by comparing diffraction data against a database maintained by the International Centre for Diffraction Data. X-ray diffraction (XRD) method is a conventional and powerful technique for the characterization of the stacking structure. One of the difficulties in the characterization of carbon materials is their low crystallinity, which leads to broadening of the corresponding XRD peak. The structure of the activated carbons was studied in terms of crystalline order with respect to graphite structure by analyzing their X- ray diffractograms. An effect of the finite crystallite sizes is seen as a broadening of the peaks in an X-ray diffraction as is explained by the Scherrer Equation.

The Scherrer equation is given as (Scherrer 1918),

$$\tau = \frac{K\lambda}{\beta \cos \theta} \qquad \text{..... (33)}$$

Where, K is the shape factor. The shape factor correlates the size of the sub-micrometer particles or crystallite in a solid to the broadening of a peak in a diffraction pattern; λ is the x-ray wavelength, typically 1.54 Å (CuKα=1.54); β is the line broadening at the half the maximum intensity (FWHM) in radian and θ is the Bragg's angle. The dimension shape factor has a typical value of about 0.9 but varies with the actual shape of the crystallite. The Scherrer equation is limited to nano scale particle but applicable to grain larger than 0.1 μm.

2.5. Results and discussion

Moisture content

The moisture content for the synthesised activated carbon from MPAC and MEAC treated with HNO_3 and H_3PO_4 are tabulated in Table 2.1. The comparatively low values of moisture content indicate higher adsorption capacity of activated carbon (Sugunadevi et al., 2002). If the moisture content of the adsorbent is more, it may reduce the efficiency for absorption by the activated carbon. Among the different activated carbon the order of the moisture content were MPAC-HNO_3 < MPAC-H_3PO_4 < MEPA-H_3PO_4 < MEAC-HNO_3

Table 2.1. Moisture content of different activated carbons

Adsorbent	Moisture content %
MPAC-HNO_3	7.92
MPAC-H_3PO_4	8.06
MEAC-HNO_3	8.59
MEPA-H_3PO_4	12.87

Volatile matter content

The values obtained for the volatile matters are presented in Table 2.2. The volatile matter of MPAC-HNO_3, MPAC-H_3PO_4, MEPA-H_3PO_4, MEAC-HNO_3 are 9.00, 7.12, 1.92, 1.00% respectively. This low value of volatile matter especially in MEAC indicates the absence of impurities in the synthesised activated carbons.

Table 2.2. Volatile matter content of different activated carbons

Adsorbent	Volatile matter content %
MPAC-HNO_3	9.00
MPAC-H_3PO_4	7.12
MEAC-HNO_3	1.92
MEPA-H_3PO_4	1.00

Acid soluble matter

Acid soluble matter present in the different activated carbon samples are tabulated in Table 2.3. The low value of acid soluble matter is an indication that the activated carbon is insoluble in acid, therefore can be engaged in treating acidic water (Rao et al., 2011).

Table 2.3. Acid soluble matter of different activated carbons

Adsorbent	Acid soluble matter %
MPAC-HNO_3	0.90
MPAC-H_3PO_4	1.30
MEAC-HNO_3	0.80
MEPA-H_3PO_4	1.10

Water soluble matter

The Water soluble matters are presented in Table 2.4. The values obtained were found to be low for all the adsorbents indicating that the carbons are almost insoluble in water and hence can be used for water analysis as it may not alter/change the physical properties of water. The low values are necessary and essential property of any adsorbent because when these adsorbents are used for water treatment, they must be least soluble in water. Among the four adsorbent, MPAC-HNO_3 have the lowest solubility in water.

Table 2.4. Water soluble matter of different activated carbons

Adsorbent	Water soluble matter %
MPAC-HNO_3	0.11
MPAC-H_3PO_4	0.15
MEAC-HNO_3	0.36
MEPA-H_3PO_4	0.45

Ash content

Low ash content is a characteristic of any activated carbon, in order to be considered as good adsorbent. Low values of ash content indicate that the pores present on the surface are welled preserved with sufficient active site for easy adsorption. The presence of impurities such as ash greatly affects the adsorption capacity of the adsorbent as most of the spaces are occupied by the ash. The results for the ash content for four different samples are given in Table 2.5. The low values of ash content suggest that the adsorption capacity of the synthesised carbons is expected to be high.

Table 2.5. Ash content of different activated carbons

Adsorbent	Ash content %
MPAC-HNO_3	0.10
MPAC-H_3PO_4	0.13
MEAC-HNO_3	1.20
MEPA-H_3PO_4	1.43

Fixed carbon

Fixed carbon is the amount of the carbon content present in the sample after exposing the sample to different physical test. The results are tabulated in Table 2.6. The high percentage of carbon content in all the four samples indicates that the raw bio-waste materials used for the synthesis of activated carbon are indeed very good source of carbon. Higher the value of fixed carbon, higher will be the surface area and active site or porosity for adsorption.

Table 2.6. Fixed carbon content of different activated carbons

Adsorbent	Fixed carbon content %
MPAC-HNO_3	81.97
MPAC-H_3PO_4	83.24
MEAC-HNO_3	87.13
MEPA-H_3PO_4	83.15

Apparent density, bulk density and porosity

The apparent density is very useful for the estimation of the packing volume or to determine the grade of carbon needed for an existing system. The relatively low density of activated carbons is attributed to random arrangement of micro-crystallites with strong cross-linking which produce porous structure. The bulk density is another important physical parameter especially for activated carbon when it is investigated for its filterability. Porosity describes the number of pores present in a sample. Porosity therefore enhances adsorption capacity of the adsorbent. The results are given in Table 2.7.

Table 2.7. Apparent density, bulk density and porosity of different activated carbon

Adsorbent	Apparent density g ml^{-1}	Bulk density g/cm^3	Porosity %
MPAC-HNO_3	0.45	0.87	0.91
MPAC-H_3PO_4	0.47	0.84	0.90
MEAC-HNO_3	0.43	0.89	0.93
MEPA-H_3PO_4	0.44	0.86	0.91

Iodine number

Iodine number (in mg g^{-1}) gives an estimate of the surface area (in m^2 g^{-1}) of activated carbon (Gergova et al., 1993; Girgis and El-Hendawy, 2002). The adsorption of aqueous iodine is considered to be a simple and quick test for evaluating the surface area of activated carbons associated with pores larger than 1 nm. The Iodine number is a fundamental parameter used to characterise activated carbon performance. The micropore content of the activated carbon is determined by Iodine number, obtained

by the adsorption of iodine from solution by the activated carbon sample. The micropores are responsible for the large surface area of activated carbon particles which are created during the activation process. It is in the micropores that adsorption largely takes place. It measures the porosity of pores with dimensions ≥ 1.0 nm. The values of iodine number obtained for different carbon samples are shown in Table 2.8.

Table 2.8. Iodine number of different activated carbons

Adsorbent	Iodine number $m^2 g^{-1}$
MPAC-HNO_3	638.61
MPAC-H_3PO_4	622.56
MEAC-HNO_3	703.74
MEPA-H_3PO_4	687.83

pH and Conductivity

The results of pH and electrical conductivity of different activated carbon samples are presented in Table 2.9. The pH of the carbon samples were found to be in the range of 6.77-7.16. It has been reported by (Ahmedna et al. 2000; Okieimen et al., 2007) that for most applications, carbon pH in the range 6-8 is acceptable. Conductivity measures the electrical current, which is proportional to the mineral matter present in water. So conductivity depends on the total dissolved solids (TDS) in water. Among the four carbon samples, MEAC-HNO_3 shows the highest electrical conductivity.

Table 2.9. pH and Conductivity measurement for different activated carbons

Adsorbent	pH	Conductivity (μS)
MPAC-HNO_3	7.16	104.30
MPAC-H_3PO_4	6.92	87.20
MEAC-HNO_3	6.80	123.60
MEPA-H_3PO_4	6.77	84.40

Zero point charge (pH_{zpc})

In order to get an idea about the surface charge density on the synthesized activated carbon, pH_{ZPC} was measured. The pH_{ZPC} values for MPAC-HNO_3, MPAC-H_3PO_4 MEAC-HNO_3 and MEPA-H_3PO_4 were found to be 6.81, 6.70, 6.96 and 6.74 respectively. This indicates that the surface is positively charged. When the pH becomes greater than pH_{zpc} the surface of the carbon is rendered negatively charged, because of the dissociation of the acidic functionalities, releasing protons into the medium. On the other hand, when the pH is less than the pH_{zpc}, the basic sites

combine with protons from the medium to leave a positively charged surface (Menendez-Diaz and Martln-Gullonb, 2006). In the present study, for every carbon, the pH value is less than its corresponding pH_{ZPC} value. This indicates that the surface is positively charged. The values of pH_{ZPC} for different carbon samples are shown in Table 2.10-2.13 and the corresponding plots are given as Fig. 2.3-2.6.

Table 2.10. Determination of initial and final pH of MPAC-HNO_3

pH_i	pH_f	pH_f - pH_i
6.82	7.02	0.20
7.09	7.26	0.17
7.25	7.39	0.14
7.47	7.59	0.12
7.58	7.64	0.06
7.75	7.71	-0.04
7.87	7.79	-0.08
8.02	7.88	-0.14
8.16	7.92	-0.24
8.37	7.98	-0.39

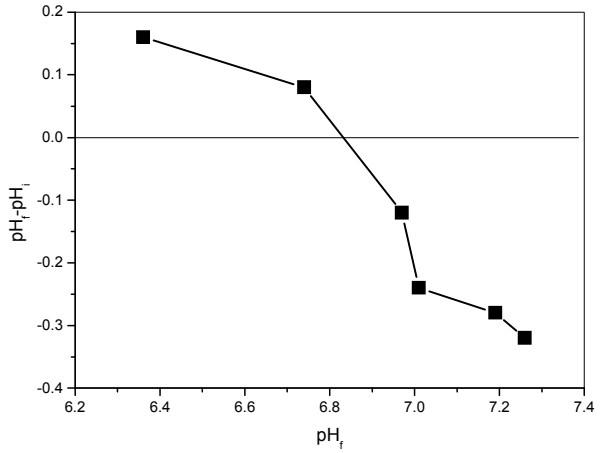

Fig. 2.3. Plot of pH_f vs pH_f-pH_i of MPAC-HNO_3

Table 2.11. Determination of initial and final pH of MPAC-H_3PO_4

pH_i	pH_f	pH_f-pH_i
7.11	7.25	0.14
7.25	7.37	0.12
7.30	7.41	0.11
7.58	7.65	0.07
7.66	7.69	0.03
7.80	7.76	-0.04
8.33	8.24	-0.09
8.46	8.32	-0.14
8.58	8.39	-0.19
8.64	8.41	-0.23

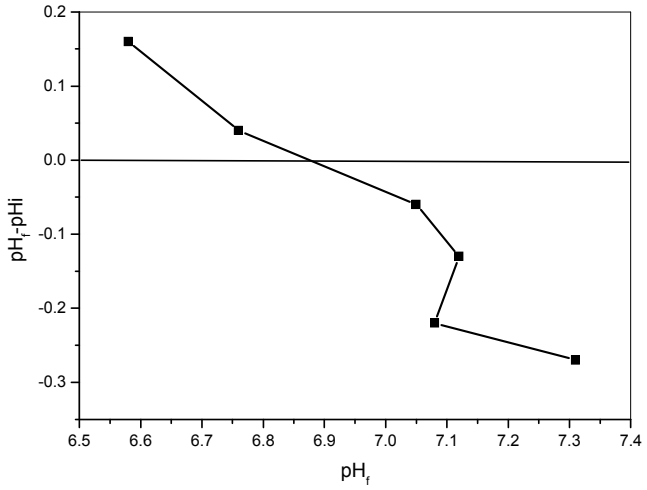

Fig. 2.4. Plot of pH_f vs pH_f-pH_i of MPAC-H_3PO_4

Table 2.12. Determination of initial and final pH of MEAC-HNO_3

pH_i	pH_f	pH_f- pH_i
7.44	7.61	0.17
7.58	7.73	0.15
7.76	7.88	0.12
7.81	7.91	0.10
8.26	8.30	0.04
8.41	8.38	-0.03
8.55	8.46	-0.09
8.64	8.51	-0.13
8.72	8.56	-0.16
8.83	8.61	-0.22

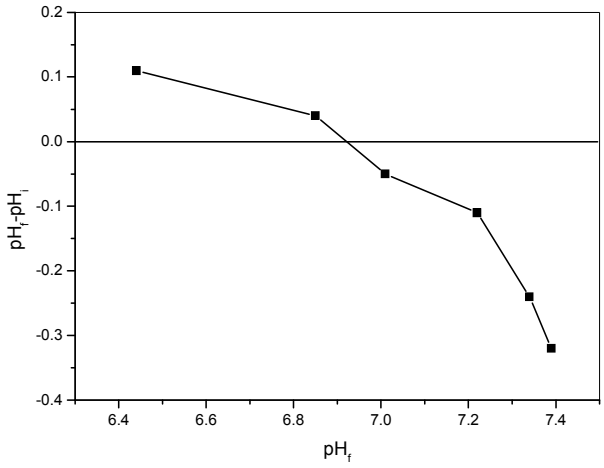

Fig. 2.5. Plot of pH_f vs pH_f-pH_i of MEAC-HNO_3

Table 2.13. Determination of initial and final pH of MEAC-H_3PO_4

pH_i	pH_f	$pH_{f\,-}\ pH_i$
7.33	7.56	0.23
7.58	7.75	0.17
7.71	7.85	0.14
7.86	7.95	0.09
8.07	8.12	0.05
8.25	8.19	-0.06
8.36	8.25	-0.11
8.42	8.27	-0.15
8.55	8.36	-0.19
8.63	8.41	-0.22

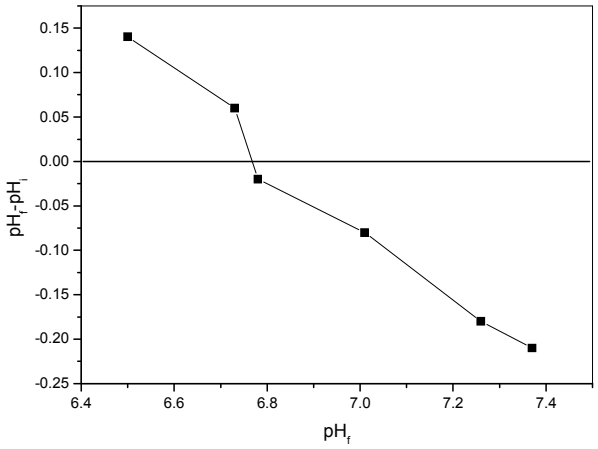

Fig. 2.6. Plot of pH_f vs pH_f-pH_i of MEAC-H_3PO_4

Oxygen containing functional groups

From Table 2.14. it is evident that the total basic groups is greater than the total acidic groups (due to carboxylic, lactonic, phenolic and carbonyl groups). The basicity may be due to oxygen functional groups, and the existence of pyrone-type structures on the edges of the polyaromatic layers (Ekpete and Horsfall 2011). The surface titration method stipulates that only strongly acidic carboxylic groups are neutralized by sodium bicarbonates (Na_2HCO_3), where as those neutralized by sodium carbonate (Na_2CO_3) are thought to be lactonic and carboxylic group. The weakly acidic phenolic groups only react with strong alkali, sodium hydroxide (NaOH). Neutralization with hydrochloric acid (HCl) characterizes the amount of surface basic group's pyrones and chromenes that are present in the activated carbon. It may be noted that the Boehm's titration for determining the amounts and types of surface functional groups on activated carbon has been widely used by many researchers (Rao et al., 2011a)

Table 2.14. Surface acid groups and total basic groups measured by Boehm's titration (mEq g^{-1}) for different activated carbon

Samples	Carboxyl	Lactonic	Phenolic	Total basic groups
MPAC-HNO_3	0.40	1.00	1.20	5.07
MPAC-H_3PO_4	0.20	0.80	0.50	3.26
MEAC-HNO_3	1.00	1.50	0.60	4.87
MEAC-H_3PO_4	0.30	0.70	0.80	3.66

Pore volume and surface area (BET method)

The surface area is one of the most important characteristic properties of any adsorbent in study. BET specific surface area was determined for four different samples and the resulting surface area varied in the range 812-931 m^2g^{-1}. Among the four samples MEAC-HNO_3 possess higher surface area and pore volume. The increasing order of the surface area among the four adsorbents is found to be MEAC-HNO_3>MEPA-H_3PO_4>MPAC-HNO_3>MPAC-H_3PO_4. The particle size and surface area plays an important role in adsorption and the adsorption capacity of any adsorbent increases with decreasing particle size. This is due to increase in the availability of active sites for adsorption. It is also observed that the surface area of the resulting activated carbons varies by activating agents. The results obtained from BET surface analyser for different carbons are tabulated in Table 2.15.

Table 2.15. BET surface area

Adsorbent	Surface area $m^2 g^{-1}$	Pore volume cc g^{-1}
MPAC-HNO_3	931	0.514
MPAC-H_3PO_4	883	0.504
MEAC-HNO_3	865	0.508
MEPA-H_3PO_4	812	0.498

Scanning electron microscopy (SEM) study

SEM micrographs of the activated carbon gives a clear picture of the porosity of an adsorbent and also shows complex disorganised surface structures of different open pore sizes, shapes and dimensions. From the SEM micrograph Fig.2.7 –2.10, slant flakes are observed in different sizes and their surfaces are observed to be rough and smooth. The rough surface micrographs showed a distinct roughness with oval patterns. Within each oval section, presence of the macro pores is clearly noticeable. The surface corrugation is clearly visible from the SEM images which may be due to HNO_3 and H_3PO_4 treatment. All the carbon samples possess many pores in a honeycomb like shape which are clearly visible on the surface. The carbon flakes are arranged randomly consisting imperfect layer planes, which are largely disorganized. In certain parts of the structure, over a short distances some parallel or near parallel alignment formation takes place which often referred to as ‘‘micro crystallites’’. Activation with HNO_3 and H_3PO_4 is effective to create well developed pores distribution on the surface of the precursor, thus leading to large surface area and porous structure of the activated carbon. Presence of different pores sizes in the synthesised activated carbon is expected to influence the adsorption process.

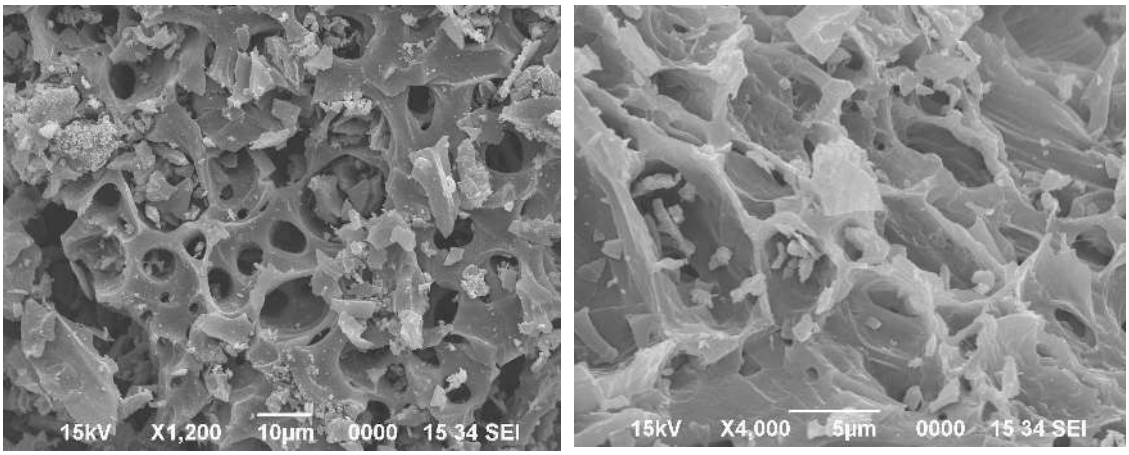

Fig. 2.7. SEM micrograph of MPAC-HNO_3 at x1200 and x4000 (Formation of numerous pores were observed)

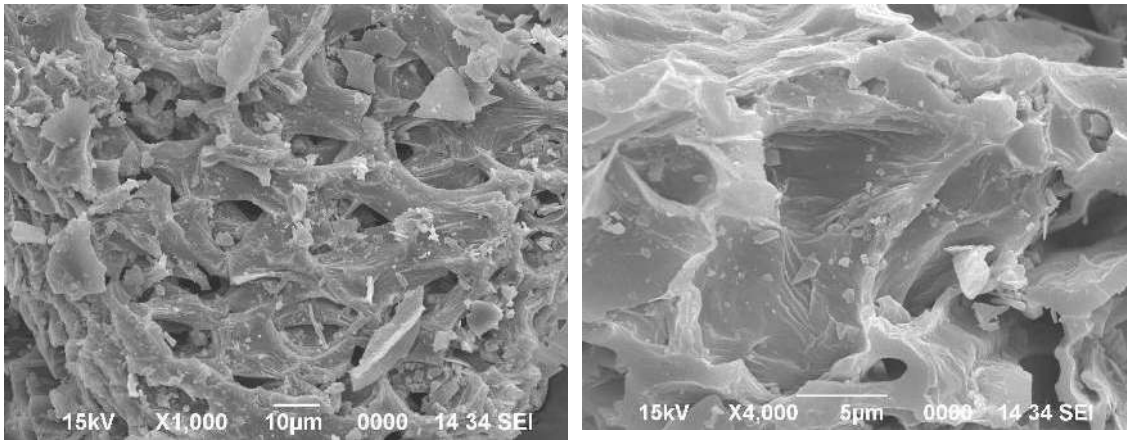

Fig. 2.8. SEM micrograph of MPAC-H_3PO_4 at x1000 and x4000 (Formation of diverse pores structure were observed)

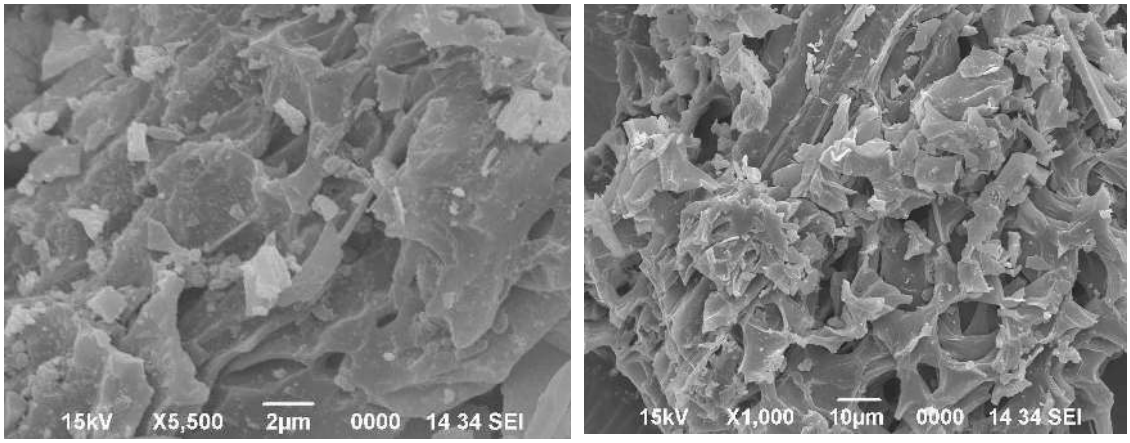

Fig. 2.9. SEM micrograph of MEAC-HNO_3 at x1000 (Disorganised surface structure with different pores dimensions were observed)

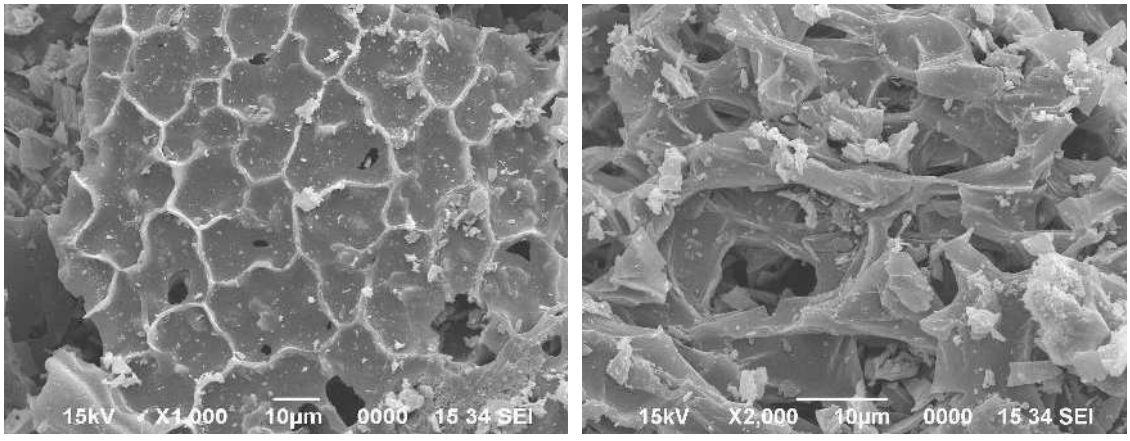

Fig. 2.10. SEM micrograph of MEAC-H_3PO_4 at x1000 and x2000 (Formation of micropores in a non-uniform pattern were observed)

Energy-Dispersive X-Ray (EDX) study

EDX study was carried out to find out the percentage composition of carbon and oxygen within the sample under investigation. The results obtained for the four different samples of activated carbon are given Fig. 2.11- 2.14 and corresponding elemental composition are given in Table 2.16-2.19.The carbon content was found to be highest for MEAC-HNO_3 and least in MEAC-H_3PO_4 whereas the Oxygen content was highest in MEAC-H_3PO_4.

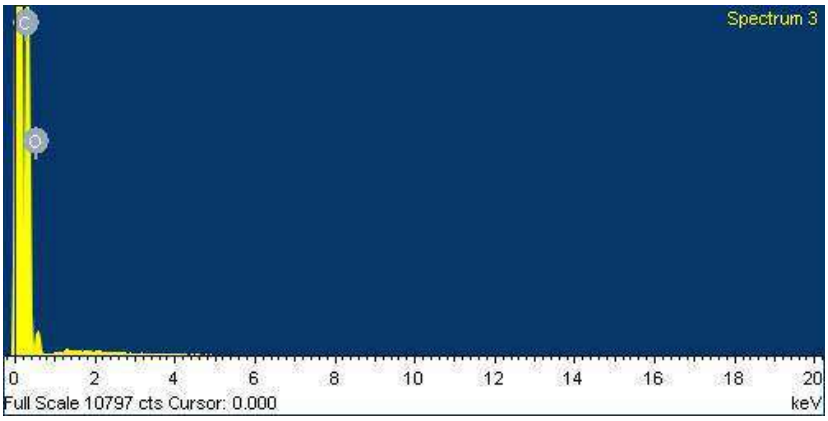

Fig. 2.11. EDX spectra of MPAC-HNO_3

Table 2.16. Elemental composition of MPAC-HNO_3

Element	Weight%	Atomic%
C K	77.46	82.07
O K	22.54	17.93
Totals	100.00	

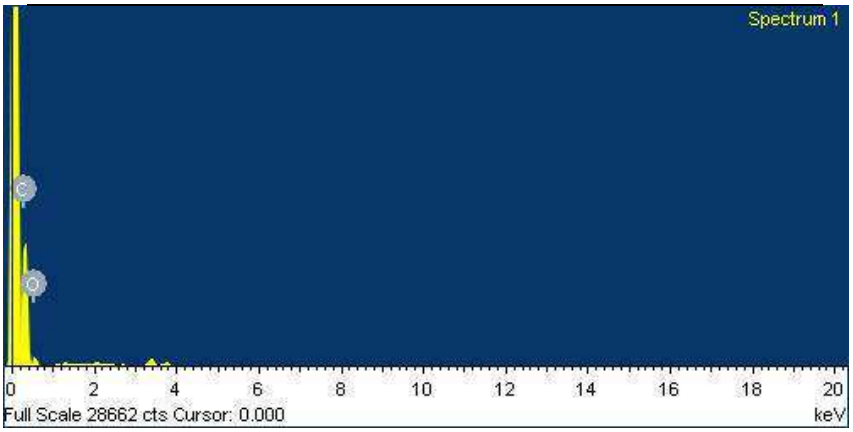

Fig. 2.12. EDX spectra of MPAC-H_3PO_4

Table 2.17. Elemental composition of MPAC-H_3PO_4

Element	Weight%	Atomic%
C K	77.12	81.78
O K	22.88	18.22
Totals	100.00	

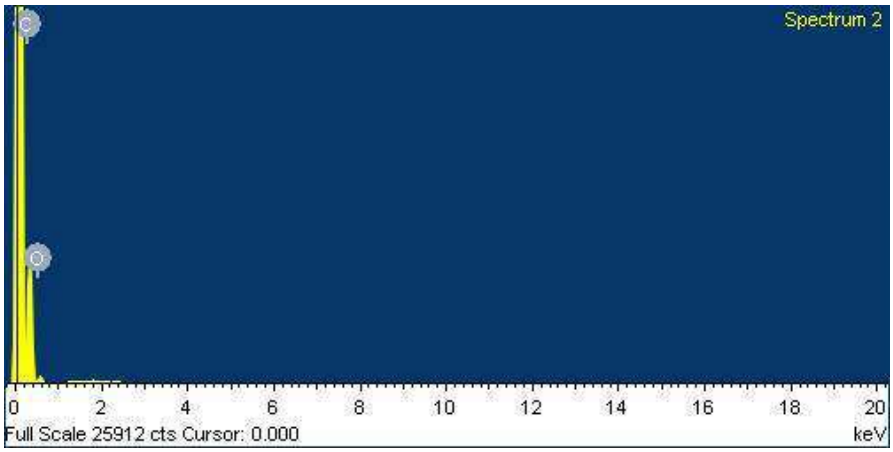

Fig. 2.13. EDX spectra of MEAC-HNO_3

Table 2.18. Elemental composition of MEAC-HNO_3

Element	Weight%	Atomic%
C K	78.23	82.72
O K	21.77	17.28
Totals	100.00	

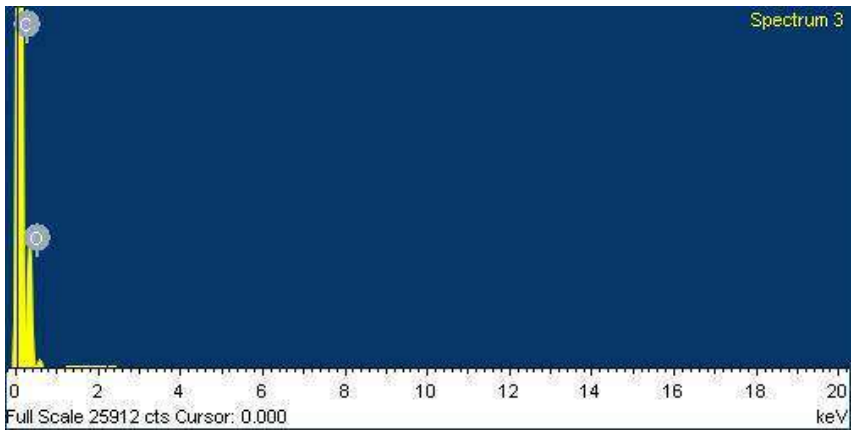

Fig. 2.14. EDX spectra of MEAC-H_3PO_4

Table 2.19. Elemental composition of MEAC-H_3PO_4

Element	Weight%	Atomic%
C K	76.17	80.98
O K	23.83	19.02
Totals	100.00	

FT-IR study

The presence of oxygen and aromatic structures were identified in prepared activated carbons by FT-IR analysis. The FT-IR spectra of MPAC-HNO_3, MPAC-H_3PO_4, MEACHNO_3 and MEAC-H_3PO_4 are shown in Fig. 2.15-2.20. Surface chemical groups were detected by absorption bands assigned to carboxyl, carbonyl, phenolic, ethers and hydroxyl groups. The different absorption peaks were observed for activated and unactivated carbon samples and are shown in Table 2.20. A very prominent peak at 3417-4346 cm^{-1} were observed for all the carbon samples, which is due to the absorption of water molecules as result of an O-H stretching mode of hydroxyl groups (John 2000). The band at 2806-2810 $cm^{-1}$is attributed to C-H stretch and has also been reported by Matsumura et al., (1976). The band of asymmetric stretching at lower wave numbers indicates the presence of strong hydrogen bonds. The peaks at 1625-1636 cm^{-1} is due to the presence of C=O group (Socrates 1994). The band appearing at 1585-1591 cm^{-1} has been assigned as aromatic structure (Donnet et al., 1993). This has been assigned to aromatic ring stretching coupled to highly conjugated carbonyl groups or attributed to the stretching vibrations of C=O moieties of conjugated systems such as diketone, keto ester and keto-enol structure (Lambart 1987). Bands at 1342-1347 cm^{-1} correspond to phenolic group (Friedel and Carlson, 1972). Some weak bands were observed in all the carbon samples in the range from 700-400 cm^{-1}, indicating the presence of C-C stretching in the carbon adsorbents (Bansal and Goyal, 2005).

Table. 2.20. FT-IR band assignment of different carbon samples

Wave number (cm^{-1})						
Unactivated *Mucuna* carbon	MPAC-HNO_3	MPAC-H_3PO_4	Unactivated *Manihot* carbon	MEAC-HNO_3	MEAC-H_3PO_4	Assignments
3446	3432	3438	3417	3424	3445	O-H steching
2807	…….	2811	2806	2808	2806	C-H vibration
1634	1637	1628	1625	1626	1626	C=O
1585	1585	1591	1587	1591	1591	aromatic structure
1345	1346	1349	1342	1347	1347	phenolic group
1015	1024	1002	1008	1015	-------	C-O strech and vibration

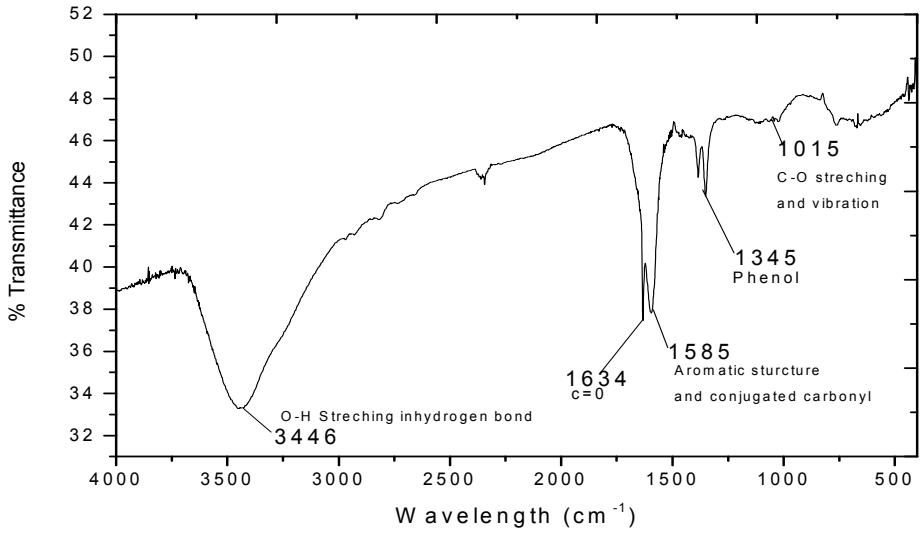

Fig. 2.15. FT-IR spectra of MPUC (*Mucuna pruriens* unactivated carbon)

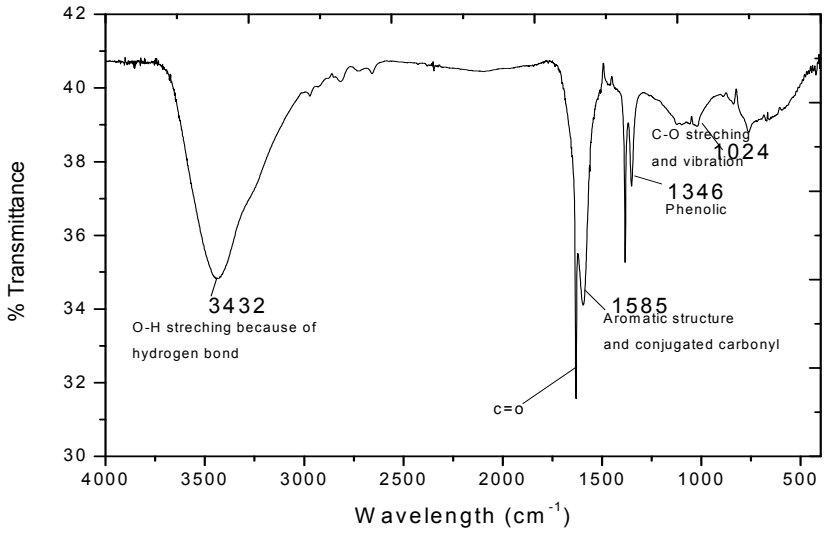

Fig. 2. 16. FT-IR spectrum of MPAC-HNO_3

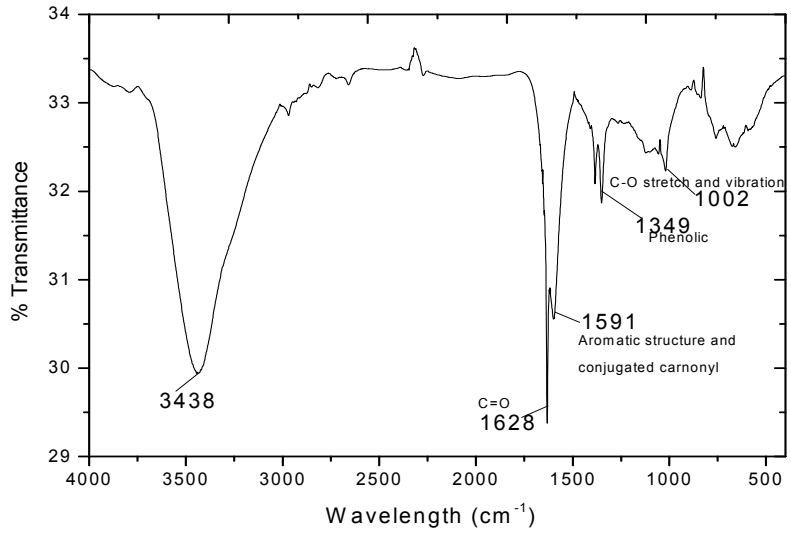

Fig. 2. 17. FT-IR spectrum of MPAC-H_3PO_4

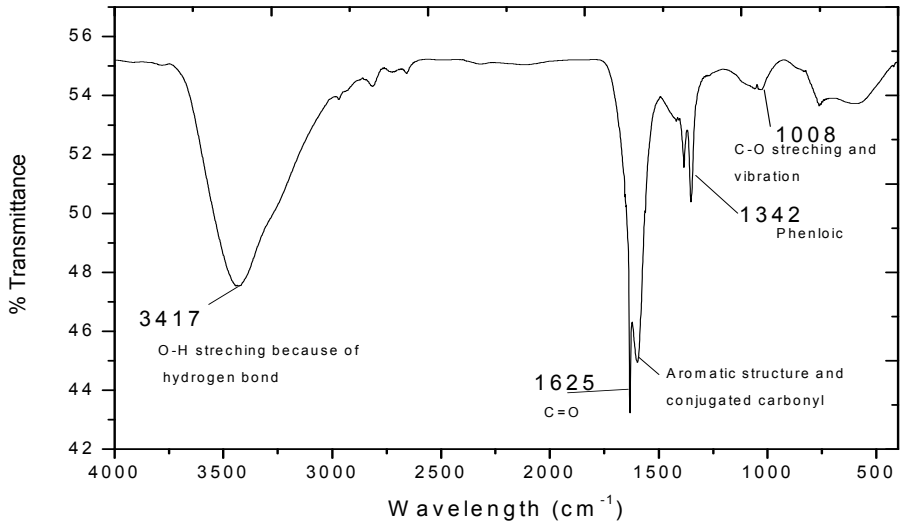

Fig. 2. 18. FT-IR spectrum UMEC (*Manihot esculenta* unactivated carbon)

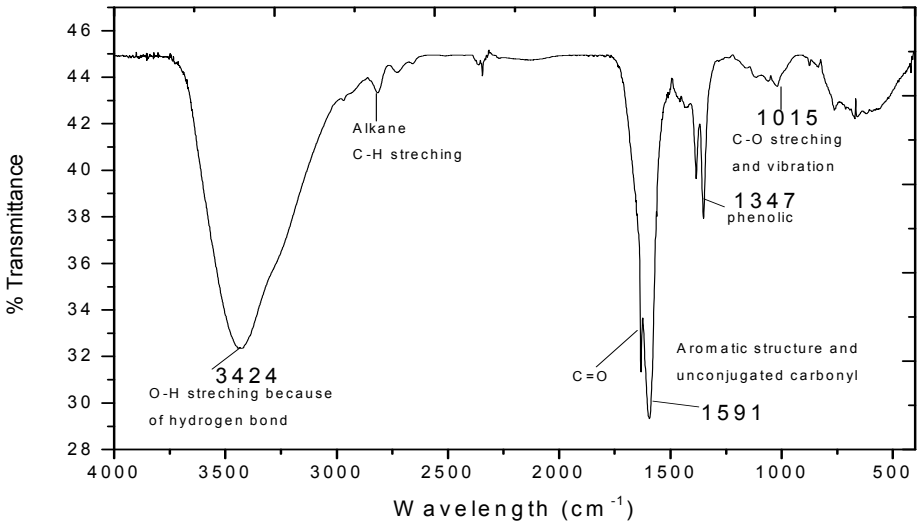

Fig. 2. 19. FT-IR spectrum MEAC-HNO_3

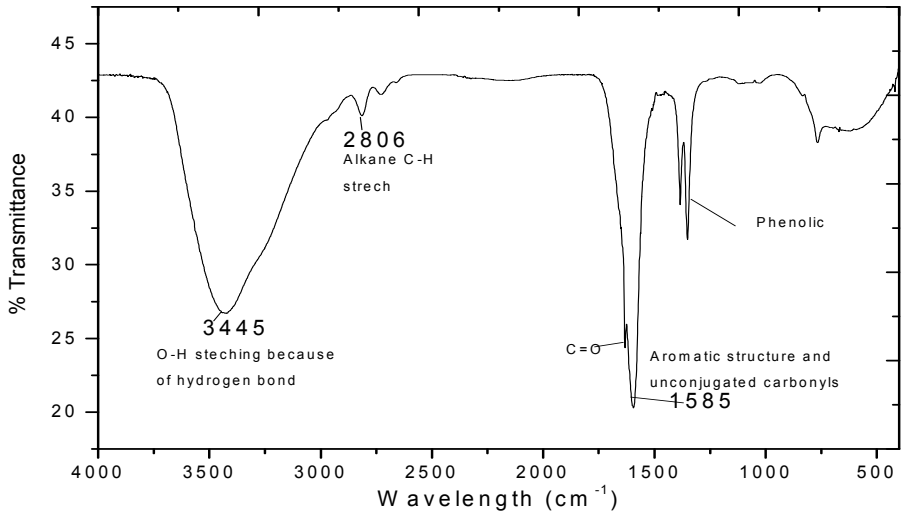

Fig. 2. 20. FT-IR spectrum MEAC-H_3PO_4

Powder X-ray Diffraction (PXRD) study

Fig. 2.21-2.26 illustrate the XRD pattern of the different activated carbon synthesised from the selected biowaste materials. All the carbons exhibit structural parameters highly disordered solid carbons as would be expected for activated carbons that 'the more disordered, the higher is its reactivity' (Garcia et al., 1998). The X- ray

diffraction profile of selected activated carbon show broad diffraction peaks corresponding to 2θ~23°, 29° and 42° which are assigned to $CaCO_3$ compound (Compared from PDF Card No.: 00-005-0586 Quality:S). Peak around 2θ~23° may correspond to graphitic basal plane reflection of carbon due to stacking structure of aromatic layers. Activated carbons are made up of graphite like crystal and the deformation of the graphite crylstals lead to the formation of turbostratic structure which make the carbon more reactive. These compounds form typical graphitic layers and stacks of planes during carbonization (Riaz et. al., 2013). The formation of pore in carbons is due to the existing defects of graphite-like crystal layer. The change in the structural parameters of MEAC-HNO_3 and MEAC-H_3PO_4 before and after activation of the carbon can be observed from the Fig. 2.21-2.23, which suggest that the activation by HNO_3 and H_3PO_4 greatly influence the structural transformation of the activated carbon. Similar pattern were also observed for MPAC-HNO_3 and MPAC-H_3PO_4 carbon sample (Fig. 2.24-2.26). Each sample has a different full width at half maximum (FWHM) value of the (104) peak, indicating the presence of a micropore wall structure (Yoshizawa *et al*., 1996). This is in consistent with fact that a decrease in the order of crystallinity in carbon materials broadens the XRD peaks and shifts the (104) reflection towards lower angles (Leon y Leon, 1992). The much wider (104) peak of the activated carbon indicates that much smaller number of layers are involved in coherently scattering structural units in these materials.

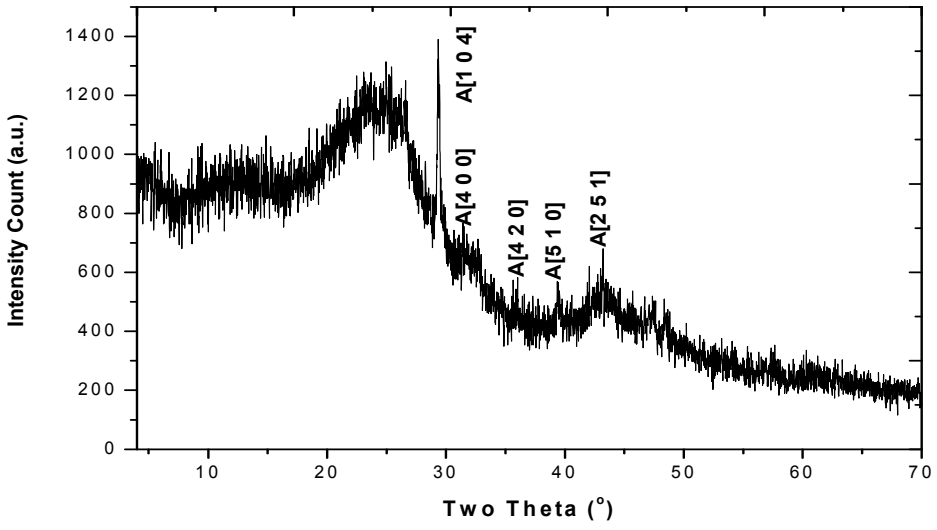

Fig. 2.21. XRD spectra of MEAC-HNO_3

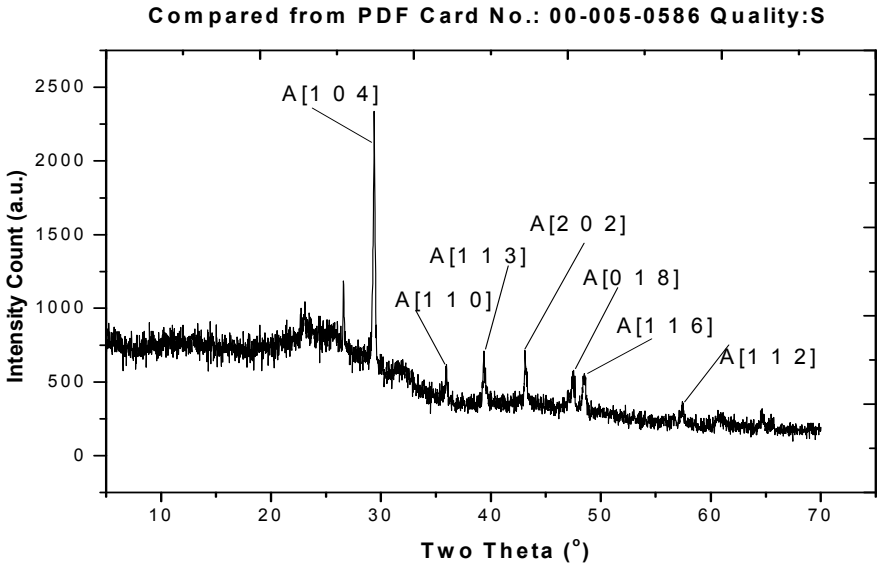

Fig. 2.22. XRD spectra MEAC-H_3PO_4

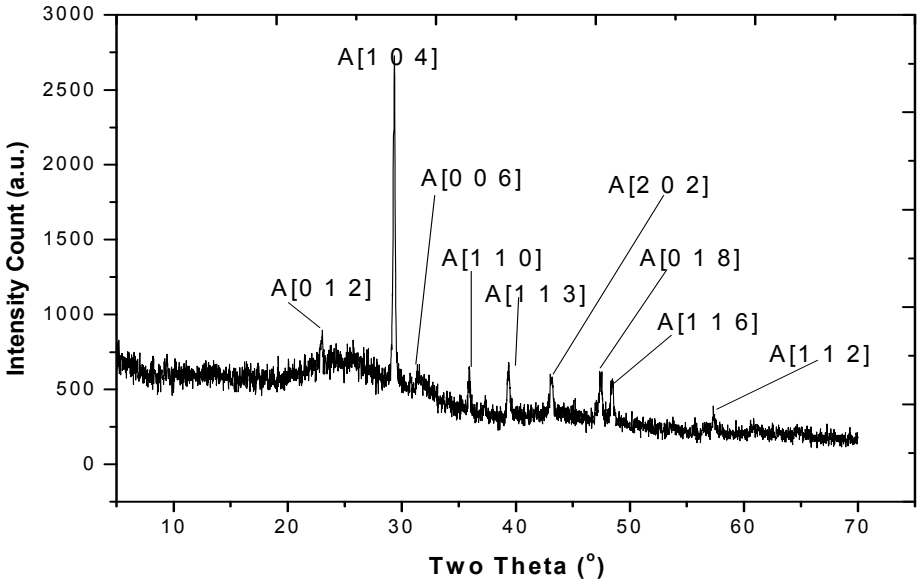

Fig. 2.23. XRD spectra ME-unactivated carbon

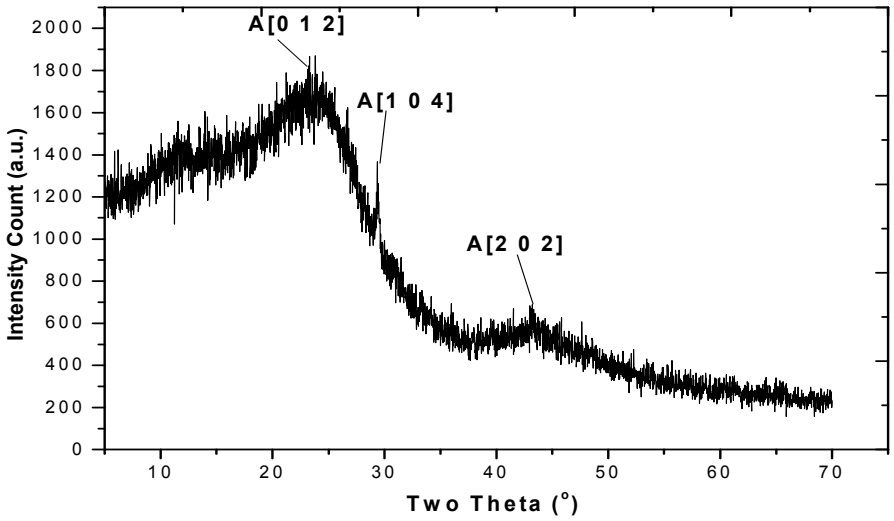

Fig. 2.24. XRD spectra MPAC-H_3PO_4

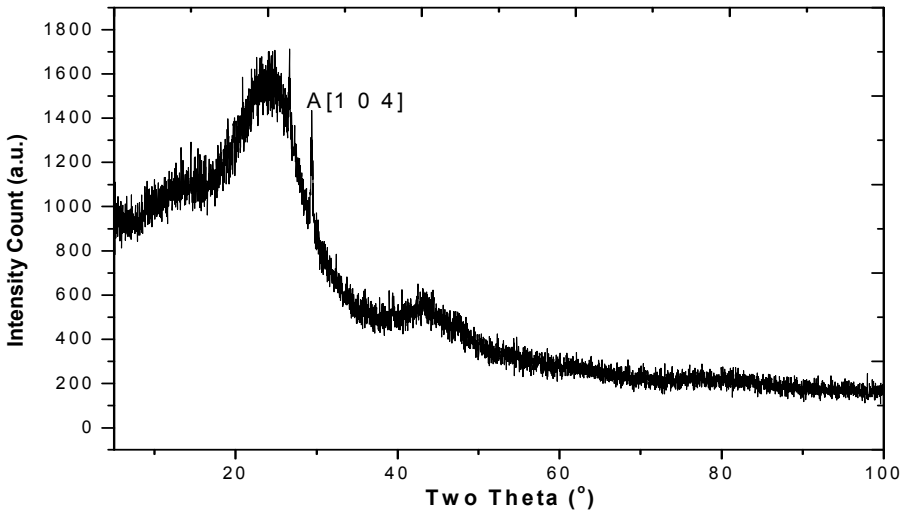

Fig. 2.25. XRD spectra MPAC-HNO_3

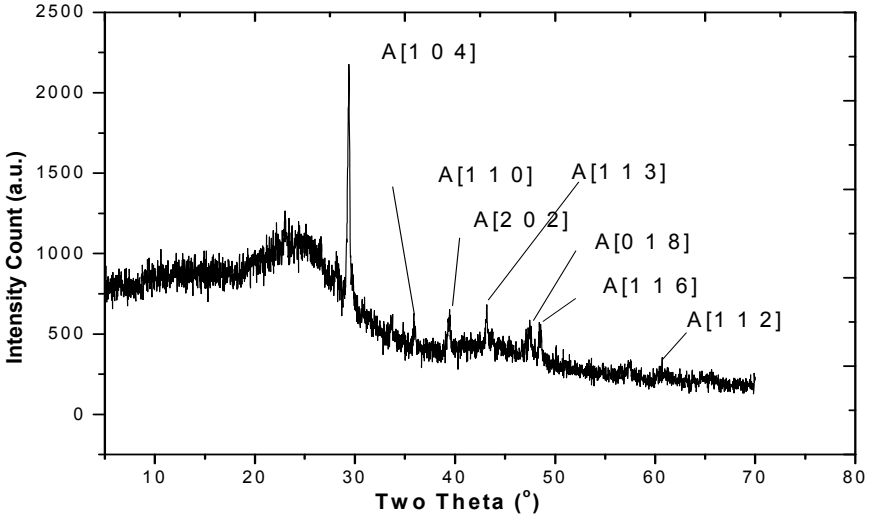

Fig. 2.26. XRD spectra MP-unactivated carbon

Thermal study

The thermograms obtained for different activated carbon samples are given in Fig. 2.27-2.30. From the thermograms it can be observed that initially a weight loss occurs at around 73-80^{o}C, corresponding to a mass lose of 7-8% which may be due to the loss of hygroscopic molecule like water and other volatile matter, impurities. Again a small weight change was observed at around 700-750^{o} C, with a percent mass loss of 13-16% which may be due to the loss of carbon dioxide and carbon monoxide (Bansal and Goyal, 2005). There is a gradual weight loss with increasing temperatures upto 900°C in all the samples, Which might be due to evaluation of CO_2 and CO from surface oxygen groups, which are formed during oxidation with HNO_3 and H_3PO_4 (El-Hendawy 2003; Teng and Suuberg, 1993). At temperature around 1000^{o}C it was observed that a mass of 62-64% was found to remain unburnt. Thus, the synthesized activated carbons show high thermal stability. It can also be observed from the DTA thermograms that the weight loss process for all the carbon samples undergo endothermic process.

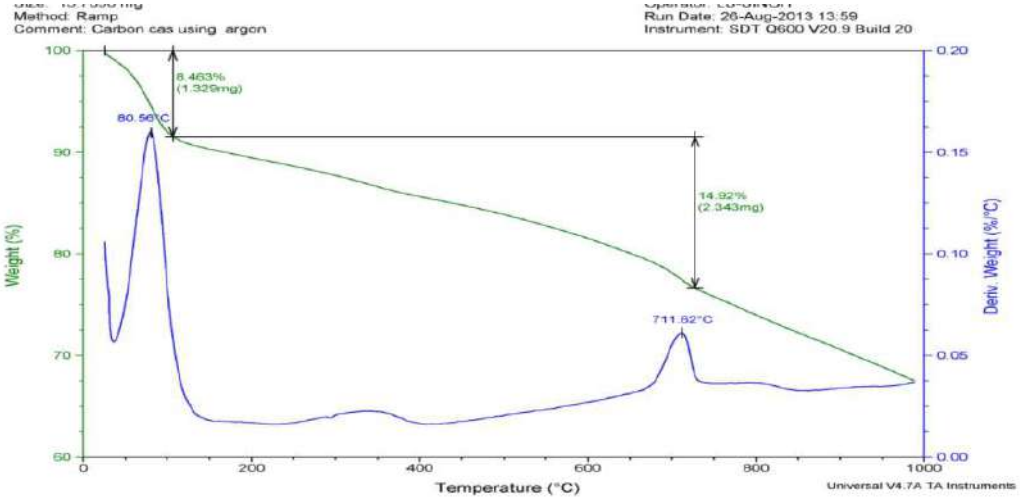

Fig. 2.27. TGA-DTA thermogram of MEAC-HNO_3

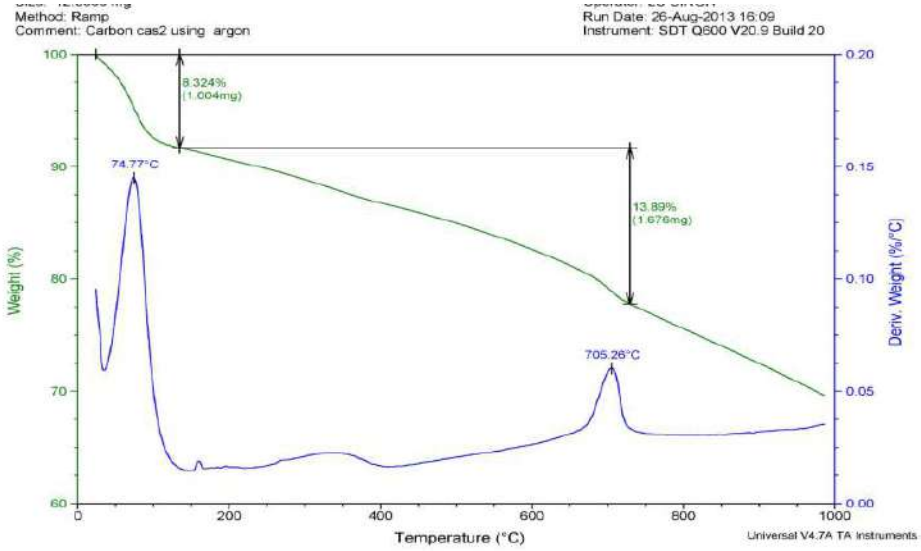

Fig. 2.28. TGA-DTA thermogram of MEAC-H_3PO_4

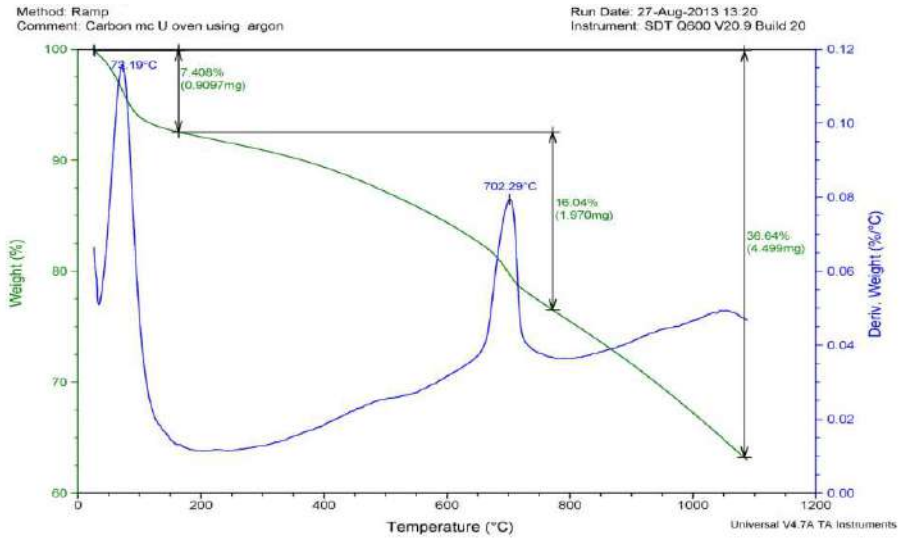

Fig. 2.29. TGA-DTA thermogram of MPAC-HNO_3

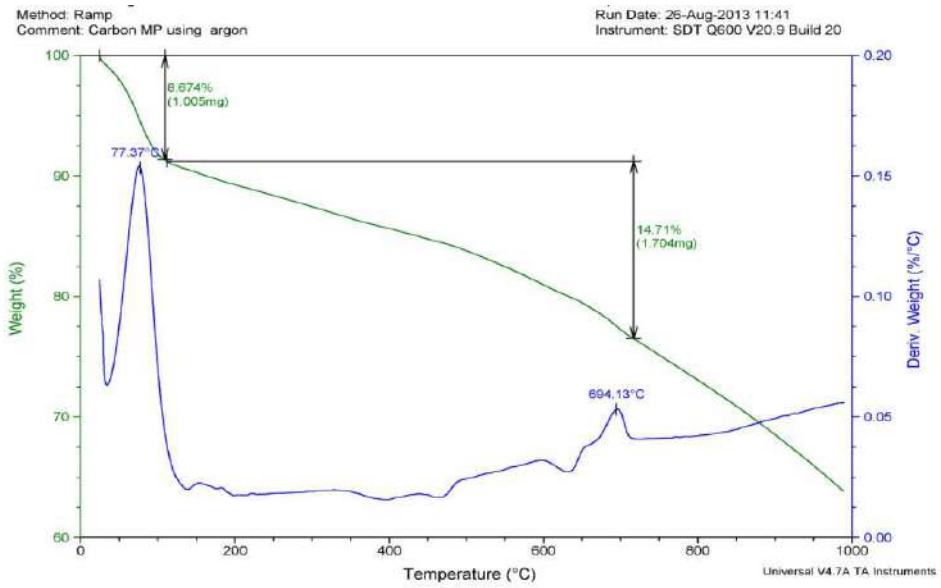

Fig. 2.30. TGA-DTA thermogram of MPAC-H_3PO_4

2.6. Conclusions

The synthesised carbon from *Mucuna pruriens* and *Manihot esculenta* plant namely MPAC-HNO_3, MPAC-H_3PO_4 and MEAC-HNO_3, MEAC-H_3PO_4 were subjected to different physico-chemical studies in order to determine their different properties. The presence of low ash content indicates that the pores within the carbon are free of impurities thus expected to have greater adsorption capacity. The low values of volatile matters reflects that the carbons were well carbonized this leads to formation of stable carbon framework. The values obtained for apparent density and bulk density are also an indicative for high adsorptive properties of the carbon samples. Boehm titration confirms the presence of basic groups is more as compared to acidic group in all the synthesised carbons and the pH values are less than its corresponding pH_{ZPC} value, which points the fact that the surface is positively charged. The spectroscopic data confirms the presence of functional different functional groups like carbonyl, phenolic, hydroxyl etc. All the synthesised carbons show high thermal stability up to 1000^{o}C. XRD analysis reveals the presence of $CaCO_3$ in all the carbon samples. The presence of characteristics graphitic crystallites and loose packing of the aromatic sheets called turbostratic structure were also determined from XRD analysis. Surface morphological studies given by SEM showed the random arrangement of carbon flakes which further confirms the probable turbostratic structure pattern

reflected by XRD. Porous nature and surface ablation caused by HNO_3 and H_3PO_4 treatment is clearly visible in the SEM micrographs.

References

Ahmedna, M., Marshall, W.E., Rao, R.M. (2000). Granular activated carbons from agricultural by –products: preparation properties and application in cane sugar refining. Bulletin of Louisana state University Agricultural centre.

Allem, A. C. (1994). The origin of *Manihot esculenta* Crantz (Euphorbiaceae) Genet. *Resources Crop Evol*, 41:133-150.

Annual book of ASTM standards. (2011). Standard test for pH of activated carbon, ASTM D 3838-05, Philadelphia PA, United State of America.

Annual book of ASTM standards. (2009). Standard test method for water soluble of activated carbon, ASTM D 5029-98, Philadelphia PA, United State of America.

Annual book of ASTM standards. (2004). Standard test method for moisture in activated carbon, ASTM D 2867-95:707-711, Philadelphia PA, United State of America.

Annual book of ASTM standards. (2003). Standard test method for volatile matter content of activated carbon sample, ASTM D 5832-95:921-922, Philadelphia PA, United State of America.

Annual book of ASTM standards. (1999). Standard test method for total ash content of activated carbon, ASTM D 2866-94:708-709, Philadelphia PA, United State of America.

Balakrishnan, N. P., Chakrabarty. T. (2007). The family Euphorbiaceae in India; a synopsis of its profile, taxonomy and bibliography. (Euphorb India), Botanical survey of India.

Bandosz, T.J. (2006). Activated carbon surfaces in environmental redemption. *Interface Sci Technol,*7:3-10.

Bansal, R.C., Goyal, M. (2005). Activated Carbon Adsorption. Boca Raton, FL: CRC Press.

Boehm, H.P. 1994. Some aspects of the surface chemistry of carbon blacks and other carbons. *Carbon*, 32:759-769.

Cao, Q., Chang, K., Lv, Y.K., Bao, W.R. (2006). Process effects on activated carbon with large specific surface area from corn cob. *Bioresour Technol*, 97:110-115.

Daifullah, A. A. M., Yakout, S. M., Elreefy, S. A. (2007). Adsorption of fluoride in aqueous solutions using $KMnO_4$-modified activated carbon derived from steam pyrolysis of rice straw. *J Hazard Mater*, 147:633-643.

Donnet, J.B., Bansal, R.C., Wang, M. (1993). Carbon Black. Second Edition, Marcel Dekker, New York.

Ekpete, O.A., Horsfall, M.Jr. (2011). Preparation and characterization of activated carbon derived from fluted pumpkin stem waste. *Res J Chem Sci*, 1(3):10-17.

El-Hendawy, A.N.A. (2003). Influence of HNO_3 oxidation on the structure and adsorptive properties of corncob-based activated carbon. *Carbon,* 41:713-722.

Friedel, R.A., Carlson, G.L. (1972). Difficult carbonaceous materials and their infra-red and Raman spectra. Reassignments for coal spectra. *Fuel,* 51:194-198.

Gergova, K., Petrov, N., Minkova, V. (1993). A comparison of adsorption characteristics of various activated carbons. *J Chem Tech Biotechnol,* 56(1):77-82.

Girgis, B.S., El-Hendawy, A.N.A. (2002). Porosity development in activated carbons obtained from date pits under chemical activation with phosphoric acid. *Microporous Mesoporous Mater,* 52:105-117.

Garcia, A.B., Martinez-Alonsoa, A., Leon y Leon, C.A., Tascon, J.M.D. (1998). Modification of the surface properties of an activated carbon by oxygen plasma treatment. *Fuel,* 77(6):613-624.

Hirunpraditkoon, S., Srinophakun, P., Sombun, Moore, N.E.J. (2015). Synthesis of activated carbon from jatropha seed coat and application to adsorption of iodine and methylene blue. *Chem Eng Communications,* 202(1):32-47.

Howard, R. (1974-1989). Flora of the lesser Antilles. Flora of Lesser Antilles. U.S national plant germplasm system.

John, C. (2000). Interpretation of infra spectra. A practical approach encyclopaedia ofanalytical chemistry. R.A. Meyers (Ed.) O John Wiley & Sons Ltd. Chichester.

Keay, R. W. J., Hepper, F. N. (1953-1972). Flora of west tropical Africa, ed. 2. *Royal Botanic Gardens.*

Kosmulski M. (2009). pH-dependent surface charging and points of zero charge. IV. Update and new approach. *J colloid Interface Sci,* 337(2):439-48.

Kulkarni, Mahdi,H.H. (2014). Adsorption of carbon dioxide on orange peel and carbon synthesized from orange peel kavita. *Int J Chem Sci*, 12(3):773-784.

Lambert. J.B. (1987). Introduction to organic spectroscopy. Macmillan publication, New York.

Leon y Leon, C.A., Solar, J.M., Calemma, V., Radovic, L.R. (1992).Evidence for the protonation of basal plane sites on carbon. *Carbon,* 30(5):797-811

Madhu, R., Sankar, K.V., Chen, S.M., Selvan, R.K. (2014). Eco-Friendly synthesis of activated carbon from dead mango leaves for the ultrahigh sensitive detection of toxic heavy metal ions and energy storage applications. *Rsc Advances,* 4:1225-1233.

Mahmoudi, K., Hamdi, N., Srasra, E. (2014). Preparation and characterization of activated carbon from date pits by chemical activation with zinc chloride for methyl orange adsorption. *J Mater Environ Sci,* 5(6):1758-1769.

Marsh, H., Rodriguez-Reinoso, F. (2006). Activated carbon. Publisher: Elsevier Science & Technology Books.

Menendez-Diaz, J.A., Martln-Gullonb, I. (2006). In: Activated carbon surfaces in environmental remediation, *Interface Sci Technol*, 7.

Okieimen F.E., Okiemen C.O., Wuana R.A. (2007). Preparation and characterization of activated carbon from rice husks. *J Chem Soc*, 32:126-136.

Peng, J., Zhang, L., Yang, K., Xia, H., Zhang, S., Guo, S.H. (2008). Preparation of activated carbon from coconut shell chars in pilot-scale microwave heating equipment at 60 kW. *Waste Manag,* 29:756-760.

Rao, M.N., Chakrapani, Ch, Reddy, B.V.R., Babu,Ch. S., Rao, Y .H., Rao, K.S, Rajesh, K. (2011a). Preparation of activated kaza's carbon from bio-materials and their characterization. *Int J Appl Bio Pharm Technol,* 2(3):610-618.

Rao, M.M., Reddy, B. V. R., Babu, Ch. S., Chakrapani, Ch., Haritha, P., Emmanuel, K. A., Rao, K.S. (2011). Sorption studies of rhodamineb dye using newly prepared kaza's carbons. *Der Pharma Chemica*, 3(6):513-520.

Riaz-Ahamed, K., Chandrasekaran, A.T., Kumar, A. (2013). Characterization of activated carbon prepared from albizia lebbeck by physical activation. *Int J interdisciplinary Res inno,* 1(1):26-31.

Rogers, D. J., Appan S. G. (1973). *Manihot*, *Manihotoides* (Euphorbiaceae) Fl. *Neotrop Monogr*, 13:25-34.

Rouquerol, F., Rouquerol, J., Sing, K. (1999). Adsorption by powders & porous solids. Academic Press, London.

Salman, J.M. (2014). Optimization of preparation conditions for activated carbon from palm oil fronds using response surface methodology on removal of pesticides from aqueous solution. *Arabian J Chem.*7(1):101–108.

Sarrano, V.G., Correa, E.M.C., Gonzalez, M.C.F., Franco, M.F.A., Garcia, A.M. (2005). Preparation of activated carbons from walnut wood: a study of microporosity and fractal dimension. *Smart Mater Struct*, 14:363-368.

Scherrer, P. (1918). The Scherrer equation versus the 'Scherrer–Gottingen equation'. *Nachr Ges Wiss Göttingen,* 26:98-100.

Shamsuddin, M.S., Yusoff, N.R.N., Sulaiman, M.A. (2016). Synthesis and characterization of activated carbon produced from kenaf core fiber using H_3PO_4 activation. *Procedia Chem,* 19:558-565.

Sing, K. (2001). The use of nitrogen adsorption for the characterization of porous materials. *Colloid Surf A: Physicochem Eng Aspects,* 187(188):3-9.

Srisa-ard, S. (2014). Preparation of activated carbon from sindora siamensis seed and canarium sublatum guillaumin fruit for methylene blue adsorption, *Int Trans J Eng Manag Appl Sci Tech,* 5(4):235-245.

Socrates, G. (1994). Infra characteristic group frequencies. New York, John Wiley.

Sugunadevi, S.R., Sathishkumar, M., Shanthi, K., Kadirvelu, K., Pattabhi, S. (2002). Removal of direct T-blue R from aqueous solution onto carbonised sugarcane baggase waste. *Indian J Environ Protection*, 22:500-505.

Supriya, S., Palanisamy, P.N., Shanthi, P. (2014). Preparation and characterization of activated carbon from casuarina for the removal of dyes from textile wastewater. *Int J Chemtech Res,* 6(7):3635-3641.

Teng, H. and Suuberg, E.M. (1993). Chemisorption of nitric oxide sorption. *J Phys Chem*, 97: 478-483.

Test method of activated carbon. (1986). European council for chemical manufacturers federations. EFIC, Press.

Verla, A.W., Horsfall (Jnr), M., Verla, E.N., Spiff, A.I., Ekpete, O.A. (2012). Preparation and characterization of activated carbon from fluted pumpkin (*Telfairia Occidentalis* Hook.F) Seed Shell. *Asian J Natur Appl Sci*, 1:39-50.

Viswanathan, B., Neel P. I., Varadarajan, T. K. (2009). Methods of activation and specific applications of carbon materials. National centre for catalysis research department of chemistry , IIT-Madras.

Wilmot-Dear, C. M. (1984). A revision of *Mucuna* (Leguminosae-Phaseoleae) in China and Japan Kew Bull. 39:61.

CHAPTER-3

REMOVAL OF FLUORIDE FROM AQUEOUS SOLUTION BY ACTIVATED CARBON

This chapter presents the application of activated carbons in removal of fluoride from aqueous solution. Batch mode of adsorption study was conducted to obtain optimum condition of adsorbent dosage, contact time, fluoride concentration, pH and contact time. Fluoride adsorption isotherm models were studied to evaluate the suitability of different adsorption model like Langmuir, Freundlich and Temkin. Four simplified kinetics models; pseudo first-order, pseudo second-order, intraparticle diffusion and Elovich have been discussed to identify the rate and kinetics of adsorption of fluoride by different activated carbons. Thermodynamic parameters involved during fluoride adsorption are also presented in this chapter.

3.1. Introduction

Fluorine is the lightest member of the halogen group and is one of the most reactive of all chemical elements (Hem 1989) and therefore, it is found as fluoride in the environment in combination with other elements, except oxygen and noble gases. Fluorine in the environment represent about 0.06–0.09 per cent of the earth's crust. The average crustal abundance is reported to be 300 mg kg^{-1} (Tebutt 1983). Fluorine has a strong tendency to acquire a negative charge, and in solution forms F^- ions. Fluoride ions have the same charge and nearly the same radius as hydroxide ions and may replace each other in mineral structures (Hem 1985). Fluoride thus forms mineral complexes with a number of cations and some fairly common mineral species of low solubility contain fluoride. Fluorides are found at significant levels in a wide variety of minerals, including fluorspar, rock phosphate, cryolite, apatite, mica, hornblende and others (Murray 1986). Fluorite (CaF_2) is a common fluoride mineral of low solubility occurring in both igneous and sedimentary rocks and thus, all the water bodies contain certain amount of fluoride released from such different sources. Presences of fluoride in low concentration possess certain health benefits but exposure to high concentration leads to serious health hazards over time. Thus fluoride pollution in water is a serious issue which needs to be controlled and addressed in a more environmentally benign manner.

Environmental occurrence

Fluoride is found in all natural waters at some concentration. Sea water typically contains about 1 mg l^{-1} while rivers and lakes generally exhibit concentrations less than 0.5 mg l^{-1} (WHO 2001). Water with high fluoride concentrations occur in large and extensive geographical belts associated with: sediments of marine origin in mountainous areas, volcanic rocks and granitic and gneissic rocks.

Toxic effects of high fluoride concentration

Fluoride has beneficial effects on teeth at low concentrations in drinking-water, but excessive exposure to fluoride in drinking-water, or in combination with exposure to fluoride from other sources, can give rise to a number of adverse effects. These range from mild dental fluorosis to crippling fluorosis and cancer. Prolong exposure to high concentration of fluoride may leads to other possible adverse outcomes such as change in DNA structure (Tsutsui 1984; Wang et al., 2004) and lesion on endocrine

glands, thyroid, liver and other organs (Lounici et al., 1997; Hichour 2000). Long-term exposure to high levels of fluoride leads to a disease called fluorosis, a chronic disease which has a serious affect on health in many parts of the world where drinking water contains more than 1–1.5 mg L^{-1} of fluoride. Occupational hazards leading to fluorosis owing to prolong exposure, such as in aluminum smelting and in glass industries and the manufacture of fertilizers, is reported (Susheela 1999; WHO 1984). Genu valgum (knock–knee syndrome) a type of the severe form of skeletal fluorosis has been reported from certain endemic areas including India (Krishnamachari and Krishnaswamy, 1973). Young people were found to be the chief victims of this syndrome. Fluorosis leads to biochemical changes in the composition of bone, urine, and plasma, and some hormonal changes (Das 1996). Fluoride also affects collagen synthesis and bone mineralization when present in higher concentration (Krishnamachari 1986; Harrison et al., 1990).

Fluoride has the ability to cross the cell membrane and enter soft tissues which results in impairment of soft-tissue function, and it has been demonstrated in fluoride-intoxicated animals (Vani and Reddy, 2000). Fluoride affects the brain and muscle by inhibiting some enzymes associated with energy production and transfer, membrane transport, and synaptic transmission (Vani and Reddy, 2000). Thus, in view of the above mentioned health hazards related to fluoride exposure, it is essential to reduce the concentration of fluoride to permissible level from drinking water by adopting an efficient environmentally benign method.

Fluoride concentration worldwide

Groundwater with high fluoride concentration occurs in many areas of the world including large parts of Africa, China, the Eastern Mediterranean and Southern Asia like India and Sri Lanka (WHO 2001). The distribution of fluoride worldwide is shown in Fig. 3.1.

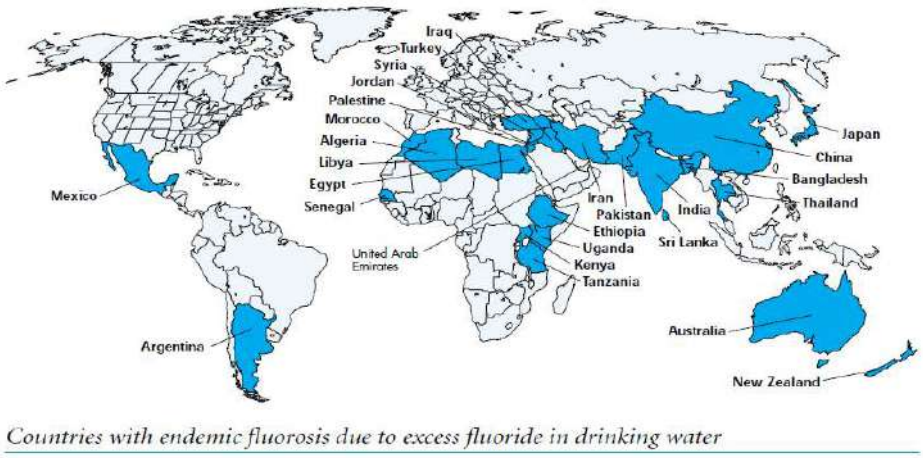

Fig. 3.1. Fluoride distribution worldwide (WHO)

Fluorosis is one of the manifestations of chronic poisoning from long-term exposure to high levels of fluoride. In India, endemic fluorosis remains a challenge and extensively studied national health problem. In 1991, 13 of India's 32 states and territories were reported to have naturally high concentrations of fluoride in water (Mangla 1991), but this had risen to 17 by 1999 (UNICEF 1999). The most seriously affected areas are Andhra Pradesh, Punjab, Haryana, Rajasthan, Gujarat, Tamil Nadu and Uttar Pradesh (Teotia et al., 1994). The high concentrations in groundwater are a result of dissolution of fluorite, apatite and topaz from the local bedrock, and Handa (1975) noted the general negative correlation between fluoride and calcium concentrations in Indian groundwater. In these states, 10 to 25 per cent of the rural population has been estimated to be at risk, and perhaps a total of 60–70 million people in India as a whole may be considered to be at risk (UNICEF, 1999).

3.2. Various defluoridation techniques

Many defluoridation techniques have been developed over the years in an effort to reduce the serious health hazards due to exposure to high level of fluoride concentration in drinking water. Lime has been used traditionally to reduce fluoride concentration from drinking water where fluoride gets precipitated as fluorite (Sollo et al., 1978). The precipitation and coagulation processes with iron (III) (Hsu 1976), activated alumina (Ghorai and Pant, 2005), alum sludge (Sujana et al., 1998) and calcium (Huang and Liu, 1999) have been widely investigated. Various techniques have been used for the removal of excess fluoride from water like adsorption (Chakrapani et al., 2010), ion exchange (Popat et al., 1994), precipitation (Bulusu et al., 1979), electrochemical process (Daifullah et al., 2007), Donnan dialysis (Kumar

and Kirthika, 2009; Jibril et al., 2013), electrodialysis, reverse osmosis (Yupeng et al., 2002). These techniques used have different requirements like high maintenance, continuous power supply, generation of additional waste/ by products, not very cost effective etc. which makes their utility somewhat limited in certain cases.

Ultimately an alternate method is desired, and among the different processes available, adsorption technique seems to be a more attractive method in terms of efficiency, durability, cost effective, simplicity of design and operation. Various materials have been used to test their efficiency in fluoride removal, such as amorphous alumina (Li et al., 2001), calcite (Yang et al., 1999), clay (Mahramanlioglu et al., 2002), zeolite (Onyango et al., 2004), activated carbon (Rao 2008), bleaching earth (Mahramanlioglu et al., 2002) and red mud (Cengeloglu et al., 2002). But some adsorbents are not capable to remove fluoride from water at low concentration (2 mg l^{-1}) (Majima and Takatsuki, 1987; Wang and Reardon, 2001) whereas other only work at extreme pH (pH≤3.0) (Suzuki et al., 1990) which might be not feasible to be applicable in natural conditions. Various defluoridation techniques and the materials used are summarized in Table 3.1.

Table 3.1. Different defluoridation techniques and the materials used (Renuka and Pushpanjali, 2013)

Carbon materials, Activated Alumina, Magnesia, Tricalcium phosphate, Calcite, Hydroxy apatite, Wood, Lignite, Activated char coal, Fish bone char, Processed bone, Nut shells, Avaram bark, Paddy husk, Coffee husk, Tea waste, Jute waste, Coir pitch, Fly ash, Bauxite, Serpentine	Ion-exchange Anion exchange resins: NCL poly anion resin, Tulsion A27, Lewatit-MIH-59, Amberlite IRA-400, Deacedodite FF-IP, Waso resin-14, Polystyrene. Cation exchange resins: Defluoron-1, Defluoron- 2, Carbion.	Precipitation Lime, Alum, Lime & Alum (Nalgonda technique), Alum flock blanket method, Poly Aluminium Chloride (PAC), Poly Aluminium Hydroxy Sulphate (PAHS), Brushite.	Others: Electrochemical method (Aluminium electrode), Electro dialysis, Electrolysis, Reverse Osmosis.

For this present study removal of fluoride from water was done by adsorption methods and activated carbons were used as adsorbent. The synthesis of activated

carbons and their characterisation are already discussed in Chapter-2 in details. Once the adsorbent were synthesised, the following experimental procedure were followed.

3.3. Materials and method

For this adsorption study, a standard stock solution of fluoride was first prepared and the removal of fluoride solution by activated carbon was studied by batch mode of adsorption. The details of the preparation of the stock solution and procedure for batch mode of adsorption study are given below.

Reagents and Apparatus

For conducting the experiments, different reagents were prepared using chemicals of analytical reagent grade.

Preparation of fluoride stock solution

1000 mg L^{-1} of fluoride solution was prepared by dissolving 2.178 g of NaF (Merck) in 1000 ml of double distilled water in a 1000 ml volumetric flask. The solution was further diluted to 500 and to 100 mg L^{-1} of fluoride solution. Different test solutions ranging from 1-10 mg L^{-1} fluoride solution were prepared from 100 mg L^{-1} fluoride solution.

Fluoride adsorption study by batch mode

Batch mode adsorption is the basis of all adsorption studies as it provides information about the different parameters that control any adsorption process. In this method different batches of samples are assembled and the changes that are undergone when exposed to different factors that may affect the adsorption process are investigated. Through this method it is possible to find out the optimum condition for the reaction to be carried out effectively. Thus, effect of temperature, contact time, adsorbent dosage, pH and concentration are studied by this method and a suitable condition is established from the different experimental data which enables to fix the experimentally obtained optimum condition that can be used to perform further experiments in future.

For this study a solution of known concentration of fluoride was prepared i.e. 5 mg L^{-1} fluoride solution with 100 ml of test solution. Studies on effect of adsorbent dosage was carried out using .25g -1.5 g and the time of contact was fixed for 80 minutes at 25±1^{o}C, effect of contact time was carried out by varying the time from 5-240 minutes, effect of temperature was carried out by varying the temperature from 298K-

313K, effect of pH was carried out by adjusting the pH of the fluoride solution ranging from 1-10, effect of concentration was carried out by varying the concentration of the test solution from 1-15 mg L^{-1}.

To study the various control parameters, the beaker along with test solution and adsorbent were shaken in a horizontal shaker at 242 rpm. When the desired contact time was reached, the conical flasks were retrieved from the shaker and the flask containing adsorbent and adsorbate was allowed to settle for sometime, which was then filtered using Whatman no. 42 filter paper and the filtrate was analysed for residual fluoride concentration by using Ion Selective Electrode (Thermo Scientific-Orion 4 star, pH/ISE).The percentage removal of the fluoride and the amount of fluoride adsorbed were calculated using the following equation (Jibril et al., 2013).

$$\% \, removal = \frac{(C_i - C_e)}{C_i} \times 100 \qquad \text{.....(34)}$$

$$Amount\ adsorbed(q_e) = \frac{(C_i - C_e)}{W} \times V \qquad \text{..... (35)}$$

Where C_i = initial concentration of fluoride solution in mg L^{-1},

C_e = equilibrium concentration of fluoride solution in mg L^{-1}

W = mass of the adsorbent in grams (g)

V = Volume of test solution in litre (L)

3.4. Adsorbent regeneration study

In order to determine the regeneration capacity of the different adsorbents after fluoride adsorption, 50 ml of 5% of NaOH was poured into a polypropylene beaker and 5 g of adsorbent were added into the beaker containing NaOH solution. The mixture was agitated at 242 rpm using magnetic stirrer for 1 hour. The mixture was filtered using Watman. No. 42 filter paper and the adsorbent so obtained were washed with double distilled water to remove excess of base from the adsorbent surface (in case present). It was than dried in the oven at 110^{o}C for 2 hours. The adsorbents were kept in vacuum desiccators for further fluoride removal study.

3.5. Results and discussion

In this part of the thesis, results on adsorption by changing the experimental condition are discussed. Subsequently applicability of different adsorption models is analysed.

Kinetics model and thermodynamic parameters on fluoride adsorption are also discussed in this section of the thesis.

Effect of adsorbent dosage

In order to find out the optimum adsorbent dosage for fluoride adsorption a fixed volume of 5 mg L^{-1} fluoride solution was taken and adsorption were studied by changing the adsorbent dosage in the range of 0.25g-1.5g. It was observed that there was an appreciable increase of fluoride adsorption by the carbon when the adsorbent dosage of the carbon increases from 0.25g to 1g (Table 3.2), because of the availability of sufficient surface area. The fluoride ion removal was maximum when the adsorbent dosage was above 1 g after which a saturation point is reached. Further increase in the adsorbent dosage does not produce any significant changes in the fluoride removal. Thus from the observed value, the optimum dosage was fixed at 1 g for the entire adsorbent sample, as the removal percentage and q_e value show good correlation. The removal percentage of fluoride is shown in Fig.3.1.

Table 3.2. Effect of adsorbent dosage on 5 mg L^{-1} fluoride solution

Adsorbent dosage (g)	MPAC-HNO_3	MPAC-H_3PO_4	MEAC-HNO_3	MEAC-H_3PO_4
	Removal %			
0.25	79.32	77.61	74.28	75.43
0.5	94.66	93.83	88.22	85.86
0.75	97.51	96.63	94.3	92.71
1	98.21	97.75	96.25	95.43
1.25	98.93	98.14	97.65	96.76
1.5	99.31	98.47	98.11	97.23

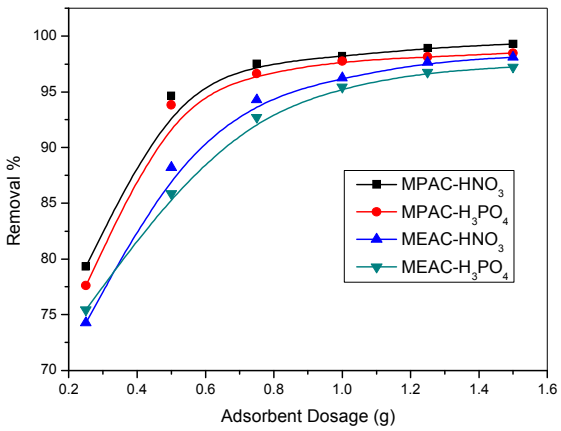

Fig. 3.2. Effect of adsorbent dosage on 5 mg L^{-1} fluoride solution

Effect of contact time

Fluoride adsorption capacity was measured at different contact time in the range of 5-240 minutes keeping the amount of adsorbent and volume of the fluoride solution fixed. In this study 1 g of adsorbent and 5 mg L^{-1} fluoride solution were used. Initially for all the carbon adsorbents, the removal percentage of fluoride increase rapidly with increasing time. This may be because of the presence of large surface area of the carbon during the initial stages of the adsorption. Significant adsorption of fluoride takes place after a time of 60 minutes and maximum adsorption of fluoride take place at around 180 minutes. From the Table 3.3, it can be observed that the adsorption of fluoride increases with the increase in contact time but it remain almost constant when equilibrium is attained at around 80 min. Thus the contact time was set at 80 minutes for further experiment. Among the four synthesised bio-adsorbent MPAC-HNO_3 show maximum removal percentage followed by MPAC-H_3PO_4, MEAC-H_3PO_4 and MEAC-HNO_3 respectively, suggesting that the oxidation by nitric acid and phosphoric acid produces adsorbent with different adsorption capacity. A plot of removal percentage vs time is shown in Fig. 3.3.

Table 3.3. Effect of contact time on different carbon samples

Time	MPAC-HNO_3	MPAC-H_3PO_4	MEAC-HNO_3	MEAC-H_3PO_4
5	48.0	59.8	60.4	44.0
10	51.0	63.4	70.0	49.8
20	68.0	68.6	72.8	65.4
40	82.8	75.8	80.0	82.8
60	91.8	83.4	83.7	87.8
80	93.5	85.2	85.3	91.1
100	94.2	88.5	88.7	94.2
120	94.4	89.0	89.0	94.7
180	97.2	92.2	93.9	97.2
240	97.2	97.5	95.9	97.2

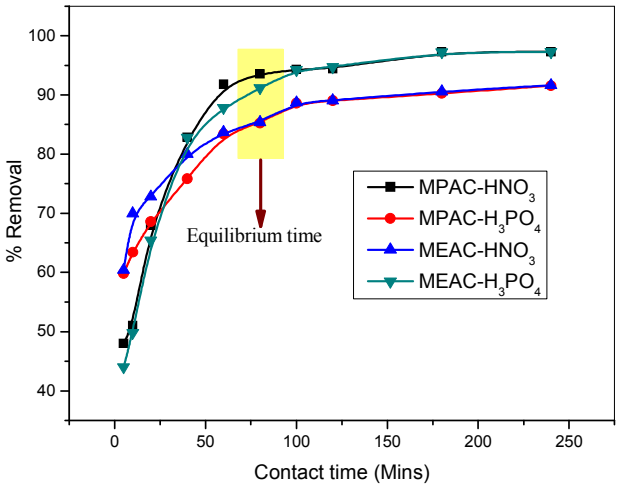

Fig. 3.3. Effect of contact time on the removal of fluoride on different activated carbon samples

Effect of pH

Surface binding sites of the adsorbents as well as the aqueous chemistry are affected by the pH of the solute (Zahra et al., 2013, Xu et al., 2008).The effect of pH on adsorption of fluoride ion was studied in the pH range of 1 to 10, keeping other parameters constant like 1 g of adsorbent and 100ml of 5 mg L^{-1} of fluoride solution with 80 minutes of contact time. Adsorption of fluoride ion was found to be more significant at pH below 5 and decreases considerably when the pH was raised above 9 (Table 3.4). This suggests the fact that the fluoride adsorption is more favourable at lower pH, this could be because of the presence of more H^+ ions at lower pH that facilitate the interaction between the oxide surface and fluoride. However, the lower adsorption capacity at higher pH may be because of the development of more negatively charge at the surface of the activated carbon which causes repulsion for the available adsorption sites. Decrease in the fluoride removal at higher pH also may be attributed to competition between OH^- and F^- for adsorption on the carbon surface. The higher removal percentage was obtained at lower pH value suggesting the fact that synthesised adsorbent has greater affinity towards fluoride adsorption at lower pH and hence can be used comfortably in fluoride removal in acidic condition. The adsorbents also show high fluoride ion intake ability even at neutral medium indicating that the synthesised adsorbent could well be used for neutral pH condition

like in drinking water treatment. The removal percentage of fluoride against different pH is shown in Fig. 3.4.

Table 3.4. Effect of pH on different carbon sample

pH	MPAC-HNO_3	MPAC-H_3PO_4	MEAC-HNO_3	MEAC-H_3PO_4
1	99.46	99.38	99.42	99.24
2	99.34	99.26	99.28	99.16
3	99.24	99.20	99.18	99.06
4	99.14	99.04	99.02	98.82
5	98.96	98.86	98.94	98.74
6	98.88	98.80	98.90	98.56
7	98.64	98.62	98.74	98.44
8	97.26	97.16	97.12	98.18
9	96.02	96.06	96.28	96.16
10	95.84	95.64	95.82	95.34

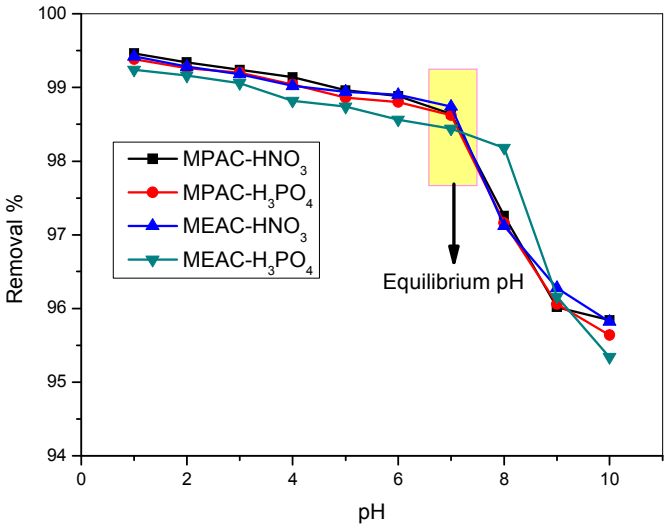

Fig. 3.4. Effect of pH on different carbon samples on the removal of fluoride

Effect of concentration

The effect of the initial concentration of fluoride adsorption was evaluated by varying the concentration of the fluoride solution in the range of 1-15 mg L^{-1} by keeping the amount of adsorbent dosage 1 g. Initially at 1 mg L^{-1} the percentage uptake of fluoride ion by all the carbon samples was around 99%. But as the concentration increase the percentage uptake of fluoride ion decreases gradually and the decrease is prominent when the concentration of the fluoride solution is above 10 mg L^{-1}. Similar trend was

observed for all the carbon samples (Table 3.5), indicating that the percentage uptake of fluoride by the adsorbent is found to be optimum at 5 mg L^{-1} since the q_e value and removal percentage at 5 mg L^{-1} fluoride solution show good correlation. The tendency to higher adsorption of fluoride ion at lower concentration is attributed to the presence of excess surface active site as compared to fluoride ion. But as the concentration increase gradually, the uptake of fluoride ions decreases which could be explained by the fact that the more fluoride ions tend to interact and occupy the limited available surface site. But it is interesting to note that as the concentration of the fluoride solution increase there is a decrease in the adsorption of fluoride, whereas the q_e value increases. This is because of the availability of more fluoride ion at higher concentration which gets adsorbed by the adsorbent. The removal percentage of fluoride at different concentration is shown in Fig. 3.5.

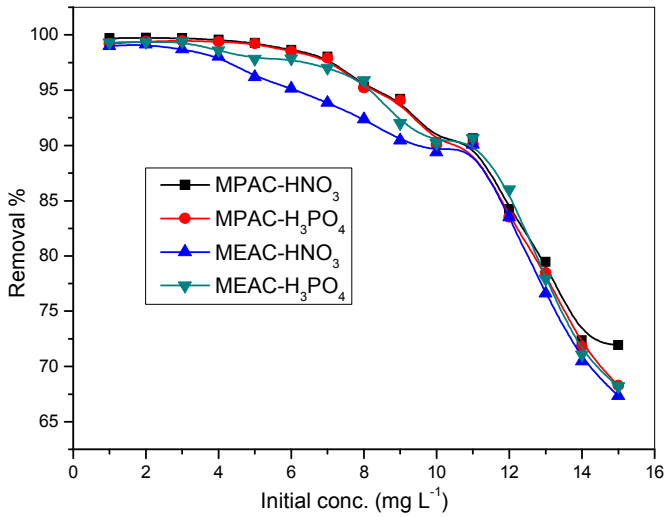

Fig. 3.5. Effect of concentration on the removal of fluoride

Table 3.5. Effect of concentration on different carbon sample

	MPAC-HNO_3			MPAC-H_3PO_4			MEAC-HNO_3			MEAC-H_3PO_4		
Conc.	C_e	q_e	R%	C_e	q_e	R%	C_e	q_e	R%	C_e	q_e	R %
1	0.003	0.99	99.70	0.008	0.99	99.20	0.010	0.99	99.00	0.007	0.993	99.30
2	0.005	0.19	99.75	0.012	0.19	99.40	0.017	0.19	99.15	0.013	0.198	99.35
3	0.009	0.29	99.70	0.016	0.29	99.46	0.039	0.29	98.70	0.018	0.298	99.40
4	0.018	0.39	99.55	0.025	0.39	99.37	0.078	0.39	98.05	0.057	0.394	98.57
5	0.037	0.49	99.26	0.039	0.49	99.22	0.190	0.48	96.20	0.109	0.489	97.82
6	0.082	0.59	98.63	0.090	0.59	98.50	0.290	0.57	95.16	0.130	0.587	97.83
7	0.138	0.68	98.02	0.147	0.68	97.90	0.430	0.65	93.85	0.210	0.679	97.00
8	0.377	0.76	95.28	0.383	0.76	95.21	0.610	0.73	92.37	0.330	0.767	95.87
9	0.522	0.84	94.20	0.533	0.84	94.07	0.860	0.81	90.44	0.720	0.828	92.00
10	0.973	0.90	90.27	0.996	0.90	90.04	1.060	0.89	89.40	0.980	0.902	90.20
11	1.030	0.99	90.63	1.090	0.99	90.09	1.090	0.99	90.09	1.030	0.997	90.63
12	1.890	1.01	84.25	1.980	1.00	83.50	1.980	1.00	83.50	1.680	1.032	86.00
13	2.670	1.03	79.46	2.800	1.02	78.46	3.040	0.99	76.61	2.870	1.013	77.92
14	3.870	1.01	72.35	3.950	1.00	71.78	4.130	0.98	70.50	4.050	0.995	71.07
15	4.210	1.07	71.93	4.760	1.02	68.26	4.900	1.01	67.30	4.770	1.023	68.20

3.5.1. Adsorption isotherm study for fluoride adsorption

In order to evaluate the adsorption capacity of fluoride by activated carbon different isotherm models were study like Langmuir, Freundlich and Temkin adsorption isotherm models which are discussed below.

Langmuir adsorption isotherm

The adsorption of fluoride onto the different chemically modified activated carbons is obtained by plotting C_e/q_e vs C_e (From Eq. (2) of Chapter-1) and is shown in Fig 3.6-3.7. The Langmuir isotherm follows a monolayer surface due to availability of finite number of identical binding sites (Dawodu et al., 2012; Boparai et al., 2010). The different experimental data obtained for Langmuir isotherm are shown in Table 3.6. From the isotherm, the value of Langmuir constant (K_L) for different activated carbon samples were found to be 1.307, 1.157, 0.958 and 0,810 for MPAC-HNO_3, MPAC-H_3PO_4, MEAC-HNO_3 and MEAC-H_3PO_4 respectively. The theoretical adsorption monolayer capacity q_m (a_L/K_L) was found to be 1.017, 1.005, 1.725 and 1.568 for MPAC-HNO_3, MPAC-H_3PO_4, MEAC-HNO_3 and MEAC-H_3PO_4 carbons respectively. The dimensionless constant separation factor (R_L), which classify the isotherm shape and indicates whether the adsorption is favorable or unfavorable has been calculated from Eq. (3) of chapter-1. Adsorption is considered favorable when

R_L value lies in the range of 0-1. In this case the values obtained were all in the range of 0-1, i.e., 0.086, 0.087, 0.083 and 0.554 for MPAC-HNO_3, MPAC-H_3PO_4, MEAC-HNO_3 and MEAC-H_3PO_4 respectively, indicating a favorable condition for adsorption. Thus, it was experimentally found that the adsorption of fluoride was very favorable on all the carbon adsorbents. It was also observed that the R_L for all the activated carbon tends more towards zero rather than unity which suggest completely ideal irreversible case. From the plot a good linear correlation co-efficient (R^2) value of 0.996, 0.997, 0.993 and 0.986 were obtained for MPAC-HNO_3, MPAC-H_3PO_4, MEAC-HNO_3 and MEAC-H_3PO_4 activated carbon respectively. All the above experimental results suggest that Langmuir adsorption of fluoride is favored. Thus it may be assumed that adsorption took place as monolayer coverage on the surface of the adsorbent containing a finite number of adsorption sites of uniform strategies of adsorption with no transmigration of adsorbate in the plane. It also indicates the homogeneous distribution of active sites on the adsorbent, since the Langmuir equation assumes that the surface is homogeneous.

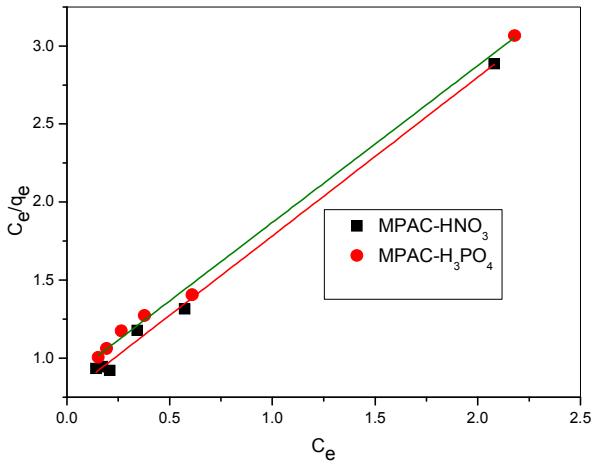

Fig. 3.6. Langmuir isotherm for fluoride adsorption by MPAC

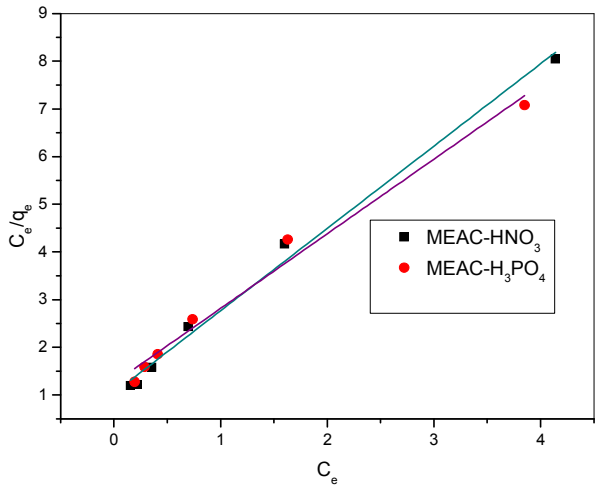

Fig. 3.7. Langmuir isotherm for fluoride adsorption by MEAC

Table 3.6. Different parameters of Langmuir adsorption isotherm for fluoride removal.

Adsorbent	R^2	a_L/k_L	K_L	a_L	R_L	$q_{e(exp)}$	$q_{e(cal)}$	χ^2
MAPC-HNO_3	0.996	1.017	1.307	1.329	0.086	0.721	0.722	0.00001
MAPC-H_3PO_4	0.997	1.005	1.157	1.162	0.087	0.711	0.777	0.0061
MEAC -HNO_3	0.993	1.725	0.958	1.653	0.083	0.515	0.505	0.0019
MEAC-H_3PO_4	0.986	1.568	0.810	1.270	0.086	0.544	0.529	0.0004

Note* unit of q_e= (mg g^{-1}). The values for χ^2 were taken up to 5th decimal for first data point and up to 4th decimal for the remaining data point.

Freundlich adsorption isotherm

A Freundlich plot was obtained by plotting $logC_e$ vs $log(X/M)$ and is shown in Fig.3.8-3.9. The plot gives the value of K and $1/n$ which were obtained from the slope and the intercept of the linear plots (Eq. (40 of chapter-1). The K value are found to be1.367, 1.234, 0.992 and 0.526 and $1/n$ value were found to be 1.230, 1.269, 0.992 and 1.008 for MPAC-HNO_3, MPAC-H_3PO_4, MEAC-HNO_3 and MEAC-H_3PO_4 respectively. Freundlich isotherm parameters for the fluoride adsorption on the activated carbons are given in Table 3.7. In this isotherm, the value of correlation coefficients R^2 was found to be 0.981 and 0.983, for MPAC-HNO_3 and MPAC-H_3PO_4, respectively, which is lower than the Langmuir value indicating the fact that experimental data in the present case is comparatively less fitted than the Langmuir model. However, for MEAC-HNO_3 and MEAC-H_3PO_4 the value for R^2 was found to be 0.995 and 0.996 which was higher than the values obtained from Langmuir

isotherm suggesting that Freundlich isotherm fit better for MEAC-HNO_3 and MEAC-H_3PO_4 adsorbent. But the value of $q_{e(cal)}$ from Freundlich isotherm is not close to the values of $q_{e(exp)}$ obtained experimentally this suggest the fact that adsorption of fluoride on carbon did not fit closely for Freundlich isotherm as it was for Langmuir.

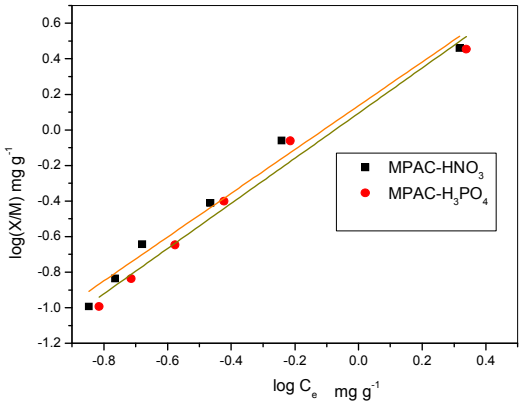

Fig. 3.8. Freundlich adsorption isotherm for fluoride adsorption using MPAC

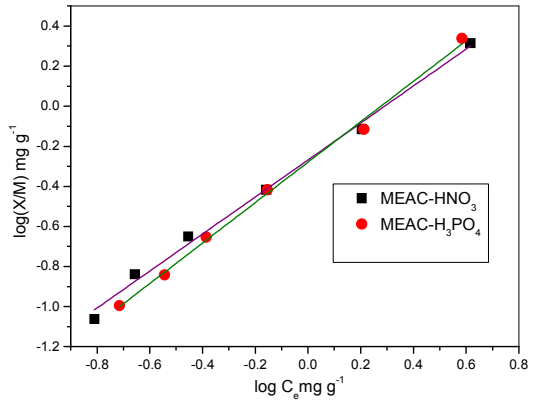

Fig. 3.9. Freundlich adsorption isotherm for fluoride adsorption using MEAC

Table 3.7. Freundlich isotherm for fluoride adsorption

Adsorbent	*logK*	*1/n*	*K*	*n*	$q_{e(exp)}$	$q_{e(Cal)}$	R^2	χ^2
MPAC-HNO_3	0.135	1.230	1.367	0.813	0.721	0.526	0.98	0.052
MAPC-H_3PO_4	0.094	1.269	1.243	0.788	0.711	0.523	0.98	0.049
MEAC-HNO_3	-0.268	0.922	0.540	1.084	0.515	0.301	0.99	0.088
MEAC-H_3PO_4	-0.279	1.008	0.526	0.992	0.544	0.353	0.99	0.067

Note* Unit of K=($mg^{1-1/n}$ $L^{1/n}$ g^{-1}), n=(g L^{-1}) and q_e=(mg g^{-1})

Temkin isotherm for fluoride adsorption

Temkin isotherm is studied by using Eq. (6) of chapter-1 i.e., q_e vs lnC_e which is shown in Fig. 3.10-3.11.The values of the Temkin constants A and B and the correlation coefficients are listed in Table 3.8. The isotherms indicate that the adsorption increases with increase in equilibrium concentration of the fluoride ion. The R^2 values of Temkin isotherm were found to be in the range of 0.899-0.991 which is again lower than both Langmuir and Freundlich value. This suggests that the Temkin isotherm model of adsorption may not be significant in this case. From the Table 3.8, it is evident that the MEAC-HNO_3 possesses maximum value of heat of sorption followed by MPAC-HNO_3, MPAC-H_3PO_4 and MEAC-H_3PO_4 respectively. The heat of adsorption gives an idea about the quality of the adsorbent thus from the present results, it may be assumed that quality of carbon adsorbents are different and it follows the order MEAC-HNO_3> MPAC-HNO_3>MPAC-H_3PO_4>MEAC-H_3PO_4 respectively.

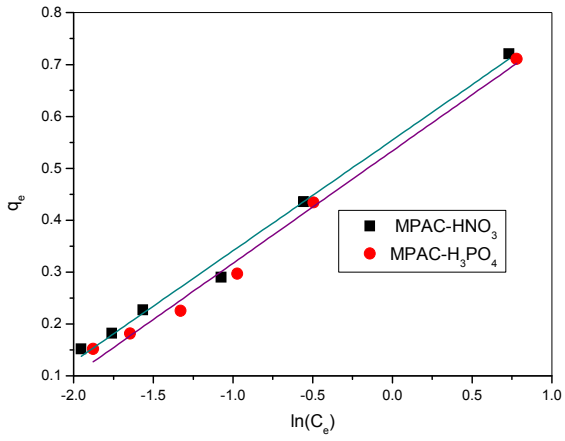

Fig. 3. 10. Temkin adsorption isotherm for fluoride adsorption by MPAC

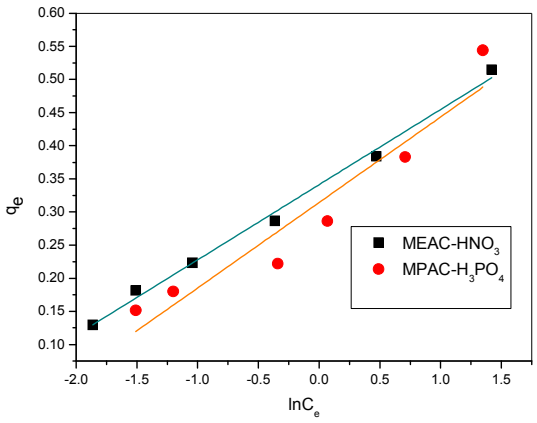

Fig. 3.11. Temkin adsorption isotherm for fluoride adsorption by MEAC

Table 3.8. Comparison of different Temkin adsorption parameters of isotherm for fluoride removal

Adsorbent	*B*	*Bln(A)*	*A*	$q_{e(exp)}$	$q_{e(cal)}$	R^2	χ^2
MPAC-HNO_3	0.213	0.554	13.47	0.721	0.709	0.991	0.0001
MPAC-H_3PO_4	0.216	0.533	12.94	0.711	0.721	0.989	0.0001
MEAC-HNO_3	0.113	0.341	20.43	0.515	0.501	0.992	0.0003
MEAC-H_3PO_4	0.129	0.314	11.41	0.544	0.487	0.899	0.0061

Note* unit of B=($L^{-1}g$), A=($L^{-1}g$) *and* q_e=(mg g^{-1})

Validity of adsorption isotherm model

In order to validate the adsorption isotherm, chi-square analysis was conducted for all the isotherms. From the χ^2 analysis (given in Eq.(7) of chapter-1) and comparing the different adsorption isotherm models, it can be concluded that Langmuir and Temkin models show lowest χ^2 values compared to Freundlich model. This suggests that the Langmuir model of adsorption fits better for fluoride adsorption compared to Temkin and Freundlich isotherm model. Thus the order of favourability for fluoride adsorption by different isotherm models follows the following order Langmuir>Temkin>Freundlich.

3.5.2. Adsorption Kinetics study for fluoride removal

To evaluate the kinetic mechanism that controls the adsorption process, different models like pseudo-first-order, pseudo-second-order, intraparticle diffusion and Elovich model were tested to interpret the experimental data which are discuss below.

For this, adsorption at different temperature were studied and the results are discussed below in details.

Effect of temperature

Effect of temperature for the adsorption of fluoride was studied at four different temperature of 25^{o}C (298K), 30^{o}C (303K), 35^{o}C (308K) and 40^{o}C (313K) and the results are given in Table 3.9-3.12. It is observed that the adsorption increased with temperature indicating chemical interaction between sorbate ions and surface functionalities of the active carbons or may be due to the increase of the intraparticle diffusion rate of sorbate ions into the pores at higher temperature (Yupeng et al., 2002).The plot of adsorption capacity as a function of temperature at different time intervals is shown in (Fig. 3.12)

Table 3.9. Fluoride removal using MPAC-HNO_3 at different temperature

Time (min)	298K			303K			308K			313K		
	C_e	q_e	R%	C_e	q_e	R%	C_e	q_e	R%	C_e	q_e	R%
5	2.60	0.24	48.00	2.58	0.24	48.40	2.53	0.24	49.40	2.48	0.25	50.40
10	2.45	0.25	51.00	2.21	0.27	55.80	2.19	0.28	56.20	2.18	0.28	56.40
20	1.60	0.34	68.00	1.40	0.36	72.00	1.38	0.36	72.40	1.29	0.37	74.20
40	0.85	0.41	82.84	0.82	0.41	83.42	0.80	0.41	83.84	0.79	0.42	84.08
60	0.41	0.45	91.80	0.32	0.46	93.60	0.28	0.47	94.40	0.26	0.47	94.80
80	0.32	0.46	93.52	0.29	0.47	94.16	0.27	0.47	94.48	0.27	0.47	94.56
100	0.28	0.47	94.28	0.27	0.47	94.44	0.26	0.47	94.72	0.25	0.47	94.84
120	0.27	0.47	94.44	0.23	0.48	95.30	0.23	0.47	95.36	0.23	0.47	95.38
180	0.13	0.48	97.26	0.12	0.48	97.50	0.12	0.48	97.54	0.11	0.48	97.62
240	0.13	0.49	97.28	0.12	0.49	97.56	0.12	0.49	97.56	0.11	0.49	97.66

Note* R%=Removal percentage

Table 3.10. Fluoride removal using MPAC-H_3PO_4 at different temperature

Time (min)	298K			303K			308K			313K		
	C_e	q_e	R%	C_e	q_e	R%	C_e	q_e	R%	C_e	q_e	R%
5	2.01	0.29	59.80	2.03	0.29	59.40	1.94	0.30	61.20	1.96	0.30	60.80
10	1.83	0.31	63.40	1.58	0.34	68.40	1.43	0.35	71.40	1.63	0.33	67.40
20	1.57	0.34	68.60	1.22	0.37	75.60	1.20	0.38	76.00	1.27	0.37	74.60
40	1.21	0.37	75.80	1.08	0.39	78.40	0.99	0.40	80.20	0.87	0.41	82.42
60	0.83	0.41	83.40	0.80	0.42	84.00	0.81	0.41	83.78	0.80	0.41	83.94
80	0.73	0.42	85.24	0.61	0.43	87.76	0.74	0.42	85.20	0.62	0.43	87.42
100	0.57	0.44	88.58	0.54	0.44	89.04	0.55	0.44	89.00	0.55	0.44	88.94
120	0.54	0.44	89.02	0.44	0.45	91.18	0.51	0.44	89.68	0.41	0.45	91.66
180	0.48	0.45	90.26	0.42	0.45	91.44	0.40	0.45	91.94	0.40	0.45	91.88
240	0.42	0.46	91.54	0.41	0.45	91.78	0.38	0.46	92.36	0.38	0.46	92.22

Note* R%=Removal percentage

Table 3.11. Fluoride removal using MEAC-HNO_3 at different temperature

Time (min)	298K			303K			308K			313K		
	C_e	q_e	R%	C_e	q_e	R%	C_e	q_e	R%	C_e	q_e	R%
5	1.98	0.30	60.40	1.96	0.30	60.80	1.92	0.30	61.60	1.92	0.30	61.60
10	1.50	0.35	70.00	1.45	0.35	71.00	1.41	0.35	71.80	1.41	0.35	71.80
20	1.36	0.36	72.80	1.28	0.37	74.40	1.20	0.38	76.00	1.20	0.38	76.00
40	1.00	0.40	80.00	1.02	0.39	79.60	0.98	0.40	80.40	0.98	0.40	80.40
60	0.81	0.41	83.72	0.81	0.41	83.78	0.80	0.41	83.92	0.80	0.41	83.92
80	0.73	0.42	85.38	0.72	0.42	85.46	0.72	0.42	85.58	0.72	0.42	85.58
100	0.56	0.44	88.70	0.55	0.44	88.96	0.54	0.44	89.02	0.54	0.44	89.02
120	0.54	0.44	89.06	0.54	0.44	89.08	0.54	0.44	89.12	0.54	0.44	89.12
180	0.47	0.45	90.56	0.46	0.45	90.76	0.46	0.45	90.80	0.46	0.45	90.80
240	0.41	0.45	91.62	0.41	0.45	91.76	0.41	0.45	91.78	0.41	0.45	91.78

Note* R%=Removal percentage

Table 3.12. Fluoride removal using MEAC-H_3PO_4 at different temperature

Time (min)	298K			303K			308K			313K		
	C_e	q_e	R%	C_e	q_e	R%	C_e	q_e	R%	C_e	q_e	R%
5	2.8	0.22	44.00	2.76	0.22	44.80	2.52	0.24	49.60	2.50	0.25	50.00
10	2.51	0.24	49.80	2.33	0.26	53.40	2.27	0.27	54.60	2.09	0.29	58.20
20	1.73	0.32	65.40	1.47	0.35	70.60	1.33	0.36	73.40	1.26	0.37	74.80
40	0.86	0.41	82.80	0.87	0.41	82.60	0.79	0.42	84.08	0.79	0.42	84.18
60	0.61	0.43	87.80	0.38	0.46	92.40	0.56	0.44	88.64	0.55	0.44	88.84
80	0.44	0.45	91.18	0.25	0.47	94.92	0.36	0.46	92.74	0.26	0.47	94.62
100	0.29	0.47	94.20	0.26	0.47	94.70	0.25	0.47	94.84	0.19	0.48	96.12
120	0.26	0.47	94.72	0.23	0.47	95.40	0.23	0.47	95.38	0.16	0.48	96.74
180	0.13	0.48	97.22	0.12	0.48	97.56	0.12	0.48	97.58	0.12	0.48	97.46
240	0.13	0.48	97.26	0.12	0.48	97.58	0.11	0.48	97.62	0.11	0.48	97.70

Note* R%=Removal percentage

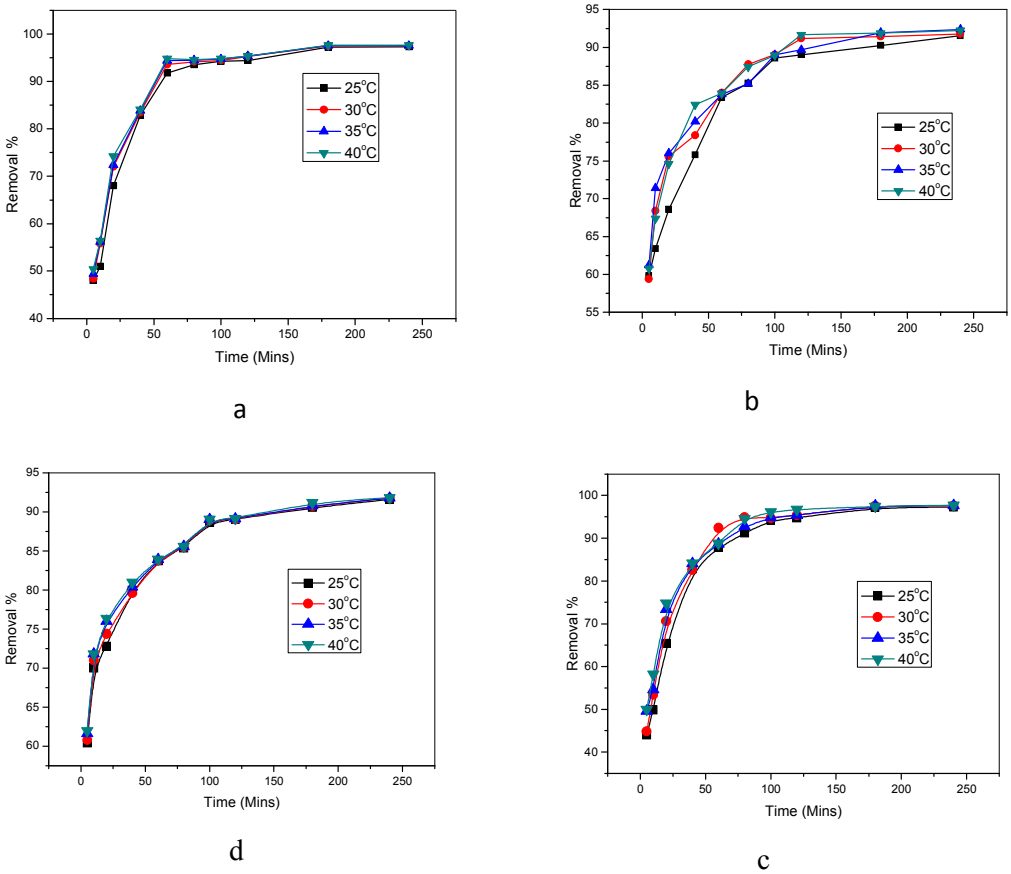

Fig. 3.12. Effect of temperature on the removal of fluoride at different time. a) MPAC-HNO_3 b)MPAC-H_3PO_4, c) MEAC-HNO_3 and d)MEAC-H_3PO_4

Pseudo first-order model for fluoride adsorption

The linearised plot of pseudo first-order kinetic model was plotted by using Eq. (8) of chapter-1, for different activated carbons and the plots are shown in Fig 3.13. The corresponding values obtained are given in Table 3.13. All the adsorbent show good correlation co-efficient, the (R^2) values was found to be 0.950, 0.977 and 0.961 for MPAC-HNO_3, MEAC-HNO_3 and MEAC-H_3PO_4 except for MPAC-H_3PO_4 which gave 0.858. Thus, it indicates that the pseudo first-order model is less suitable model of adsorption for MPAC-H_3PO_4 activated carbon. The values of rate constant (k_1) and $q_{e(cal)}$ were determined for each adsorbent from the slope and intercept. It can also be observed that the values of $q_{e(cal)}$ for the adsorbent are quite different than $q_{e(exp)}$ which signifies the fact that the adsorption process was not controlled by pseudo first-order model.

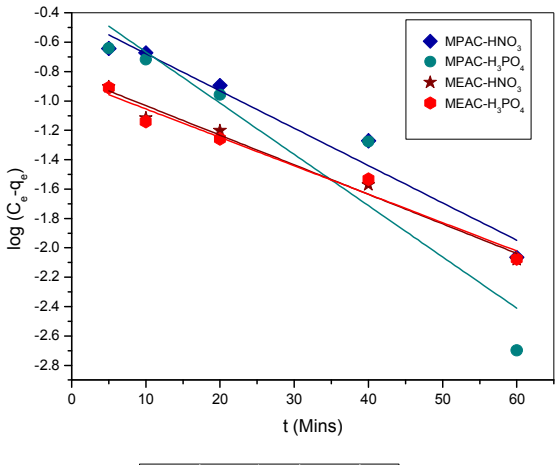

Fig. 3.13. Pseudo first-order model for MPAC and MEAC

Table. 3.13. Different parameters for Pseudo first-order model for fluoride adsorption.

Adsorbent	$q_{e(exp)}$	k_1x10^{-1}	$q_{e(cal)}$	*SSE*	R^2
MPAC-HNO_3	0.486	0.025	0.423	0.016	0.950
MPAC-H_3PO_4	0.457	0.034	0.316	0.095	0.858
MEAC-HNO_3	0.458	0.020	0.830	0.659	0.977
MEAC-H_3PO_4	0.486	0.019	0.860	0.592	0.961

Note* q_e= (mg g^{-1}) and k_1=(min^{-1})

Pseudo second-order model for fluoride adsorption

The linearised pseudo second-order plots of t/q_t vs t (from Eq. (9) of chapter-1) for the different adsorbents are shown in Fig. 3.14-3.17 and the corresponding values obtained are tabulated in Table 3.14. All the adsorbent gives good consistent correlation co-efficient (R^2) values.The values obtained for R^2 are 0.999, 0.999, 0.999 and 0.999 for MPAC-HNO_3, MPAC-H_3PO_4, MEAC-HNO_3 and MEAC-H_3PO_4 respectively. The R^2 values in the present case are found to be higher than that of pseudo first-order model, suggesting the fact that kinetics data fits better in pseudo second-order model. The values obtained from *SSE* (Squared Sum of Errors) analysis also indicate that the adsorption kinetics of fluoride onto all the carbon adsorbents could be better described and approximated more favourably by pseudo second-order model. Further, the close values of $q_{e(cal)}$ and $q_{e(exp)}$ suggest that adsorption mechanism probably follow pseudo second-order kinetics model. Similar trend has been observed and reported for adsorption of fluoride on various adsorbents (Daifullah et al., 2007; Liao and Shi, 2005).

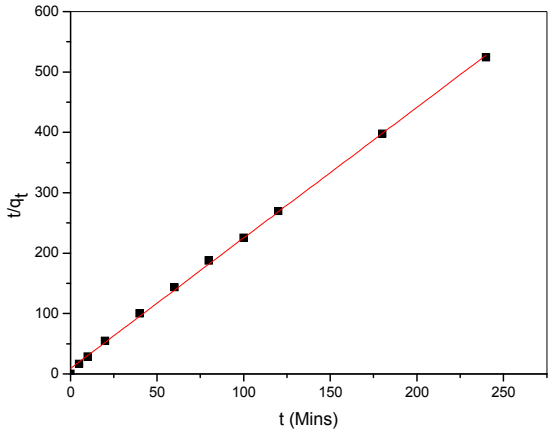

Fig. 3.14. Pseudo second order adsorption plot of MEAC-HNO_3

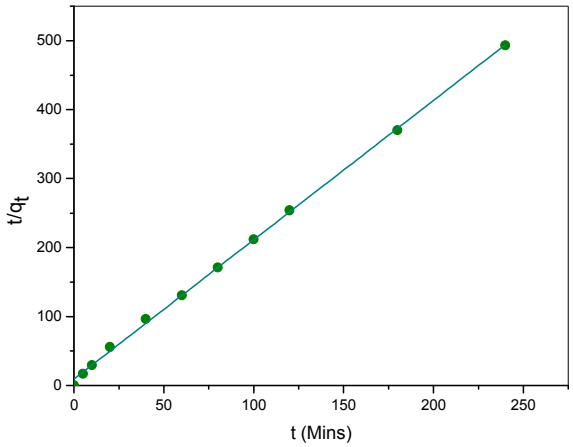

Fig. 3.15. Pseudo second order adsorption plot of MPAC-HNO_3

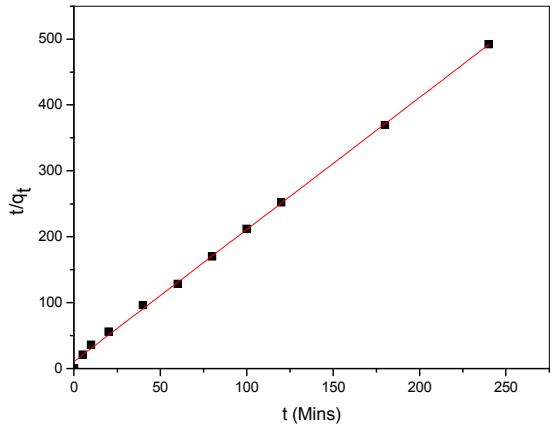

Fig. 3.16. Pseudo second order adsorption plot of MPAC-H_3PO_4

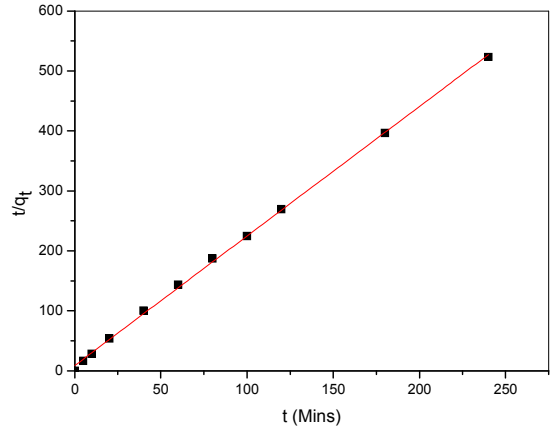

Fig. 3.17. Pseudo second order adsorption plot of MEAC-H_3PO_4

Table 3.14. Different parameters for Pseudo second-order model of fluoride adsorption

Adsorbent	$q_{e(exp)}$	k_2x10^{-1}	$q_{e(cal)}$	*SSE*	R^2
MPAC-HNO_3	0.486	0.440	0.494	0.0003	0.999
MPAC-H_3PO_4	0.457	0.373	0.499	0.0084	0.999
MEAC-HNO_3	0.458	0.552	0.462	0.0065	0.999
MEAC-H_3PO_4	0.486	0.530	0.463	0.0022	0.999

Note* Unit of q_e=(mg g^{-1}), k_2=(g $mg^{-1}min^{-1}$).

Weber and Morris intraparticle diffusion model for fluoride adsorption

Intraparticle diffusion plots of q_t versus $t^{1/2}$ (From Eq. (10) of chapter-1) are shown in Fig 3.18-3.21 and the corresponding values obtained from the plot are summarized in Table 3.15. The value of intercept gives about the thickness of the boundary layer and hence, larger the value greater will be the boundary layer (Daifullah et al., 2007 and Kumar et al., 2009). It is evident from the plots that there are two separate stages are involved. In Stage I, the fluoride uptake by the adsorbent was found to be very rapid over a short period of time because of the immediate utilization of the most readily available active sites by the fluoride ion on the adsorbent surfaces. However, in Stage II, the rate of adsorption slows down. It may be due to slow diffusion of adsorbate from surface site into the innerpores is observed. The correlation co-efficient values for all the adsorbent were found to be low i.e., in the range 0.80-0.89. This may be due to the difference in the rate of mass transfer in the initial and final stages of adsorption (Panday et al., 1986). MEAC-HNO_3 show highest value of A suggesting thickest boundary layer and hence a slow intra particle transport (k_b) is expected with maximum fluoride ion uptake from the aqueous solution. Whereas MPAC-H_3PO_4 show thinnest boundary layer with least fluoride ion uptake and hence show higher k_b value.

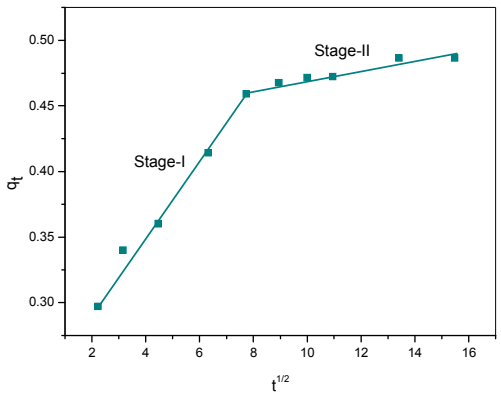

Fig .3.18. Weber and Morris intraparticle diffusion plots of fluoride adsorption for MPAC-HNO_3

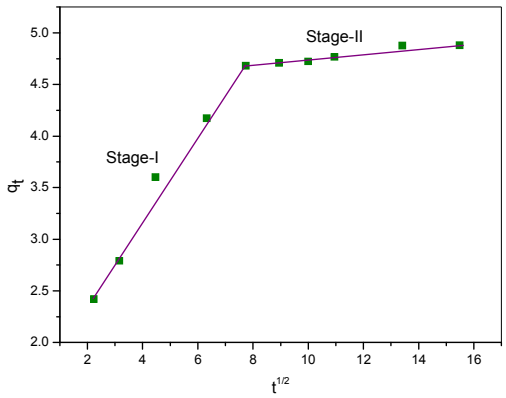

Fig .3.19. Weber and Morris intraparticle diffusion plots of fluoride adsorption for MPAC-H_3PO_4

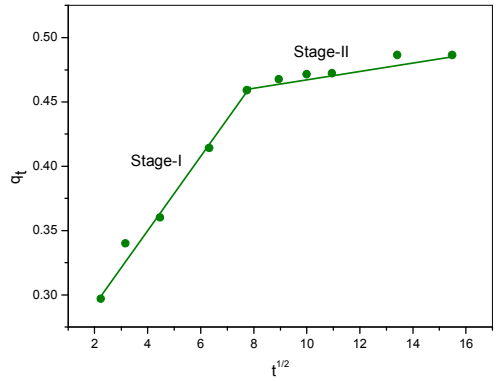

Fig. 3.20. Weber and Morris intraparticle diffusion plots of fluoride adsorption for MEAC-HNO_3

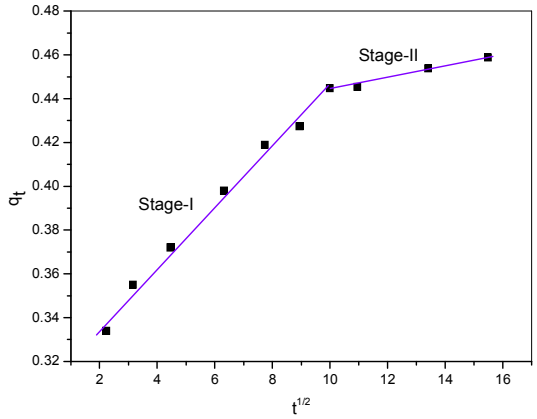

Fig. 3.21. Weber and Morris intraparticle diffusion plots of fluoride adsorption for MEAC-H_3PO_4

Table. 3.15. Different parameters obtained for intraparticle diffusion model

Adsorbent	$q_{e(exp)}$	$k_b x10^{-1}$	A	R^2
MPAC-HNO_3	0.486	0.014	0.306	0.897
MPAC-H_3PO_4	0.457	0.018	0.298	0.801
MEAC-HNO_3	0.458	0.009	0.330	0.836
MEAC-H_3PO_4	0.486	0.002	0.306	0.802

Note* Unit of k_b=(mg g-^{1} min^{-1}), q_e=(mg g^{-1}) and A=(mg g^{-1}).

Elovich model for fluoride adsorption

The plot of Elovich model of q_t vs *ln(t)* (From Eq.(11) of chapter-1) are presented in Fig. 3.22-3.25 and the results obtained from the plot are shown in Table 3.16. The correlation co-efficient values were found to be in the range of 0.97-0.989 which suggests that diffusion accounted for the Elovich kinetics pattern (Aharoni et al., 1991) and this equation alone might be taken as evidence that the rate-determining step is diffusion in nature (Pavlatou and Polyzopouls, 1988). Elovich equation is applicable only at conditions where desorption rate can be ignored (Rudzinksi et al., 1998).

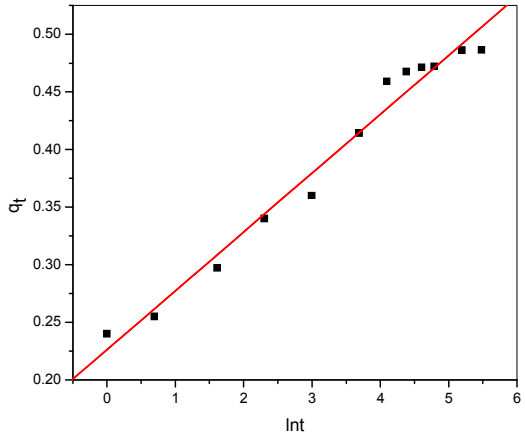

Fig. 3.22. Elovich plot for fluoride adsorption by MPAC-HNO_3

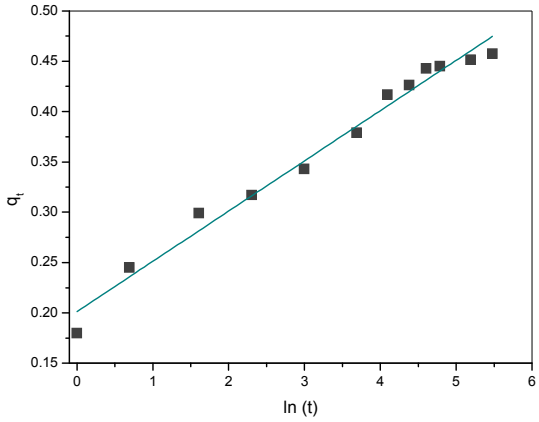

Fig. 3.23. Elovich plot for fluoride adsorption by MPAC-H_3PO_4

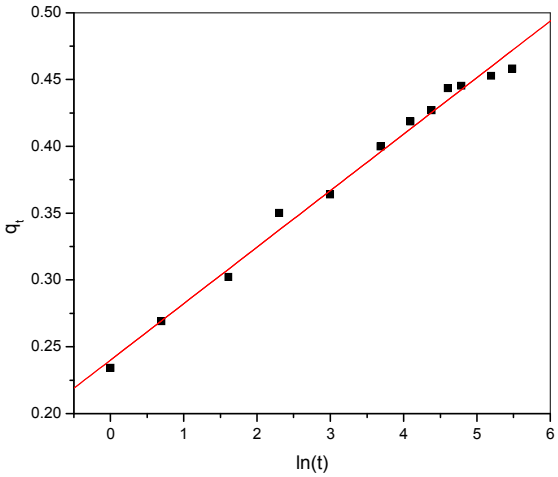

Fig. 3.24. Elovich plot for fluoride adsorption by MEAC-HNO_3

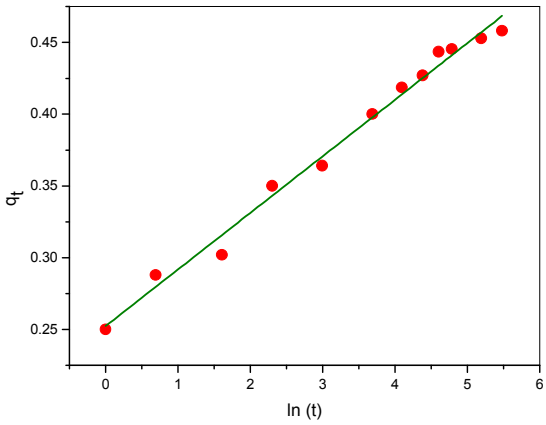

Fig. 3.25. Elovich plot for fluoride adsorption by MEAC-H_3PO_4

Table 3.16. Different parameters obtained from Elovich model

Adsorbent	$q_{e(exp)}$	β	R^2	α
MPAC-HNO_3	0.486	0.226	0.975	0.051
MPAC-H_3PO_4	0.457	0.201	0.980	0.049
MEAC-HNO_3	0.458	0.240	0.989	0.042
MEAC-H_3PO_4	0.486	0.252	0.987	0.039

Note* Unit of q_e=(mg g^{-1})

3.5.3. Thermodynamic parameters study for fluoride adsorption

Thermodynamic studies were determined by carrying out adsorption experiments at four different temperatures, i.e., 298, 303, 308 and 313 K. For this study, the plot of Vant Hoff lnK_d vs $1/T$ was obtained by using Eq. (15) of chapter-1 and the plots are shown in Fig.3.26-3.29. The values of rate constant K_d are given Table 3.16. The thermodynamic parameters ΔH^0 and ΔS^0 were obtained from slope and intercept of the plot. The value ΔG^0 was calculated using Eq. 16. The different thermodynamic parameters are tabulated in Table 3.17. The positive value of ΔH^0 is an indicative of endothermic nature of adsorption and it is also supported by the increase in K_0 value with increase in temperature. The entropy was found to be positive for the entire carbon sample after fluoride adsorptions which suggest that a change might have occurred in the internal structure of sorbents during the adsorption of fluoride ion. The negative ΔG^0 indicates that the reaction involved in fluoride adsorption by the adsorbent might be of spontaneous nature. The value of ΔH^0 obtained for all the adsorbent in the range 0.789-4.546 KJ mol^{-1} in the present thermodynamic study indicates that the fluoride sorption is chemical in nature which may be attributed to the higher electronegativity of fluoride and the specific substitution of fluoride for hydroxide onto carbon surface (Daifullah et al., 2007).

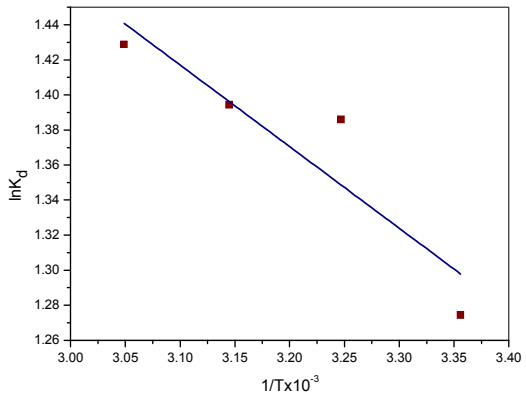

Fig 3.26. Vant Hoff plot for fluoride adsorption by MPAC-HNO_3

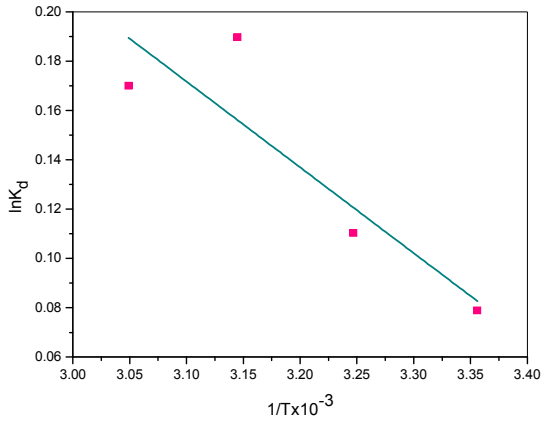

Fig 3.27. Vant Hoff plot for fluoride adsorption by MPAC-H_3PO_4

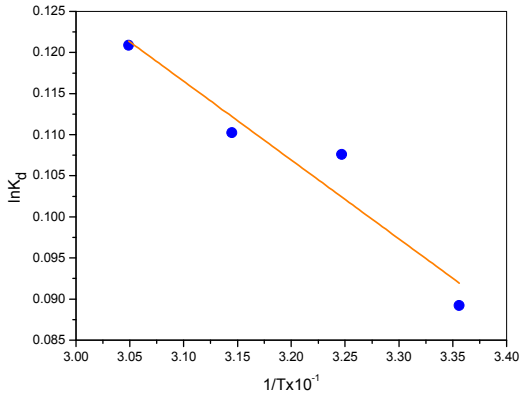

Fig 3.28. Vant Hoff plot for fluoride adsorption by MEAC-HNO_3

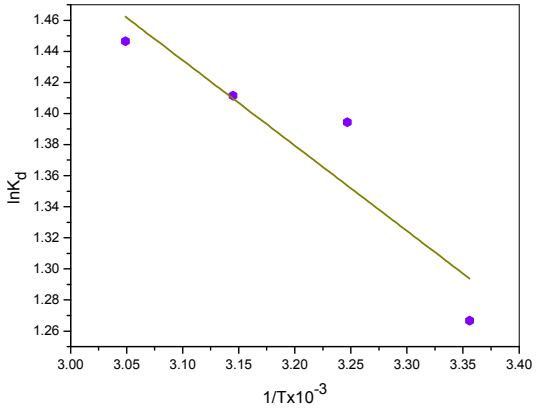

Fig 3.29. Vant Hoff plot for fluoride adsorption by MEAC-H_3PO_4

Table 3.16. Effect of temperature on the removal of fluoride using different adsorbents

Adsorbent	T(K)	C_e	q_e	k_d	Lnk_d	$1/T(K)$
MPAC-HNO_3	298	0.136	0.486	3.576	1.274	0.0033
	308	0.122	0.487	3.998	1.385	0.0032
	318	0.121	0.487	4.032	1.394	0.0031
	328	0.117	0.488	4.173	1.428	0.0030
MPAC-H_3PO_4	298	0.423	0.457	1.082	0.078	0.0033
	308	0.411	0.458	1.116	0.110	0.0032
	318	0.382	0.461	1.208	0.189	0.0031
	328	0.389	0.461	1.185	0.170	0.0030
MEAC-HNO_3	298	0.419	0.458	1.093	0.089	0.0033
	308	0.412	0.458	1.113	0.107	0.0032
	318	0.411	0.458	1.116	0.110	0.0031
	328	0.407	0.459	1.128	0.120	0.0030
MEAC-H_3PO_4	298	0.137	0.486	3.549	1.266	0.0033
	308	0.121	0.487	4.032	1.394	0.0032
	318	0.119	0.488	4.101	1.411	0.0031
	328	0.115	0.488	4.247	1.446	0.0030

Table 3.17. Different thermodynamic parameters for removal of fluoride using various carbon adsorbents

Adsorbent	ΔH^0	ΔS^o	ΔG^0			
			298(K)	303(K)	308(K)	313(K)
MPAC-HNO_3	3.795	23.780	-7.086	-7.205	-7.325	-7.443
MPAC-H_3PO_4	2.892	10.394	-3.198	-3.150	-3.188	-3.240
MEAC-HNO_3	0.789	3.4400	-1.024	-1.042	-1.059	-1.076
MEAC-H_3PO_4	4.564	26.066	-7.767	-7.894	-8.027	-8.158

Note* Unit of ΔH^0 =(KJ mol^{-1}), ΔS^o=(J $mol^{-1}K^{-1}$) and ΔG^0 =(KJ mol^{-1})

3.6. Adsorbent regeneration study

The regeneration of the adsorbents was done using 5% NaOH solution. The fluoride loaded carbon adsorbents were treated with NaOH solution in order to regenerate the surface active site. However, the percentage removal of fluoride after regeneration was poor (Table 3.18). This may be attribute to the strong binding of the fluoride ions on to the surface of the adsorbent through ion exchange interaction. And as such, regeneration of active site becomes somewhat limited; hence, regeneration of adsorbent was not satisfactory for all the carbon samples. However, since the starting raw materials used for the synthesis of different adsorbent are available in plenty, activated carbon can be readily synthesized and can be used for different adsorption

process. The removal percentage of fluoride by different adsorbents after regeneration is shown in Fig 3.30.

Table 3.18. Removal of fluoride after adsorbent regeneration

Adsorbent	C_e	q_e	Removal %
MPAC-HNO_3	6.0	0.040	40
MPAC-H_3PO_4	6.8	0.032	32
MEAC-HNO_3	5.6	0.044	44
MEAC-H_3PO_4	7.1	0.029	29

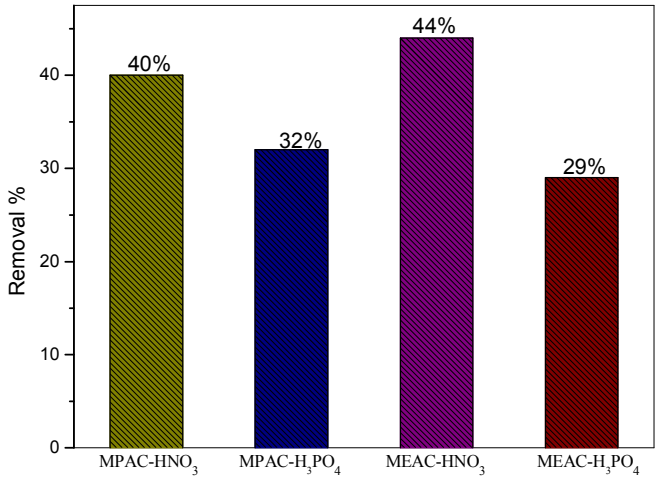

Fig. 3.30. Removal percentage of fluoride from regenerated adsorbents

3.6. Conclusion

From the present study, it was observed that the all the four adsorbent show good adsorption capacity. It was observed that the percentage removal of fluoride increased with increase in adsorbent dosage, contact time and temperature but decreased with increase in concentration of the fluoride solution. The fluoride adsorption was found to be more suitable under acidic condition. Analysis of different adsorption model like Langmuir, Freundlich and Temkin gave the impression that Langmuir isotherm model fitted best followed by Temkin and Freundlich isotherms models. This suggests homogeneous nature of the adsorbent active site and thus, it may be assumed that fluoride adsorption is limited with monolayer coverage only. It was also found that the rate of adsorption can be better described by pseudo second-order model which is an indication for chemisorptive rate-limiting reaction. The good fitting of Elovich equations indicates that pore diffusion plays a vital role in controlling the rate of

reaction. The endothermic nature of adsorption is reflected by the positive value of ΔH^0. The negative ΔG^0 reflects the spontaneous nature of fluoride adsorption reaction. It is clear from these studies fluoride sorption is chemical in nature (ΔH^o in the range 0.789-4.546 KJ mol^{-1}). The fluoride loaded carbons was regenerated with 5% NaOH solution but only around 30-40% could be regenerated.

References

Aharoni, C., Ungarish, M. (1977). Kinetics of activated chemisorption. Part-2. Theoretical models. *J Chem Soc Faraday Trans 1: Phys Chem Condens Phases,* 73(3):456–464.

Boparai, H, K., Meera, J., Denis, M.O. (2010). Kinetics and thermodynamics of cadmium ion removal by adsorption onto nano zero valent iron particle. *J HazardMater,*188(1):458-465.

Bulusu, K.R., Sundaresan, B.B., Pathak, B.N., Nawlakhe, W.G., Kulkarni, D. N., Thergoankar, V. P. (1979). Fluorides in water, defluoridation methods and their limitations. *J Inst Eng Environ Eng Div*, 60:1-25.

Cengeloglu, Y., Kir, E., Ersoz, M. (2002). Removal of fluoride from aqueous solution by using red mud. *Sep Purif Technol*, 28(1):81-86.

Chakrapani, C., Babu, C. S., Vani K.N.K., Rao, K.S. (2010). Adsorption kinetics for the removal of fluoride from aqueous solution by activated carbon adsorbents derived from the peels of selected citrus fruits. *E-J Chem,* 7:149-427.

Daifullah, A.A.M., Yakout, S.M., Elreefy, S.A. (2007). Adsorption of fluoride in aqueous solutions using KMnO4–modified activated carbon derived from steam pyrolysis of rice straw. *J Hazard Mater*, 147: 633-643.

Das, A.A. (1996). Fluorosis. In Text Book of Human Nutrition (Bamji, M.S., Rao, N.P., Reddy, V. Eds.), Oxford & IBH Publishing, New Delhi.

Dawodu, F.A., Akpomie G.K., Ogbu I.C. (2012). Isotherm modeling on the equilibrium sorption of cadmium (II) from solution by agbani clay. *Int J Multidiscipl Sci Eng,* 3(9):9-14.

Ghorai, S., Pant, K.K. (2005). Equilibrium, kinetics and breakthrough studies for adsorption of fluoride on activated alumina. *Sep Purif Technol,* 42:265-271.

Harrison, J.E., Hitchman, A.J., Hitchman, A., Haltrope, M.E. (1990). The effects of fluoride on ectopic bone formation. *J Bone Miner Res,* 5(1):81-85.

Handa, B.K. (1975). Geochemistry and genesis of fluoride-containing groundwaters in India. *Groundwater*, 13:275–281.

Hem, J.D. (1989). Study and interpretation of the chemical characteristics of natural water.Water Supply Paper 2254 3rd edition*, US Geological Survey, Washington, D.C.,* 263.

Hichour, M., Persin, F., Sandeaux, J., Gavach, C. (2000). Fluoride removal from water by Donnan analysis. *Sep Purif Technol,* 18:1-11.

Hingston, F.J., Posner, A.M., Quirk, J.P. (1972). Anion adsorption by goethite and

gibbsite. I. The role of proton in determining adsorption envelops. *J Soil Sci,* 23:177–192.

Hinz, B., Chevts, J., Renner, B. (2005). Bioavailability of diclofenacpotassium at low doses. *Brit J Clinic Pharma*, 59(1):80-84.

Hsu, P.H. (1976). Comparison of iron(III) and aluminum in precipitation of phosphate from solution. *Water Res,* 10:903-907.

Huang, C.J., Liu, J.C. (1999). Precipitate flotation of fluoridecontaining wastewater from a semiconductor manufacturer. *Water Res*, 33:3403-3412.

Jibril, M., Noraini, J., Poh, L.S., Evuti, A.M. (2013). Removal of colour from waste water using coconut shell activated carbon (CSAC) and commercial activated carbon (CAC). *J Teknologi (Sci & Eng),*60(1):15–19.

Krishnamachari, K.A.V.R., Krishnaswamy, K. (1973). Genu valgum and osteoporosis in an area of endemic fluorosis. *Lancet,* 2:877-879.

Krishnamachari, K.A.V.R. (1986). Skeletal fluorosis in humans: A review of recent progress in the understanding of the disease. *Prog Food Nutr Sci.* 10:279-314.

Kumar, E., Bhatnagar, A., Ji, M., Jung, W., Lee, S.H., Kim, S.J., Lee, G., Song, H., Choi, J.Y., Yang, J.S., Jeon, B.H.(2009). Defluoridation from aqueous solution by granular ferric hydroxide(GFH). *Water Res,* 43(2):490-498.

Kumar, P.S., Kirthika, K. (2009). Equilibrium and kinetic study of adsorption of nickel from aqueous solution onto bael tree leaf powder. *J Eng Sci Technol,* 4(4):351-363.

Lagergren, S. (1898). About the theory of so-called adsorption of soluble substances. *K. Svenska Vetenskapsakad Handl,* 24:1– 39.

Liao, X.P.,Shi, B. (2005). Adsorption of fluoride on zirconium(IV)-impregnated collagen fiber. *Environ SciTechnol*, 39:4628–4632.

Lounici, H., Addour, L., Belhocine, D., Grib, H., Nicolas, S., Bariou, B., Mameri, N. (1997). Study of a new technique for fluoride removal from water. *Desalination*, 114(3): 241-251.

Li, Y.H., Wang, S., Cao, A., Zhao, D., Zhang, X., Xu, C., Luan, Z., Ruan, D., Liang, J., Wu, D., Wei, B. (2001). Adsorption of fluoride from water by amorphous alumina supported on carbon nanotubes. *Chem Phys Lett,* 350(6):412-416.

Mahramanlioglu, M., Kizilcikli,I., Bicer, I.O. (2002). Adsorption of fluoride from aqueous solution by acid treated spent bleaching earth. *J Fluorine Chem*, 115(1):41-47.

Majima, T., Takatsuki, H. (1987). Fluoride removal from smokewashing wastewater by using CaF_2 separating method. *Water Purif Liq Wastes Treatment*, 28(7):433-443.

Mangla, B. (1991). India's dentists squeeze fluoride warnings off tubes. *New Scientist*, 131:16.

Mali, D., Srivastava,V., Agarwall, N.(2006). Removal of orange G andmethyl violet dyes by adsorption onto bagasse fly ash kinetics study and equilibrium isotherm analysis. *Dyes Pigments, 69*:210- 223.

Meenakshi, S., Viswanathan, N. (2007). Identification of selective ion exchange resin for fluoride sorption. *J Colloid Interface Sci*, 308:438–450.

Mishra, P.C., Patel, R.K.(2009). Removal of lead and zinc ions from water by low cost adsorbents. *J Hazard Mater,*168:319–325.

Murray, J.J. (1986). Appropriate Use of Fluorides for Human Health. *World Health Organization Geneva.*

Ngamsopasiriskum,C., Charnsethikul, S. (2010). Removal of phenol inaqueous solution by nano crystalline TiO2/ activated carbon compositecatalyst. *KasetsartJ Nat Sci,*1176-1182.

Onyango, M.S., Kojima, Y., Aoyi, O., Bernardo, E.C., Matsuda, H. (2004). Adsorption equilibrium modeling and solution chemistry dependence of fluoride removal from water by trivalentcation-exchanged zeolite F-9. *J Colloid Interface Sci,* 279(2): 341- 350.

Panday, K.K., Prasad, G., Singh, V.N. (1986). Mixed adsorbent for Cu(II) removal from aqueous solution. *Environ Tech Lett,* 50:547–554.

Pavlatou, A., Polyzopouls, N.A.(1988). The role of diffusion in the kinetics of phosphate desorption: the relevance of the Elovich equation. *Eur J Soil Sci,*39:425–436.

Popat, K.M., Anand, P.S., Dasare, B.D.(1994). Selective removal of fluoride ion from water by the aluminium, from the aminomethyl phosphoric acid type ion exchange resin. *React Poly*, 23:23-32.

Raichur, A.M., Basu, M.J.(2001). Adsorption of fluoride onto mixed rare earth oxides. *Sep Purif Technol*, 24:121–127.

Renuka, P., Pushpanjali, K.(2013). Review on Defluoridation Techniques of Water. *Int J Eng Sci,* 2(3):86-94.

Rao, K. S. (2008). Kaza's carbons are low cost adsorbents for defluoridation of potable water-a review. *Asian J Chem Environ Res*, 1:1-12.

Rudzinksi, W., Panczyk, P. (1998). In: J.A. Schwarz, C.I. contescu (eds.), surfaces of nanoparticles and porous materials. *Dekker New York*, 355.

Susheela, A.K. (1999). Dark side of fluoride. The Daily Star, February 20, Features, 16(col. 5).

Mohan, S., Karthikeyan, J. (1997). Removal of lignin and tannin color from aqueous solution by adsorption on to activated carbon solution by adsorption on to activated charcoal. *Environ Pollut 97*,183-187.

Suzuki, T., Kanesato, M., Yokoyama, T. (1990). Removal of fluorides from aqueous solutions. *Japanese Kokai Tokkyo Koho (Patent number 02191543).*

Tebutt, T.H.Y. (1983). Relationship Between Natural Water Quality and Health, United Nations Educational, *Scientific and Cultural Organization, Paris*.

Teotia, S.P., Teotia, M. (1994). A disorder of high fluoride and low dietary calcium interactions (30 years of personal research). *Fluoride*, 27:59-66.

Tsutsui, A., Yagi, M., Horowitz, A.M. (2000). The prevalence of dental caries and fluorosis in Japanese communities with up to 1.4 ppm of naturally occurring fluoride. *J Public Health Dentistry*, 60(3):147-153.

UNICEF. (1999). State of the art report on the extent of fluoride in drinking water and the result in gendemicity in India. Report by Fluorosis Research & Rural Development Foundation for UNICEF, New Delhi.

Vani, M.L., Reddy, K.P. (2000). Effects of fluoride accumulation on some enzymes of brain and gastrocnemius muscle of mice. *Fluoride,* (33)17-26.

Wang, A.G., Xia, T., Chu, Q.L., Zhang, M., Liu, F., Chen, X.M., Yang, K.D. (2004). Effects of fluoride on lipid peroxidation, DNA damage and apoptosis in human embryo hepatocytes. *Biomed EnvironSci,*17(2):217-222.

Wang, Y., Reardon, E.J. (2001). Activation and regeneration of a soil sorbent for defluoridation of drinking water. *Appl Geochem,* 16:531–539.

Weber Jr., W.J., Morris J.C. (1963). Kinetics of adsorption on carbon from solution. *J Sanit Eng Div,* 89:31–59.

WHO. (1984). Fluorine and Fluorides, Environmental Health Criteria 36. World Health Organization, Geneva.

Xu, D., Tan, X.L., Chen, C.L., Wang, X.K. (2008). Adsorption of Pb(II) from aqueous solution to MX-80 bentonite: Effect of pH, ionic strength, foreign ions and temperature. *Appl Clay Sci*, 41: 37-46.

Yang, M., Hashimoto, T., Hoshi, N. Myoga, H. (1999). Fluoride removal in a fixed bed packed with granular calcite. *Water Res,* 33(16): 3395-3402.

Yupeng, G., Jurui, Q., Shaofeng, Y., Kaifeng, Y., Zichen W.,Hongding, X. *(*2002).

Adsorption of Cr(VI) on micro and mesoporous rice husk-based active carbon. *Mater Chem Phy,* 78:132–137.

Zahra, D., Mohammad, A. B., Mojdeh, R., Mohammad, F. (2013). Adsorption of methylene blue dye from aqueous solution by modified pumice stone: kinetics and equilibrium studies. *Health scope*, 2(3): 136-144.

CHAPTER-4

REMOVAL OF METHYLENE BLUE (MB) FROM AQUEOUS SOLUTION

In this chapter removal on methylene blue (MB) dye by activated carbon has been discussed in details. Batch mode adsorption study was conducted to evaluate the optimum condition of pH, adsorbent dose, contact time and dye concentration on methylene blue adsorption study. The equilibrium isotherm for adsorption was studied by Langmuir, Freundlich and Temkin isotherms models. The kinetic study of adsorption of methylene blue molecules onto the activated carbons were studied by different models such as pseudo first-order, pseudo second-order, intraparticle diffusion and Elovich models. The determination of thermodynamics parameters are also discussed in this chapter.

.

4.1. Introduction

Water is one of the major elements essential for sustenance of all forms of life on earth. Unlike most natural resources, water is a renewable resource yet its availability is limited by many physical, climatic and geographical factors. Around the world it is estimated that only 3% of the world's water supply is fresh water and of this, only a third is available as either surface water or groundwater and the remaining are locked in polar ice cap (UN 2016). And gradually the least available fresh water which is the last resort for sustaining and survival of mankind is becoming polluted and limited for human consumption. The world population is ever increasing and the demand for freshwater is surging up. And as a result there is a water crises situation in many parts of the world. Now the point has reached where all sources of drinking water, including municipal water system, wells, lakes, rivers, and even glaciers, contain some level of contamination which is not safe for drinking due to heavy industrial and environmental pollution (Schwarzenbach et al., 2010). About half of the world's population is exposure to poor water quality and it has a tremendous impact on human health (Saravanan et al., 2011). Environmental water contamination is the leading worldwide cause of death and disease and it adversely affects over 1 billion people every day in developing countries. Though science has contributed significantly in addressing the threat from water-related diseases, solutions to these complex problems are still sought in a simple, one-dimensional 'cause effect remedy' context (Saravanan et al., 2011). Over the decade's urbanisation, industrialisation, mismanagement and over exploitation of natural resources have caused major effect on our environment. Thus, the modern world needs to be equipped with advanced environmentally benign technology to address such serious problems. For water treatment, the production of porous materials has been the subject matter for many researchers, in an effort to find its application in various water purification processes. Activated carbon is such one of the most important microporous adsorbents from an industrial point of view (Ismadji et al., 2005). It occupies a special place in terms of producing a clean environment involving water purification as well as separations and purification in the chemical and associated industries. Thus, activated carbon plays an important role in the removal of many types of pollutants from waste water.

Out of many number of pollutants, synthetic dyes are one of the major pollutants in industrial wastewater. Dyeing industry effluents constitute one of the most

problematic wastewaters to be treated due to their high chemical and biological oxygen demands, suspended solids, content in toxic compounds and also for colour, which are the first contaminant to be recognized by the human eye (Aksu 2005). About 15% of the total world production of dyes is lost during the dyeing process and is released as liquid Effluents (Zolllinger 1987). The treatment of dyes in industrial wastewater presents several problems since dyes usually have a synthetic origin and complex aromatic molecular structures which make them very stable and generally difficult to be biodegraded and photodegraded (Lorenc-Grabowska and Gryglewicz, 2007; Gupta 2009). Methylene blue is a thiazine (cationic) dye, which is most commonly used for coloring among all other dyes of its category (structure shown in Fig. 4.1). It is present in noticeable amount in industrial wastewater, which imparts blue colour. The dye causes eye burns, which may be responsible for permanent injury to the eyes of human and animals. If swallowed, the dye causes irritation to the gastrointestinal tract with symptoms of nausea, vomiting and diarrhea. It may also cause methemoglobinemia, cyanosis, convulsions, tachycardia and dyspnea, if inhaled. It is likely to cause irritation to the skin (Senthilkumar 2004). Many treatment techniques have been applied to a broad range of water and wastewater contaminated with dyes including physical or chemical treatment processes (Cengiz and Cavas, 2008). These include chemical coagulation, flocculation (Mohammad and Muttucumlutants, 2009; Zahra et al., 2013) ozonation, oxidation, photodegradation (Aksu 2005), ion exchange, irradiation, precipitation (Robinson et al., 2001). Membrane filtration (Mishra and Tripathy, 1993), Electro kinetic coagulation (Gahr et al. 1994), microbial cultures (Knapp and Newby, 1995) and various other techniques (Table 4.1) have been employed. However, these methods are not widely used due to their high cost which requires various tools and are generally not feasible on large scale industries. In contrast, an adsorption technique is by far the most versatile and widely used. The most common adsorbent materials are; alumina silica (Josefa and Oliveira, 2003), metal hydroxides (Wu and Tseng, 2006) and activated carbon (Malik et al., 2002). It has been reported that the adsorption onto activated carbon, have proven to be the most efficient and reliable method for the removal of many pollutants, including different dyes (Aksu 2005). Although commercial activated carbon is very effective adsorbent, its high cost requires the search for alternatives and low cost adsorbents (Pollard 1992). Several low cost adsorbents have been tested for removing dyes (Garg et al., 2004) including carbon from palm-tree cobs (Avom et al.,

1997), plum kernels (Wu et al., 1999), cassava peel (Rajeshwarisivaraj et al., 2001), bagasse (Tsai et al., 2001), jute fiber (Senthilkumaar et al., 2005a), rice husks (Yalc and Sevinc¸ 2000), olive stones (El-Sheikh and Newman, 2004), date pits (Girgis and El-Hendawy, 2002), fruit stones and nutshells (Aygun et al., 2003). The advantage of using agricultural by-products as raw materials for manufacturing activated carbon is that these raw materials are renewable and potentially less expensive to manufacture. Plant biomass is a natural renewable resource that can be converted into useful materials and energy (Klass 1998). The present study is an attempt to use *Mucuna pruiens* and *Manihot esculenta*, as a source of non conventional low-cost adsorbent for removal of MB dye from aqueous solution. The capacity of adsorbent for adsorbate is obtained by adsorption isotherm model, which is the equilibrium relationship between adsorbent/adsorbate systems. In this study, three models (Langmuir, Freundlich and Temkin) (Otero et al., 2003; Haimour and Sayed, 1997) have been used to describe the sorption process of MB onto four absorbents.

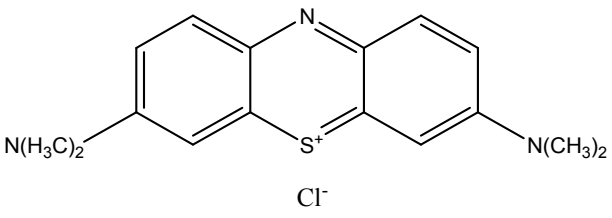

B

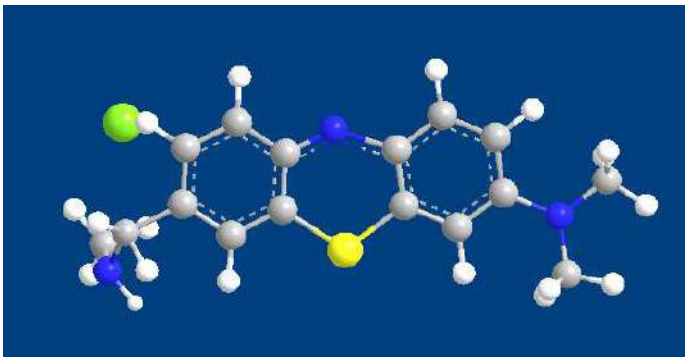

A

Fig.4.1. a) Structure of Methylene blue. b) 3D Structure of MB showing active site for possible interaction with activated carbon.

Table 4.1 Various methods for the removal of Methylene Blue

Techniques	Reference
Photo electrochemical degradation method	(An et al., 2001)
Adsorption of methylene blue onto Perlite	(Mehmet et al., 2000)
Adsorption of methylene blue onto Pithophora sp	(Kumar et al., 2004)
Bio-adsorption of methylene blue on Baggage	(Raghuvamsi et al., 2004)
Utilization of commercially available carbons	(Kahn, 2002)
Utilization of Biogas slurry	(Namasivayam and Yamuna, 1994)
Utilization of fly ash	(Ghouti et al., 2003)
Guava seeds as a source of activated carbon	(Rahman and Saad, 2003)
Utilization of Gulmohar tree fruit carbon (GTFC)	(Manickavasakam et al., 2004)
Utilization of firewood	(Wu and Tseng, 2006)
Utilization of Sheep Wool fiber and Cotton fiber for removal o f methylene blue	(Khan et al., 2005)

4.2. Materials and Methods

Reagents and Apparatus

Reagents. A stock solution of methylene blue was prepared by dissolving 1gm of methylene blue in 1000 ml of double distilled water and subsequently diluted with deionised water to the required concentration. The resultant solution contains 1000 mg L^{-1} of methylene blue. This solution is said to be stock solution of methylene blue. The pH of the working solution was adjusted to the desired value with 0.1M HCl and 0.1M NaOH. All chemicals used were of analytical reagent grade.

The apparatus used are

1) UV-Visible Spectrophotometer (PerkinElmer, lamda-25)

2) Elico-pH Meter

4.3. Adsorption Studies of methylene blue on activated carbons by batch method

In order to understand the adsorption behaviour of methylene blue, the effect of various experimental parameters has been investigated using batch adsorption experiments conducted at various pH values with different amounts of adsorbent. The

effect of initial concentration is studied by varying methylene blue concentrations between 2-20 mg L^{-1}. The effect of adsorbent dose on percent removal was studied with 0.1 g to 1g of adsorbent with 10 mg L^{-1} dye concentration. The effect of contact time was studied by varying the agitating time (range 2-60 min) at fixed optimum initial concentration of methylene blue (10 mg L^{-1}) with optimum dose of adsorbents (0.5 g) and also the effect of pH was studied ranging from 2-10. The equilibrium concentrations of each solution were determined from the absorbance of the solution measured by a spectrophotometer (UV-Visible, lambda 25-PerkinElmer) at the λmax value, which is 665 nm for methylene blue. The amount of MB adsorbed onto the activated carbon surface was determined by the difference between the initial and remaining concentrations of MB solution. The amount of adsorbed MB at equilibrium, q_e (mg g^{-1}) was calculated by the percentage removal of the dye and the amount of dye adsorbed were calculated by using Eq. (34) and Eq. (35) given under section 3.3 in chapter 3.

4.4. Result and discussion

Batch mode adsorption study for methylene blue adsorption

Different experiments were conducted in batches for methylene blue adsorption to obtain a suitable optimum condition. The results are discussed below under different headings.

Effect of adsorbent dosage

The adsorbent dose is an important parameter in adsorption studies because it determines the optimum amount of carbon required for the removal of dye solution. The percentage removal of methylene blue by adsorption on the selected adsorbents was studied with different adsorbent dosages (0.25-1 g) with 50 ml of dye solution and contact time of 50 min for MPAC-HNO_3, and MPAC-H_3PO_4, and 60 mins for MEAC-HNO_3 and MEAC-H_3PO_4 maintained at 25±1 ° C. The amount of dye adsorbed increased with increase in the amount of activated carbon as more number of available adsorption sites will be available at a higher concentration of the adsorbent for the adsorption of methylene blue dye (Ahmad 2009). Initially the rate of removal of dye was found to increase rapidly which slowed down as the dose increased, this may be due to the reduction in effective surface area available for adsorption (Franca et al., 2009). The plots of adsorbent dosage versus percent removal

are shown in Fig 4.1. This suggests that the adsorbed solute may either block the access to the internal pores or cause particles to aggregate and thereby reducing the availability of active sites for adsorption (Kannan and Vanangamudi, 1991a; Kannan and Karuppasamy, 1998b). The relative percent removal for all the activated carbon samples seems to be gradually increasing. Adsorbent MEAC-HNO_3 shows the highest percent removal at 1 g L^{-1} dose of the adsorbent where as MPAC-H_3PO_4 show the least removal percent. From the plot, an idea is obtained that all the adsorbents are a good source for MB dye removal as the percentage removal were high in all the cases.

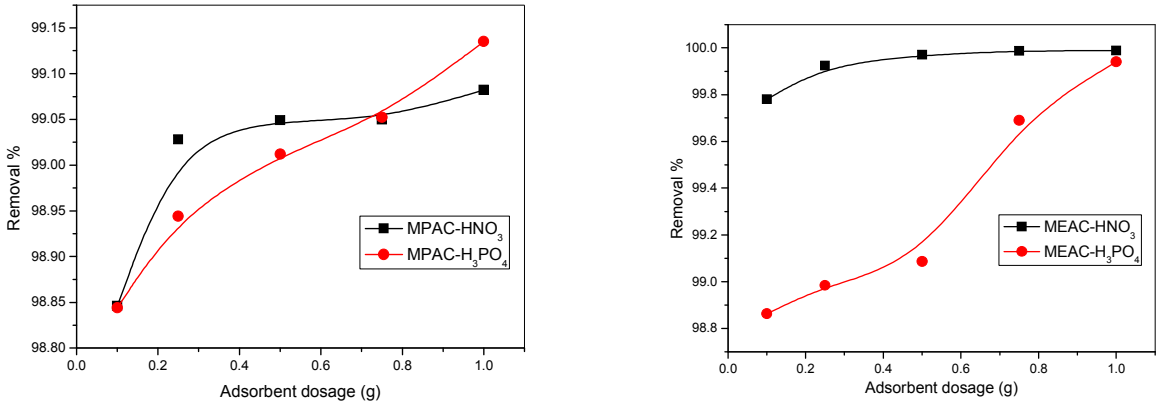

Fig. 4.1. Effect of adsorbent dosage on MB dye removal using different adsorbents

Effect of contact time

The effect of contact time on the removal of methylene blue dye was studied by varying the agitating time (range 2-60 min) at fixed optimum initial concentration of methylene blue (10 mg L^{-1}) and adsorbents dose of 0.5 g. The contact time plot shows the removal of methylene blue is rapid in early stages but it gradually slows down until it reaches the equilibrium. The initial rate of adsorption was greater because the diffusion of dye molecules through the solution to the surface adsorbents is affected by the dye concentration. Once equilibrium was attained, the percentage sorption did not change with further increases of time. The equilibrium was attained after agitating for 60 min at 242 rpm in an orbital shaker. The decrease in the extent of removal of methylene blue after 60 min of contact time in some cases may be due to the desorption process(Senthilkumar et al., 2005). The relation between contact time and percent removal of methylene blue is shown in the Fig. 4.2.

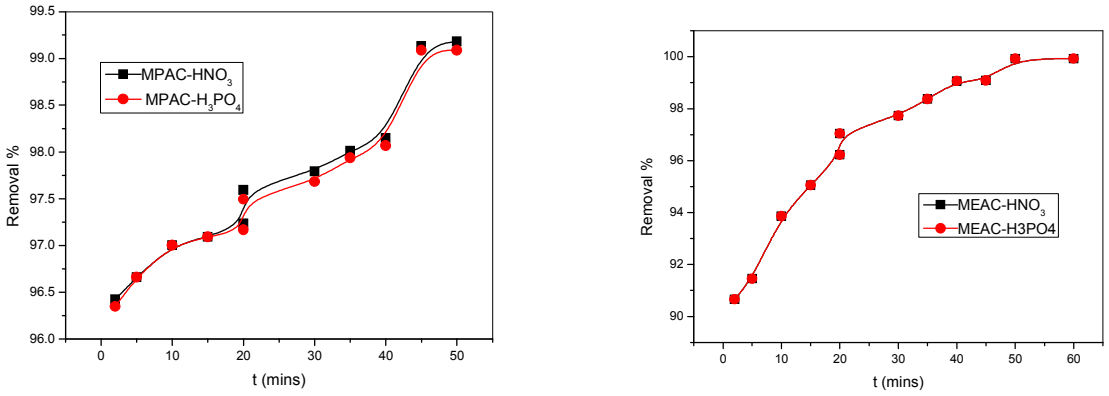

Fig. 4.2. Removal percentage of MB using different adsorbent at varying contact time

Effect of pH

The pH of a medium controls the magnitude of electrostatic charges which are imparted by the ionized dye molecules. As a result, the rate of adsorption will vary with the pH of an aqueous medium (Önal et al., 2006). The effects of initial pH on dye solution were investigated by varying the pH from 3 to 10 and using initial dye concentration of 10 mg L^{-1} with contact time of 50 mins for MPAC-HNO_3 and MPAC-H_3PO_4, and 60 mins for MEAC-HNO_3 and MEAC-H_3PO_4 maintained at 25±1°C. At pH 3 the removal was minimum but it increased along with increasing pH of dye solution. The result in the Fig. 4.3 shows that the maximum adsorption was observed at pH above 7 for all the adsorbents. The maximum adsorption was observed for MEAC-HNO_3 when pH was around 9 and 10. However, it may be noted that the percentage removal is appreciable good from pH above 4, suggesting the vast applicability of the adsorbent in; acidic, neutral and basic medium. The MB adsorption usually increases as the pH is increased. Lower adsorption of MB at acidic pH is probably due to the presence of excess H^+ ions competing with the cation groups on the dye for adsorption sites. At higher pH, the surface of activated carbon particles may get negatively charged, which enhances the adsorption of positively charged dye cations through electrostatic forces of attraction (Hameed et al., 2008a). Such observations were also reported by Hameed and Khaiary and others (Hameed and Khaiary, 2008b; Cengiz and Cavas, 2008).

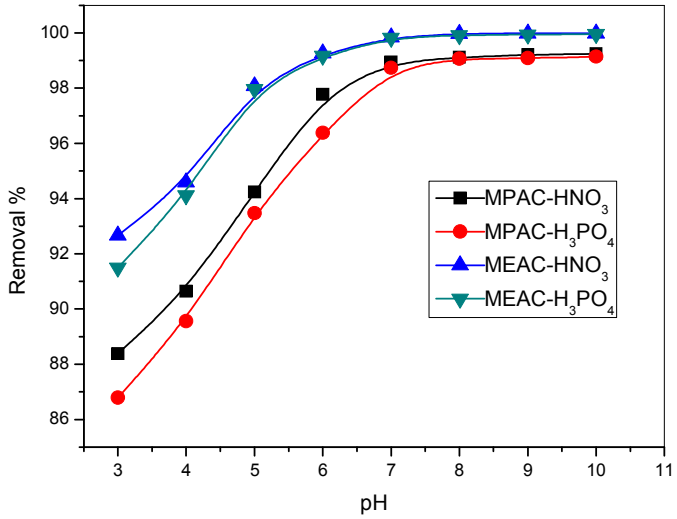

Fig. 4.3. Effect of pH on percent removal of methylene blue dye

Effect of concentration

The effect of concentration on the adsorption of methylene blue was studied by varying the dye concentration between 2-20 mg L^{-1} in 50 ml of methylene blue dye solution by adding .5 g of adsorbent and contact time of 60 mins. The effect of the dye concentration depends on the immediate relation between the dye concentration and the available binding sites on an adsorbent surface (Salleh et al., 2011). Thus, to find out the optimum relationship between the amounts of fixed adsorbent used against different dye concentration were studied with four adsorbents (MPAC-HNO_3, MPAC-H_3PO_4, MEAC-HNO_3 and MEAC-H_3PO_4). Generally the percentage of dye removal decreases with an increase in dye concentration, which may be due to the saturation of adsorption sites on the adsorbent surface (Eren and Acar, 2006). At low concentration, there will be unoccupied active sites on the adsorbent surface, and when the initial dye concentration increases, the active sites required for adsorption of the dye molecules will disappear (Kannan and Sundram, 2001c). However, the increase in the initial dye concentration will cause an increase in the loading capacity of the adsorbent and this may be due to the high driving force for mass at a high initial dye concentration (Gouamid et al., 2006). In other words, the residual concentration of dye molecules will be higher for higher initial dye concentrations. The variation of percent removal of methylene blue with increasing concentration is shown in Fig. 4.4. And variation of the amount of methylene blue adsorbed with increasing

concentration is shown in Fig. 4.5. The relevant data shows that the amount adsorbed exponentially increases while the percentage removal exponentially decreases with the increase in initial concentration of the methylene blue.

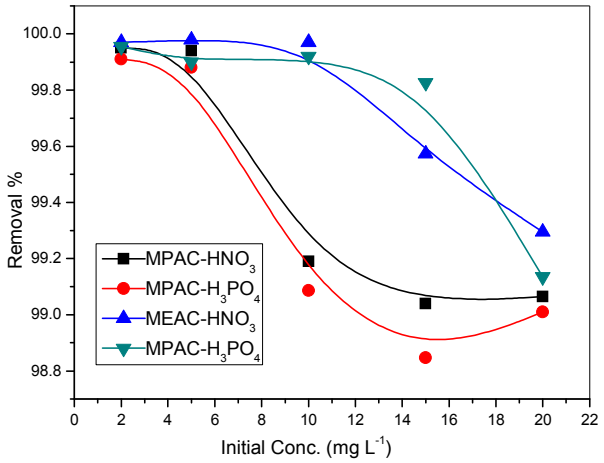

Fig 4.4. Variation of percent removal of methylene blue with increasing concentration.

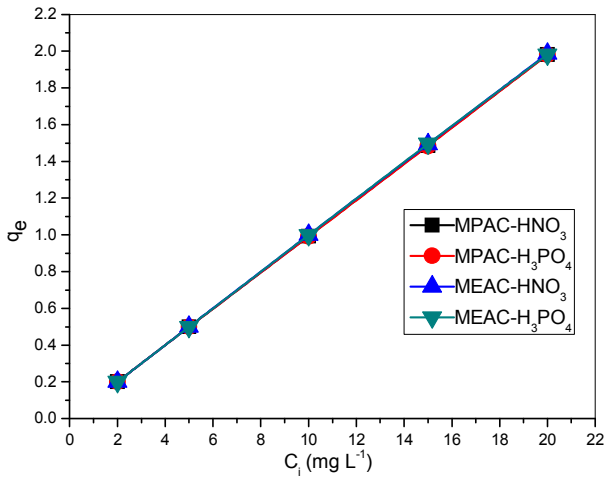

Fig. 4.5. Variation of the amount of methylene blue adsorbed with increasing concentration

Table 4.1. Different calculated values for adsorption study of MB by MPAC-HNO_3

Time (mins)	*Ce*	R %	q_e	C_e/q_e	$logC_e$	$logq_e$	q_t	$log(q_e-q_t)$	t/q_t	$t^{1/2}$
2	0.357	96.42	0.964	0.370	-0.446	-0.0158	0.9642	-1.5595	2.074	1.41
5	0.334	96.66	0.966	0.345	-0.476	-0.0147	0.9666	-1.5984	5.172	2.23
10	0.299	97.00	0.970	0.309	-0.523	-0.0132	0.9700	-1.6617	10.30	3.16
15	0.290	97.09	0.970	0.299	-0.536	-0.0128	0.9709	-1.6798	15.44	3.87
20	0.276	97.23	0.972	0.284	-0.558	-0.0121	0.9723	-1.7106	20.56	4.47
25	0.240	97.59	0.975	0.246	-0.618	-0.0105	0.9759	-1.7991	20.49	5.00
30	0.220	97.79	0.977	0.225	-0.656	-0.0097	0.9779	-1.8573	30.67	5.47
35	0.198	98.01	0.980	0.202	-0.701	-0.0087	0.9801	-1.9321	35.70	5.91
40	0.184	98.15	0.981	0.188	-0.733	-0.0081	0.9815	-1.9871	40.75	6.32
45	0.086	99.13	0.991	0.087	-1.061	-0.0037	0.9913	-3.3187	45.39	6.70
50	0.081	99.18	0.991	0.082	-1.086	-0.0035	0.9918	0.0000	50.41	7.07

Note* R%=Removal percentage. For different adsorption kinetics study, the values were taken up to 4^{th} decimals

Table 4.2. Different calculated values for adsorption study of MB by MPAC-H_3PO_4

Time (Mins)	*Ce*	R%	q_e	C_e/q_e	$logC_e$	$logq_e$	q_t	$log(q_e-q_t)$	t/q_t	$t^{1/2}$
2	0.365	96.34	0.963	0.379	-0.437	-0.0161	0.9634	-1.5476	2.07	1.41
5	0.341	96.66	0.965	0.353	-0.467	-0.0150	0.9659	-1.5865	5.17	2.23
10	0.303	97.00	0.969	0.312	-0.518	-0.0133	0.9696	-1.6548	10.31	3.16
15	0.298	97.09	0.970	0.307	-0.524	-0.0131	0.9701	-1.6639	15.46	3.87
20	0.283	97.16	0.971	0.291	-0.547	-0.0124	0.9716	-1.6961	20.58	4.47
25	0.250	97.49	0.974	0.257	-0.601	-0.0110	0.9749	-1.7728	20.51	5.00
30	0.231	97.68	0.976	0.237	-0.635	-0.0101	0.9768	-1.8244	30.71	5.47
35	0.206	97.93	0.979	0.210	-0.685	0.0090	0.9793	-1.9051	35.73	5.91
40	0.193	98.06	0.980	0.197	-0.713	-0.0084	0.9806	-1.9535	40.78	6.32
45	0.091	99.08	0.990	0.092	-1.039	-0.0039	0.9908	-3.0268	45.41	6.70
50	0.091	99.08	0.990	0.092	-1.039	-0.0039	0.9908	-3.0222	50.46	7.07

Note* Note* R%=Removal percentage. For different adsorption kinetics study, the values were taken up to 4^{th} decimals

Table 4.3. Different calculated values for adsorption study of MB by MEAC-HNO_3

Time (Mins)	*Ce*	R%	q_e	C_e/q_e	$logC_e$	$logq_e$	q_t	$log(q_e-q_t)$	t/q_t	$t^{1/2}$
2	0.613	93.87	0.938	0.653	-0.212	-0.0274	0.9387	-1.2748	2.13	1.41
5	0.421	95.79	0.957	0.439	-0.375	-0.0186	0.9579	-1.4696	5.21	2.23
10	0.206	97.85	0.978	0.210	-0.686	-0.0094	0.9785	-1.8758	10.21	3.16
15	0.215	97.94	0.979	0.219	-0.667	-0.0090	0.9794	-1.9062	15.31	3.87
20	0.139	98.29	0.982	0.141	-0.856	-0.0074	0.9829	-2.0501	20.34	4.47
25	0.171	98.61	0.986	0.173	-0.767	-0.0060	0.9861	-2.2433	20.28	5.00
30	0.138	98.62	0.986	0.139	-0.860	-0.0060	0.9862	-2.2510	30.41	5.47
35	0.091	99.09	0.990	0.091	-1.040	-0.0039	0.9909	-3.0409	35.32	5.91
40	0.051	99.49	0.994	0.051	-1.292	-0.0022	0.9949	0.0000	40.20	6.32
45	0.038	99.62	0.996	0.038	-1.420	-0.0016	0.9962	0.0000	45.17	6.70
50	0.003	99.97	0.999	0.003	-2.522	-0.0001	0.9997	0.0000	50.01	7.07
60	0.003	99.97	0.999	0.003	-2.522	-0.0001	0.9997	0.0000	60.01	7.74

Note* Note* R%=Removal percentage. For different adsorption kinetics study, the values were taken up to 4th decimals

Table 4.4. Different calculated values for adsorption study of MB by MEAC-H_3PO_4

Time (Mins)	*Ce*	R%	q_e	C_e/q_e	$logC_e$	$logq_e$	q_t	$log(q_e-q_t)$	t/q_t	$t^{1/2}$
2	0.934	90.66	0.906	1.030	-0.029	-0.0425	0.9066	-1.0695	2.20	1.41
5	0.855	91.45	0.914	0.934	-0.068	-0.0388	0.9145	-1.1117	5.46	2.23
10	0.614	93.86	0.938	0.654	-0.211	-0.0275	0.9386	-1.2740	10.65	3.16
15	0.495	95.05	0.950	0.520	-0.305	-0.0220	0.9505	-1.3839	15.78	3.87
20	0.378	96.22	0.962	0.392	-0.422	-0.0167	0.9622	-1.5285	20.78	4.47
25	0.296	97.04	0.970	0.305	-0.528	-0.0130	0.9704	-1.6693	20.61	5.00
30	0.227	97.73	0.977	0.232	-0.643	-0.0099	0.9773	-1.8383	30.69	5.47
35	0.163	98.37	0.983	0.165	-0.787	-0.0071	0.9837	-2.0909	35.57	5.91
40	0.094	99.06	0.990	0.094	-1.026	-0.0041	0.9906	-2.9172	40.37	6.32
45	0.092	99.08	0.990	0.092	-1.036	-0.0040	0.9908	-2.9956	45.41	6.70
50	0.089	99.92	0.999	0.008	-2.096	-0.0003	0.9992	0.0000	50.04	7.07
60	0.008	99.92	0.999	0.008	-2.096	-0.0003	0.9992	0.0000	60.04	7.74

Note* Note* R%=Removal percentage. For different adsorption kinetics study, the values were taken up to 4th decimals

Effect of Temperature

The effect of temperature on the removal of MB was studied at four different temperatures of 298K, 308K, 318K and 328K. The results are tabulated in Table 4.5-4.8 and the graphical representation of removal percentage of MB dye against temperature is shown in Fig. 4.6. The experimental results indicated that the magnitude of adsorption was proportional to the solution temperature. When the temperature increased from 298-328K, there was an increased in the adsorption of

MB onto the activated carbon samples. It is evident from the Table 4.5 the increase in the temperature show only a small degree of changes in the adsorption of MB. However, the temperature factors does not produce any significant adsorption of MB from aqueous solution, it was observed that the maximum removal of MB dye was at 328K for the entire carbon absorbents under investigation. This is also an indication about the utility of activated carbon performance under varying temperature on the removal of dye.

Table 4.5. Effect of temperature on removal MB dye using MPAC-HNO_3 at different T(K)

Time	298K		308K		318K		328K	
(mins)	C_e	R%	C_e	R %	C_e	R%	C_e	R %
2	0.357	96.42	0.356	96.43	0.350	96.49	0.348	96.51
5	0.334	96.66	0.325	96.66	0.313	96.66	0.307	96.66
10	0.299	97.00	0.293	97.00	0.290	97.00	0.283	97.00
15	0.290	97.09	0.280	97.09	0.278	97.09	0.270	97.09
20	0.276	97.23	0.269	97.30	0.260	97.39	0.256	97.43
20	0.240	97.59	0.239	97.60	0.228	97.71	0.221	97.78
30	0.220	97.79	0.220	97.80	0.216	97.83	0.208	97.91
35	0.198	98.01	0.191	98.08	0.186	98.13	0.180	98.19
40	0.184	98.15	0.174	98.25	0.170	98.29	0.167	98.32
45	0.086	99.13	0.086	99.13	0.084	99.15	0.083	99.16
50	0.081	99.18	0.081	99.19	0.078	99.21	0.073	99.26

Note* R%=Removal percentage

Table 4.6. Effect of temperature on removal MB dye using MPAC-H_3PO_4 at different T(K)

Time	298K		308K		318K		328K	
(mins)	C_e	R %	C_e	R%	C_e	R%	C_e	R %
2	0.365	96.34	0.357	96.42	0.356	96.43	0.351	96.48
5	0.341	96.66	0.334	96.66	0.331	96.66	0.327	96.66
10	0.303	97.00	0.299	97.00	0.291	97.00	0.288	97.00
15	0.298	97.09	0.290	97.09	0.286	97.09	0.280	97.09
20	0.283	97.16	0.276	97.23	0.267	97.32	0.261	97.38
20	0.250	97.49	0.240	97.59	0.239	97.60	0.231	97.69
30	0.231	97.68	0.220	97.79	0.218	97.81	0.210	97.89
35	0.206	97.93	0.198	98.01	0.190	98.09	0.187	98.12
40	0.193	98.06	0.184	98.15	0.178	98.21	0.171	98.28
45	0.091	99.08	0.086	99.13	0.085	99.14	0.085	99.14
50	0.091	99.08	0.088	99.11	0.085	99.15	0.085	99.16

Table 4.7. Effect of temperature on removal MB dye using MEAC-HNO_3 at different T(K)

Time	298K		3 08K		318K		328K	
(mins)	C_e	R%	C_e	R %	C_e	R%	C_e	R%
2	0.613	93.87	0.601	93.99	0.589	94.11	0.563	94.37
5	0.421	95.79	0.396	96.04	0.357	96.43	0.321	96.79
10	0.206	98.05	0.294	97.99	0.244	98.22	0.218	98.24
15	0.195	97.94	0.201	97.06	0.178	97.56	0.176	97.82
20	0.191	98.29	0.188	98.32	0.161	98.53	0.149	98.67
25	0.171	98.09	0.168	98.12	0.147	98.39	0.133	98.51
30	0.138	98.62	0.136	98.64	0.132	98.68	0.110	98.90
35	0.091	99.09	0.089	99.11	0.084	99.16	0.081	99.19
40	0.051	99.49	0.050	99.50	0.050	99.50	0.049	99.50
45	0.038	99.61	0.034	99.63	0.034	99.65	0.034	99.66

Note* R%=Removal percentage

Table. 4.8. Effect of temperature on removal MB dye using MEAC-H_3PO_4 at different T(K)

Time	298K		308K		318K		328K	
(mins)	C_e	R %	C_e	R %	C_e	R %	C_e	R%
2	0.934	90.66	0.901	90.99	0.885	91.15	0.873	91.27
5	0.855	91.45	0.818	91.82	0.800	92.00	0.798	92.02
10	0.614	93.86	0.577	94.23	0.516	94.84	0.501	94.99
15	0.495	95.05	0.443	95.57	0.400	96.00	0.396	96.04
20	0.378	96.22	0.316	96.84	0.298	97.02	0.228	97.72
20	0.296	97.04	0.211	97.89	0.201	97.99	0.190	98.10
30	0.227	97.73	0.209	97.91	0.193	98.07	0.188	98.12
35	0.163	98.37	0.114	98.86	0.101	98.99	0.096	99.04
40	0.094	99.06	0.091	99.09	0.089	99.11	0.087	99.13
45	0.092	99.08	0.089	99.11	0.087	99.13	0.085	99.15

Note* R%=Removal percentage

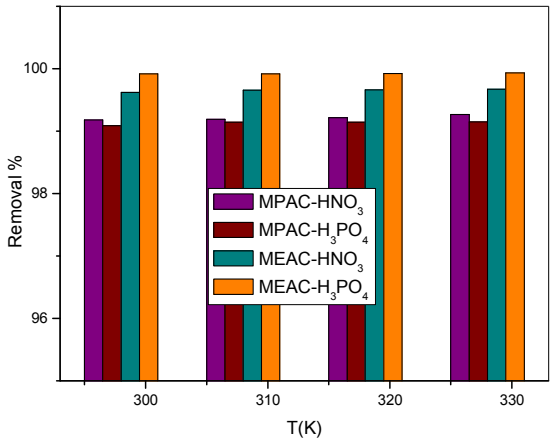

Fig. 4.6. Graphical representation of the removal of MB dye by different adsorbents at different temperature

4.4.1. Adsorption isotherm study of methylene blue adsorption

Methylene blue kinetic and isotherm adsorption experiments were carried out to evaluate the adsorption performance of chemically modified activated carbon. An adsorption isotherm gives the relationship between the amount of a substance adsorbed at constant temperature and its concentration in the equilibrium solution (Ketcha1et al., 2012). Langmuir, Freundlich and Temkin adsorption isotherm models are employed in this study to describe the experimental adsorption isotherm.

Langmuir adsorption isotherm for MB adsorption

The Langmuir isotherm model was obtained by using Eq. (2) of chapter-1 i.e., C_e vs C_e/q_e (the values of C_e and C_e/q_e are shown in Table 4.1-4.4). The plot of Langmuir model is shown in Fig. 4.8-4.9. The different experimental data obtained for Langmuir isotherm are shown in Table 4.9. From the isotherm, the theoretical monolayer capacity (q_m) was found to be 1.044, 1.045, 1.062 and 1.099 for MPAC-HNO_3, MPAC-H_3PO_4, MEAC-HNO_3 and MEAC-H_3PO_4 respectively. Among the four adsorbent the value of Langmuir constant (K_L) was found to be highest for MPAC-HNO_3 (256.41 g L^{-1}) and least for MEAC-H_3PO_4 (90.90). This indicates that the surface modification by different activating agent produces adsorbent with different properties, hence, different adsorption capacities. The favourability of adsorption of adsorbate onto the adsorbent has been defined by a factor called dimensionless constant separation factor denoted by R_L. Adsorption onto adsorbent is considered favourable when R_L value lies in the range of 0-1, in this present study, the value obtained were all in the favourable adsorption range, i.e., 0.0003, 0.0004, 0.004 and 0.0009 for MPAC-HNO_3, MPAC-H_3PO_4, MEAC-HNO_3 and MEAC-H_3PO_4 respectively. The degree of favourability for all the activated carbon tented more towards zero rather than unity which suggest completely ideal irreversible case. A good linear correlation co-efficient value was obtained from the plot 0.999, 0.999, 0.999 and 0.999 for all the carbon samples under study. Thus, it was experimentally determined that the adsorption of MB dye was very favourable on all the carbon samples. Thus, from the experimentally determined data it can be noted that the adsorption of MB dye is favoured in the form of monolayer coverage on the surface of the adsorbent containing a finite number of adsorption sites of uniform strategies of adsorption with no transmigration of adsorbate in the plane and also indicate the

homogeneous distribution of active sites on the adsorbent, since the Langmuir equation assumes that the surface is homogeneous

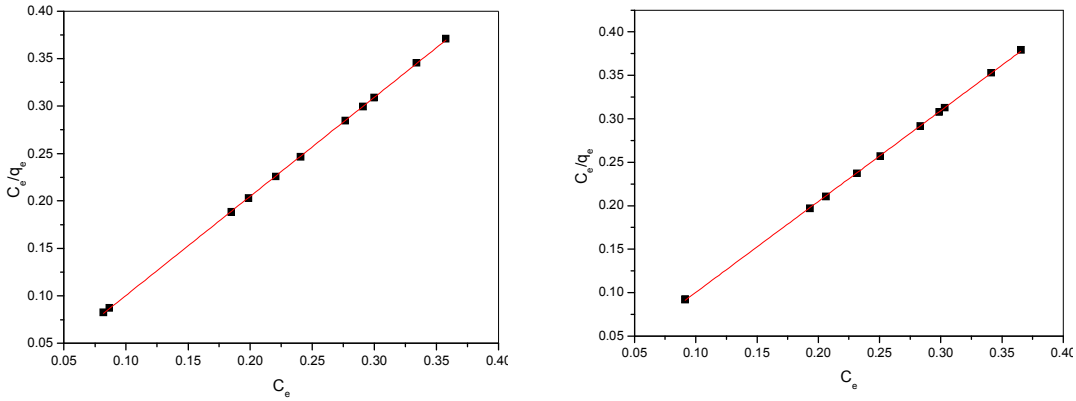

Fig. 4.8. Langmuir adsorption isotherms for the removal MB dye by a)MPAC-HNO_3 b)MPAC-H_3PO_4

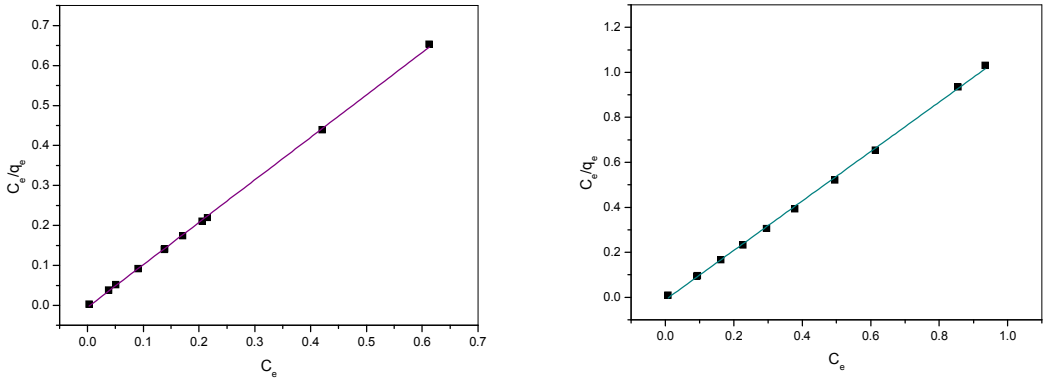

Fig. 4.9. Langmuir adsorption isotherms for the removal MB dye a) MEAC-HNO_3 b)MEAC-H_3PO_4

Table 4.9. Different parameters of Langmuir adsorption isotherm for MB dye removal.

Adsorbent	a_L/k_L	K_L	a_L	R_L	R^2	$q_{e(exp)}$	$q_{e(cal)}$	χ^2
MPAC-HNO_3	1.044	256.40	267.69	0.0003	0.999	0.991	0.954	0.0014
MPAC-H_3PO_4	1.045	232.55	234.02	0.0004	0.999	0.990	0.989	0.00002
MEAC-HNO_3	1.062	227.27	241.36	0.0004	0.999	0.999	0.937	0.0038
MEAC-H_3PO_4	1.099	90.900	99.910	0.0009	0.999	0.999	0.900	0.0096

Note* Unit of q_e=(mg g^{-1})

Freundlich adsorption isotherm for MB adsorption

A Freundlich isotherm model is obtained by plotting $logC_e$ vs $logq_e$ from Eq.4 of chapter-1 (the values of $logC_e$ and $logq_e$ are given in table 4.1-4.4.) and are shown in

Fig. 4.10-4.11. The values of adsorption capacity *K* and *1/n* are obtained from the slope and the intercept of the linear Freundlich plots. The *K* value was found to be 0.949, 0.948, 0962, 0.938 and *1/n* value were found to be -0.018, -0.019, -0.008 and -0.016 for MPAC-HNO_3, MPAC-H_3PO_4, MEAC-HNO_3 and MEAC-H_3PO_4 respectively. The negative *1/n* values suggest that the adsorption data are not significantly suite for this model which was also supported by low correlation factor obtained from the plot. Freundlich isotherm parameters for the MB dye adsorption on the different carbons samples are tabulated in Table 4.10. Thus, the experimental data suggest that the Freundlich isotherm is less suited for adsorption of MB dye onto activated carbon samples under study.

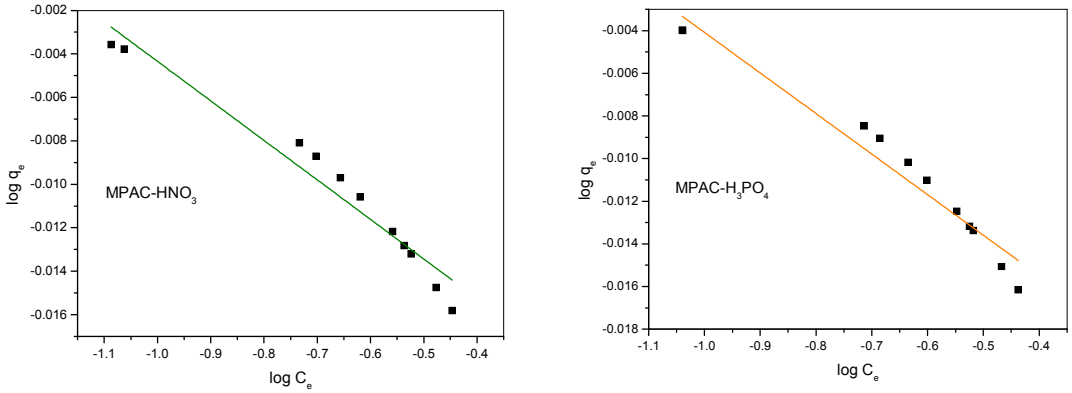

Fig. 4.10. Freundlich adsorption isotherms for the removal of MB dye by different adsorbents.

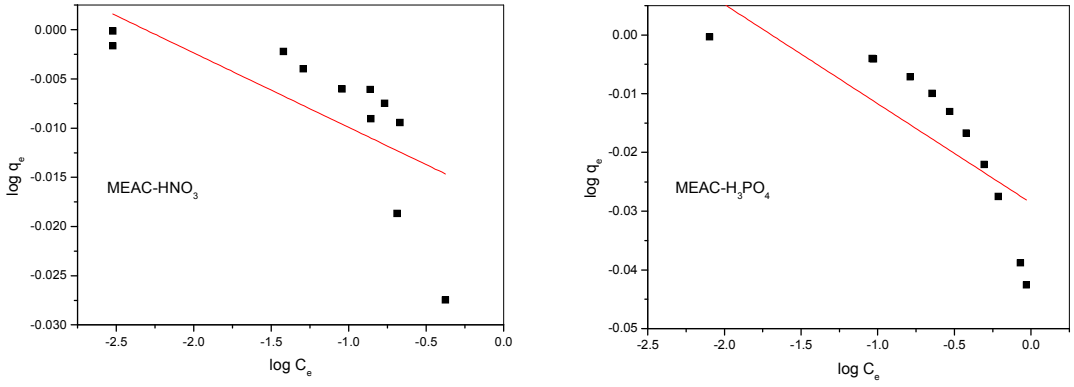

Fig. 4.11. Freundlich adsorption isotherms for the removal of MB dye by different adsorbents.

Table 4.10. Freundlich isotherm for MB dye adsorption

Adsorbent	*logK*	*1/n*	*K*	*n*	R^2	$q_{e(exp)}$	$q_{e(Cal)}$	χ^2
MPAC-HNO_3	-0.022	-0.018	0.949	-55.5	0.949	0.9918	0.994	0.000004
MAPC-H_3PO_4	-0.023	-0.019	0.948	-52.6	0.953	0.9908	0.993	0.000005
MEAC-HNO_3	-0.017	- 0.008	0.962	-125	0.503	0.9997	0.989	0.00011
MEAC-H_3PO_4	-0.028	- 0.016	0.938	-62.5	0.043	0.9992	0.942	0.00250

Note* Unit of K=($mg^{1-1/n}\ L^{1/n}\ g^{-1}$), n=($g\ L^{-1}$) and q_e=($mg\ g^{-1}$)

Temkin adsorption isotherm for MB adsorption

The plot of Temkin isotherm q_e vs lnC_e (the values of q_e vs lnC_e were obtained from Table 4.1-4.4.). The values of the Temkin constants A and B and the correlation coefficients are listed Table 4.12. From the Table 3.9, it can be concluded that the MEAC-H_3PO_4 possess maximum value of heat of sorption and the maximum binding energy values was shown by MEAC-HNO_3. The R^2 value of Temkin isotherm were in the range of 0.54-0.95 which is lower than both Langmuir and Freundlich values, which show poor linearity. This suggests that the Temkin isotherm may not be applicable for adsorption study of MB dye removal.

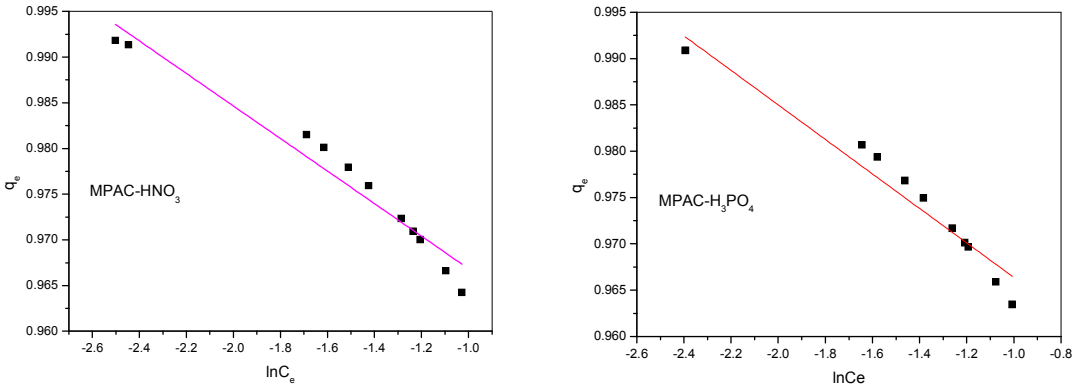

Fig.4.12. Temkin adsorption isotherms for the removal of MB dye by different adsorbents.

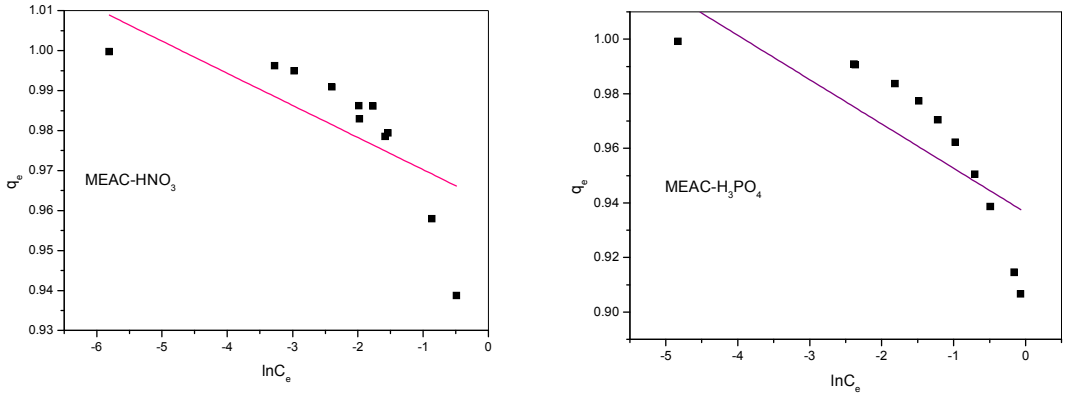

Fig.4.13. Temkin adsorption isotherms for the removal of MB dye by different adsorbents.

Table 4.11. Comparison of different parameters of Temkin adsorption isotherm for MB dye removal.

Adsorbent	*B*	*Bln(A)*	*A*	R^2	$q_{e(exp)}$	$q_{e(cal)}$	χ^2
MPAC-HNO_3	0.017	0.949	55.82	0.951	0.994	0.906	0.007
MPAC-H_3PO_4	0.018	0.947	52.61	0.955	0.993	0.903	0.008
MEAC-HNO_3	0.008	0.541	67.62	0.541	0.989	0.494	0.256
MEAC-H_3PO_4	0.016	0.654	40.87	0.654	0.942	0.577	0.157

Note* unit of *B*=($L^{-1}g$), *A*=($L^{-1}g$) *and* q_e=(mg g^{-1})

Chi-square analysis

Validity of the adsorption model was studied by chi-square analysis using Eq. (7) of chapter-1. From the χ^2 analysis and comparing the different adsorption isotherm models of Langmuir, Freundlich and Temkin isotherms from the corresponding χ^2 values, it can be concluded that Langmuir models show lowest χ^2 values compared to Freundlich and Temkin isotherm. Suggesting that the Langmuir adsorption model is best suited for MB dye adsorption from aqueous solution.

4.4.2. Adsorption Kinetics for methylene blue adsorption

Adsorption kinetics is one of the most important aspects for the consideration of adsorption efficiency (Hirunpraditkoon et al., 2015). The evaluation of kinetics is necessary in designing of sorption system. The overall adsorption process can typically be controlled by one or more activities, e.g., by film or external diffusion, surface diffusion, adsorption on the pore surface, pore diffusion, or a combination of these processes. Generally, both pore diffusion and film diffusion were considered to be the major factor in controlling the rates of sorption. Four simplified kinetics

models; pseudo first-order, pseudo second-order, intraparticle diffusion and elovich have been discussed to identify the rate and kinetics of adsorption of Methylene blue by different activated carbon samples.

Pseudo first-order model for MB adsorption

The linearised plot of pseudo first-order kinetic model was plotted using Eq. (8) of chapter-1, i.e., t/q_t vs t for adsorption of methylene blue by activated carbon. The plots are shown in Fig. 4.14-4.15 and the kinetic data for the adsorption of MB dye onto the activated carbons under different conditions were calculated from the related plots and are summarized in Table 4.12. All the adsorbents show good correlation co-efficient values in the range of 0.928-0.980. Thus, it indicates that the pseudo first-order model of adsorption is suitable for MB dye adsorption onto activated carbons.

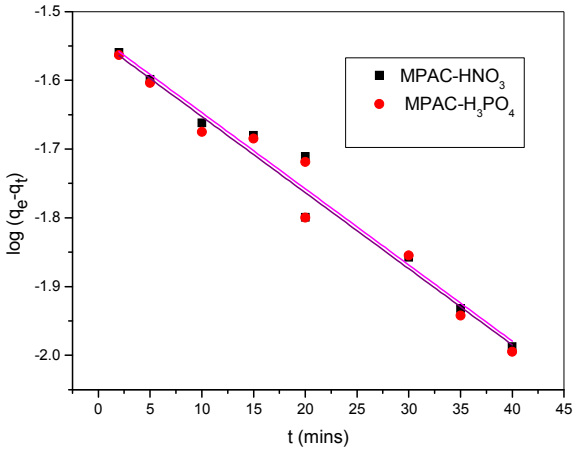

Fig. 4.14. Pseudo first-order plot for adsorption of MB dye by different adsorbents

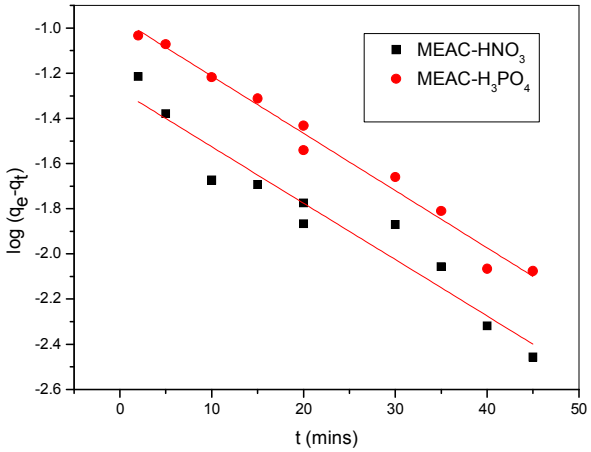

Fig. 4.15. Pseudo first-order plot for adsorption of MB dye by different adsorbents

Table. 4.12. Different parameters for Pseudo first order model for MB adsorption.

Adsorbent	$q_{e(exp)}$	$k_1 x10^{-1}$	$q_{e(cal)}$	*SSE*	R^2
MPAC-HNO_3	0.994	0.1108	0.980	0.0250	0.968
MPAC-H_3PO_4	0.993	0.1107	0.848	0.0250	0.967
MEAC-HNO_3	0.989	0.2495	1.001	0.0001	0.928
MEAC-H_3PO_4	0.942	0.2533	1.000	0.0002	0.980

Note* Unit of q_e = (mg g^{-1}) and k_1=(min^{-1})

Pseudo second-order model for MB adsorption

The linearised pseudo second-order model was plotted using Eq. (9) of chapter-1 i.e., *t/qt* vs *t* for the different adsorbents and are shown in Fig. 4.16-4.17 and the different values obtained from the plot are tabulated in Table 4.13. All the adsorbent gives good consistent correlation co-efficient (R^2) values of 0.999, 0.999, 0.999 and 0.999. The R^2 values are found to be considerably higher than that of pseudo first-order model, indicating that the pseudo second-order model fits better for MB dye adsorption on carbon samples. The favourability of pseudo second-order over pseudo first order is also supported by the lower values obtained from *SSE* analysis which reflects that the adsorption kinetics of MB dye onto all the adsorbents could be better described and approximated more by pseudo second-order model. Further, the close values of $q_{e(cal)}$ and $q_{e\ (exp)}$ also suggest that adsorption system follow pseudo second-order model. Similar trend have also been observed and reported for adsorption of MB dye on various adsorbents by several authors (Kavitha and Namasivayam 2007; Garagoz et al., 2008).

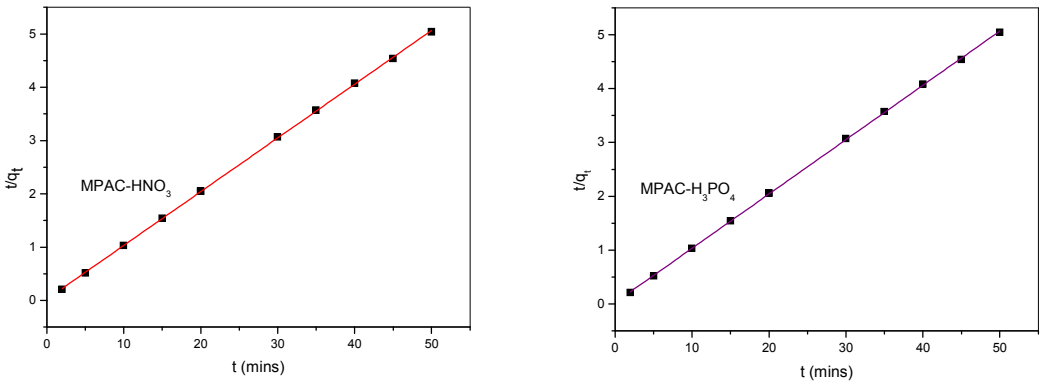

Fig. 4.16. Pseudo second-order isotherm for adsorption for MB dye by different adsorbents

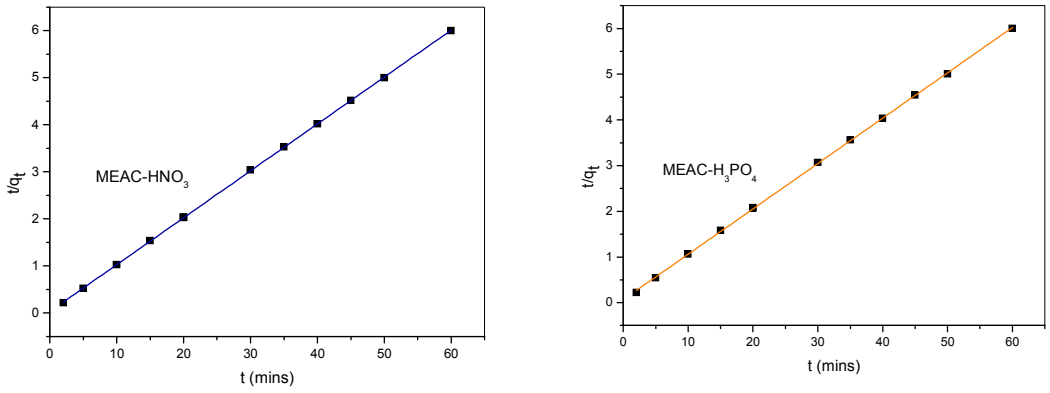

Fig. 4.17. Pseudo second-order plot for MB dye adsorption by different adsorbents

Table 4.13. Different parameters for Pseudo second-order model for MB adsorption

Adsorbent	$q_{e(exp)}$	k_2x10^{-1}	$q_{e(cal)}$	*SSE*	R^2
MPAC-HNO_3	0.994	0.1008	0.990	0.00001	0.999
MPAC-H_3PO_4	0.993	0.1009	0.997	0.00001	0.999
MEAC-HNO_3	0.989	0.0997	0.966	0.0005	0.999
MEAC-H_3PO_4	0.942	0.0992	0.924	0.0003	0.999

Note* Unit of q_e=(mg g^{-1}) and k_2=(g $mg^{-1}min^{-1}$)

Intraparticle diffusion model for MB adsorption

According to this model, the plot of the uptake, q_t, versus the square-root of time, $t^{1/2}$ is linear. Hence, using Eq. (10) of chapter-1, Weber and Morris equation for intraparticle diffusion, the plots of q_t vs $t^{1/2}$was plotted and are shown in Fig. 4.18 and the different values obtained are listed in Table 4.14. The value of intercept reflects about the thickness of the boundary layer, hence, larger the value thicker will be the boundary layer (Daifullah et al., 2007; Kumar et al., 2008). The correlation co-efficient values for all the adsorption were found to be low 0.75-0.80 except 0.96 in MEAC-H_3PO_4 which show deviation of straight lines from the origin. The highest value of *A* was found for MPAC-HNO_3 (0.95) suggesting thickest boundary layer Whereas MEAC-H_3PO_4 show thinnest boundary layer (0.88). The intraparticle diffusion is considered as the rate-controlling step model involved in the adsorption process if the line passes through the origin (Bhattacharyya and Sharma, 2004; Chen et al., 2003). But it is evident from the plot that the intercept of the line fails to pass through the origin in each case which may be due to difference in the rate of mass transfer (Panday et al., 1986), hence cannot be considered as a rate-limiting step. The divergence of slope values indicates that besides intraparticle diffusion process, there

may be other processes controlling the rate of adsorption, and all of which may be operating simultaneously.

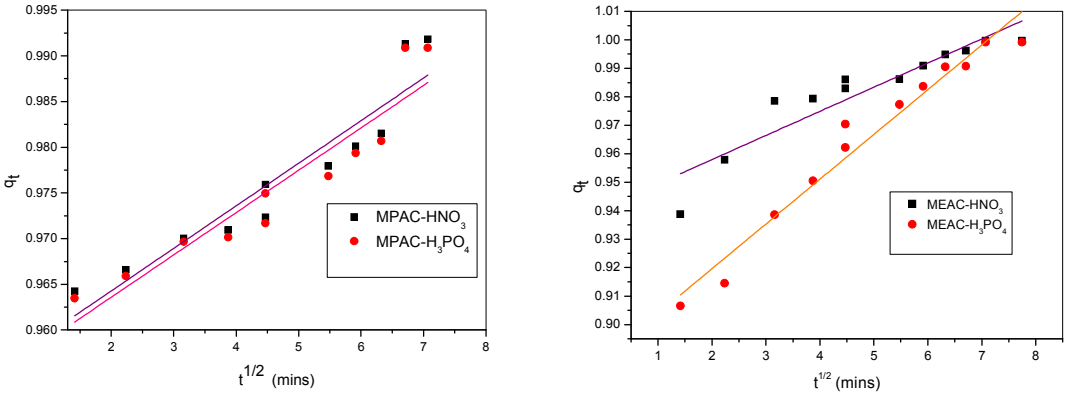

Fig. 4.18. Intraparticle diffusion plots of MB dye adsorption on various carbon adsorbents.

Table. 4.14. Different parameters obtained for intraparticle diffusion model

Adsorbent	$q_{e(expt)}$	$k_b x10^{-1}$	A (mg g^{-1})	R^2
MPAC-HNO_3	0.994	0.0047	0.955	0.897
MPAC-H_3PO_4	0.993	0.0046	0.954	0.801
MEAC-HNO_3	0.989	0.0080	0.940	0.836
MEAC-H_3PO_4	0.942	0.0015	0.888	0.802

Note* Unit of q_e = (mg g^{-1}), k_b=(mg g^{-1} min$^{-0.5}$) and A= (mg g^{-1}k$_b$)

Elovich model for MB adsorption

The Elovich model was plotted using Eq. (11) of chapter-1, i.e., q_t vs *ln(t)* which are presented in Fig. 4.19 and the corresponding results obtained from the plot are summarized in table 4.15. The correlation co-efficient values were found to be in the range 0.741 and 0.736 for MPAC-HNO_3 and MPAC-H_3PO_4 whereas MPAC-HNO_3 and MPAC-H_3PO_4 gives good correlation co-efficient values of 0.965 and 0.964.this suggest that diffusion accounted for the Elovich kinetics pattern is more significant in MPAC-HNO_3 and MPAC-H_3PO_4.

Form the comparisons among different model of kinetics study; it is apparent that the good fitting of the kinetic values from the observed R^2 is shown by pseudo second-order model (Table 4.13). Thus, the dynamics of sorption could be better described by pseudo second-order model for adsorption of methylene blue.

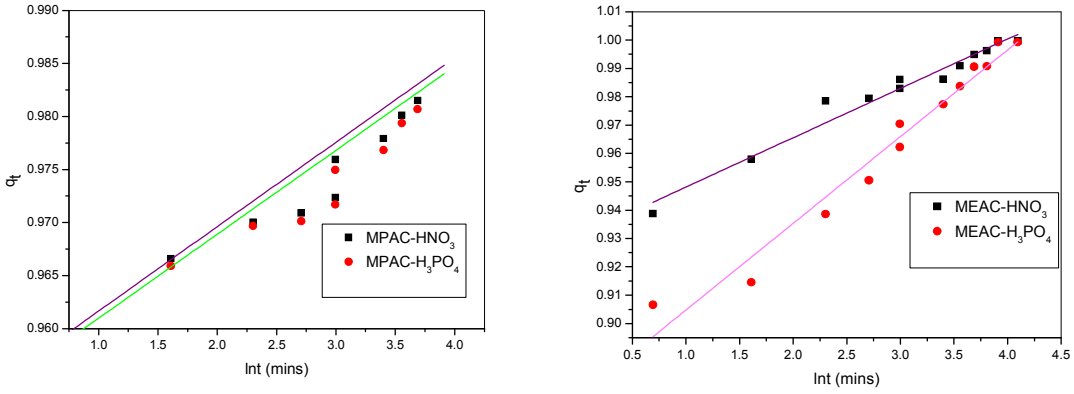

Fig. 4.19. Elovich plots for the removal of MB dye by adsorption on various adsorbents.

Table 4.15. Different parameters obtained from Elovich model

Adsorbent	$q_{e(exp)}$	β	R^2	α
MPAC-HNO_3	0.994	0.9537	0.741	0.0080
MPAC-H_3PO_4	0.993	0.9537	0.736	0.0079
MEAC-HNO_3	0.989	0.9300	0.965	0.0017
MEAC-H_3PO_4	0.942	0.8740	0.964	0.0303

Note*Unit of q_e =(mg g^{-1})

4.2.3. Thermodynamic parameters study

In order to determine the thermodynamic parameters involved in the adsorption of MB dye, adsorption experiments was carried out at four different temperatures range of 298, 308, 318 and 328 K. The values rate constant K_d are given in Table 4.16. The plot of lnK_d vs $1/T$ from Eq. (15) of chapter-1, which is a Vant Hoff plot, is shown in Fig.4.20 and 4.12. Different thermodynamic parameters ΔH^0 and ΔS^0 were obtained from slope and intercept of the plot. The value ΔG^0 was calculated using Eq. (16) of chapter-1. The endothermic nature of adsorption is indicated by positive value of ΔH^0 and this is also supported by the increase in K_0 value with increase in temperature. The change in the surface morphology during the adsorption reaction is suggested by positive value of $\Delta S.^0$ The Gibbs free energy changes (ΔG^0) of adsorption is normally negative for a better adsorption. Hence, in the present case the negative ΔG^0 indicates that the reaction involved during MB dye adsorption by the carbon adsorbent is a spontaneous process and it suggest that the adsorption of MD dye is favoured onto different carbon samples.

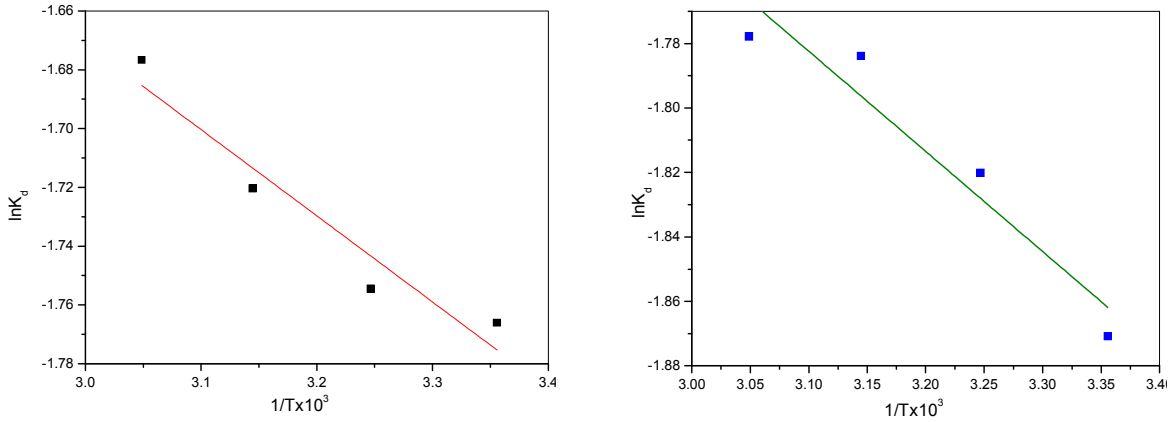

Fig. 4.20. Vant Hoff plot of MPAC-HNO_3 and MPAC-H_3PO_4

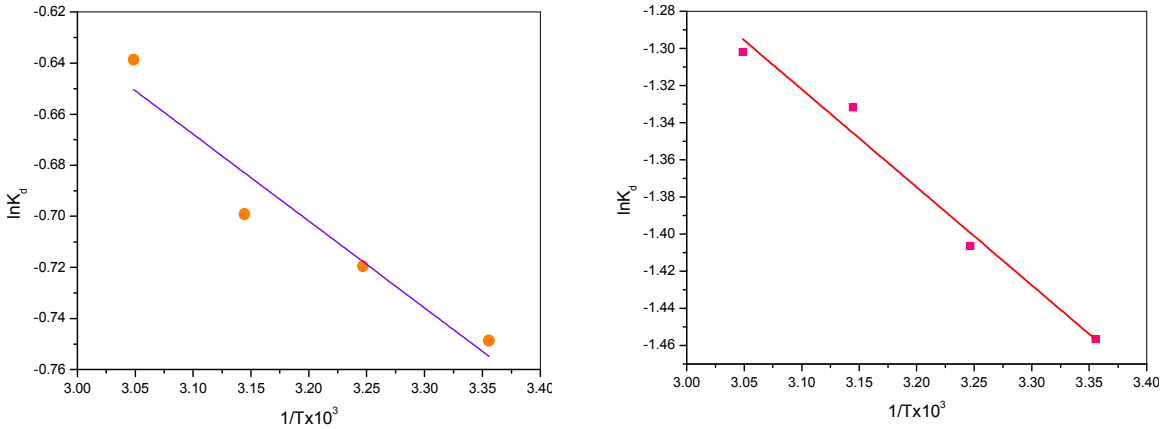

Fig. 4.21. Vant Hoff plot of MEAC-HNO_3 and MEAC-H_3PO_4

Table 4.16. Effect of temperature on the removal of MB dye using different adsorbents

Adsorbent	*T(K)*	C_e	q_e	k_d	lnk_d	*1/T(K)*
MPAC-HNO_3	298	0.081	0.991	12.110	2.494	0.0033
	308	0.081	0.991	12.200	2.501	0.0032
	318	0.078	0.992	12.682	2.540	0.0031
	328	0.073	0.992	13.516	2.603	0.0030
MPAC-H_3PO_4	298	0.038	0.996	26.215	3.266	0.0033
	308	0.034	0.996	28.885	3.363	0.0032
	318	0.034	0.996	29.139	3.372	0.0031
	328	0.034	0.996	29.311	3.377	0.0030
MEAC-HNO_3	298	0.091	0.991	10.847	2.383	0.0033
	308	0.088	0.991	11.189	2.415	0.0032
	318	0.085	0.991	11.551	2.446	0.0031
	328	0.085	0.990	11.602	2.451	0.0030

MEAC-H_3PO_4	298	0.008	0.999	117.547	4.766	0.0033
	308	0.008	0.999	118.947	4.778	0.0032
	318	0.008	0.999	120.381	4.790	0.0031
	328	0.007	0.999	136.886	4.919	0.0030

Table 4.17. Different thermodynamic parameters for removal of MB dye using various carbon adsorbents

Adsorbent	ΔH^0	ΔS^o	ΔG^0			
			298(K)	303(K)	308(K)	313(K)
MPAC-HNO_3	2.963	30.5	-6.126	-6.431	-6.763	-7.041
MPAC-H_3PO_4	2.493	26.2	-5.315	-5.577	-5.8386	-6.101
MEAC-HNO_3	2.838	36.8	-8.128	-8.496	-8.896	-9.265
MEAC-H_3PO_4	3.748	52.1	-11.77	-12.298	-12.819	-13.34

Note* Unit of ΔH^0 =(KJ mol^{-1}), ΔS^o=(J $mol^{-1}K^{-1}$) and ΔG^0 =(KJ mol^{-1})

4. 5. Conclusions

Adsorption studies of methylene blue on activated carbons was studied where effect of initial concentration, adsorbent dose, contact time and pH were the parameters considered to determine the adsorption efficiency of the carbon samples. The results of the percentage removal of methylene blue dye increased with the increase of contact time, pH and the dose of adsorbent. On the contrary, the removal percentage decreased with the increase in concentration of the standard methylene blue solution. The basic medium highly influences the higher removal of the dye which may due to the preference of the cations present on the dye molecule for basic sites. The results suggest that intra particle adsorption is very important in adsorption processes. The adsorption processes is found to be pseudo second order. The equilibrium data have been analyzed using Langmuir, Frendulich and Temkin isotherms. The adsorption data obeyed Langmuir isotherms and indicates the formation of uni-molecular layer of adsorption. Out of three isotherm models studied for this adsorbent-adsorbate system, Langmuir model shows best fit with consistent correlation coefficient of 0.999, 0.999, 0.999 and 0.999 for all the adsorbents. So, these activated carbons can be effectively used for the removal of methylene blue dye from aqueous solution. Among the four low-cost adsorbents under consideration, the order of adsorption capacity of the various adsorbents is as follows: MEAC-HNO_3 > MEAC-HNO_3>MEAC-H_3PO_4 > MPAC-H_3PO_4. MEAC-HNO_3 possesses the highest or the maximum adsorption capacity. Hence it is the best and the most effective adsorbent in the removal of methylene blue content in water. The suggested adsorbent materials are very cheap and are abundantly available. Because of their economic viability, these low cost

adsorbents can be used in the process of eliminating the undesirable and unwanted ingredients in water.

References

Ahmad, R. (2009). Studies on adsorption of crystal violet dye from aqueous solution onto coniferous pinus bark powder (CPBP*). J Harz Mater,* 171(1):767-173.

Aksu, Z. (2005). Application of biosorption for the removal of organic pollutants: a review. *Process Biochem,* 40(3-4):997-1026.

An, T., Li, G., Xiong, Y., Zhu, X., Xing, H., Liu, G. (2001). Photo electrochemical degradation of methylene blue with nano TiO_2 under high potential bias. *Mater Phys Mech*, 4:101-106.

Avom, J., Mbadcam, J.K., Noubactep, C, Germain, P. (1997). Adsorption of methylene blue from an aqueous solution onto activated carbon from palm-tree cobs. *Carbon*, 35: 365–369.

Aygun, A., Yenisoy-Karakas, S., Duman, I. (2003). Production of granular activated carbon from fruit stones and nutshells and evaluation of their physical, chemical and adsorption properties. *MicroporMesopor Mater,* 66:189–195.

Bhattacharyya, K.G., Sharma, A., (2004). Azadirachta indica leaf powder as an effective biosorbent for dyes: A case study with aqueous Congo red solutions. *J Environ Manage*, 71:217–229.

Cengiz, S., Cavas, L. (2008). Removal of methylene blue by invasive marine seaweed: *Caulerpa recemosa* var, cylindracea. *Bioresour Technol,* 99(7):2357-2363.

Chen, J.P., Wu, S., Chong, K.H. (2003). Surface modification of a granular activated carbon by citric acid for enhancement of copper adsorption. *Carbon* 41:1979–1986.

Daifullah, A.A.M., Yakout, S.M., Elreefy, S.A. (2007). Adsorption of fluoride in aqueous solutions using $KMnO_4$–modified activated carbon derived from steam pyrolysis of rice straw. *J Hazard Mater*, 147: 633-643.

El-Sheikh, A. H., Newman, A.P. (2004). Characterization of activated carbon prepared from a single cultivar of Jordanian olive stones by chemical and physiochemical techniques. *J Analy Appl Pyrol,* 71:151–164.

Eren, z., Acar, F.N. (2006). Adsorption of reactive black 5 from an aqueous solution: equilibrium and kinetic studies. *Desalination,* 194-201.

Franca, A.S., Oliveira, L.S., Ferreira, M.E. (2009). Kinetics and equilibrium studies of methylene blue adsorption by spent coffee grounds. *Desalination*, 249:267–272.

Gahr, F., Hermanutz, F., Opperman, W. (1994). Ozonation: An important technique to comply with new German law for Textile wastewater treatment. *Water Sci Technol,* 30:255-263.

Garg, V.K., Amita, M., Kumar, R., Gupta, R. (2004). Basic dye (methylene blue) removal from simulated waste-water by adsorption using indian rosewood sawdust: a timber industry waste. *Dyes and Pigments*, 63(3):243-250.

Girgis, B.S., El-Hendawy, A.A. (2002). Porosity development in activated carbons obtained from date pits under chemical activation with phosphoric acid. *Micropor Mesopor Mater*, 52:105–117.

Ghouti, M.A., Khraisheh, M.A., Allen, S.J., Ahmad, M.N. (2003). The removal of dyes from textile waste water: A study of the physical characteristics and adsorption mechanisms of diatomaceous earth. *J Environ Manage*, 69(3):229-238.

Gouamid, M., Ouahrani, M.R., Bensaic, M.B. (2006). Adsorption equilibrium, kinetics and thermodynamics of methylene blue from aqueous solutions using date palm leaves. *Desalination,* 194-259.

Gupta, V. (2009). Application of low-cost adsorbents for dye removal: a review. *J EnvironmManag,* 90(8):2313-2342.

Haimour, N., Sayed, S. (1997). The adsorption kinetics of methylene blue dye on jift, Dirsat. *Natur Eng Sci,* 24:215-224.

Hameed, B.H., Mahmoud, D.K., Ahmad, A.L. (2008a). Equilibrium modelingand kinetic studies on the adsorption of basic dye by a low-cost adsorbent: Coconut (*Cocosnucifera*) bunch waste. *J Hazard Mater*, 158:65–72.

Hameed, B.H., Khaiary. M.I.E. (2008b). Sorption kinetics and isotherm studies of a cationic dye using agricultural waste: broad bean peels. *J Hazard Mater,* 154:639–648.

Hirunpraditkoon, Srinophakun, P., Sombun, N. (2015). Synthesis of activated carbon from jatropha seed coat and application. 202(1):32-47.

Ismadji, S., Sudaryanto, Y., Hartono, S.B., Setiawan, L.E.K., Ayucitra, A. (2005). Activated carbon from char obtained from vacuum pyrolysis of teak sawdust: pore structure development and characterization. *Bioresour technol,* 96(12):1364–1369.

Josefa, S.Y.M., Oliveira, E.D. (2003). Heavy metals removal in industrial effluents by sequential adsorption treatment. *Adv Environ Res*, 7: 263-272.

Kannan, N., Karuppasamy, K. (1998b). Low cost adsorbents for the removal of phenylacetic acid from aqueous solution. *Indian J Environ Pro*, 18(9):683-686.

Kannan, N., Vanangamudi, A. (1991a). A study on the removal of Chromium (VI) by adsorption on lignite coal. *Indian J Environ Prot,* 11:241-245.

Kannan, N., Sundaram, M.M. (2001c). Kinetics and mechanism of removal of methylene blue by adsorption on various carbons-a comparative study. *Dyes and Pigments,* 51:25-40.

Karagoz, S., Tay, T., Ucar, S., Erdem, M. (2008). Activated carbons from waste biomass by sulfuric acid activation and their use on methylene blue adsorption. *Bioresour Technol,* 99:6214–6222.

Kavitha, D., Namasivayam, C. (2007). Experimental and kinetic studies on methylene blue adsorption by coir pith carbon. *Bioresour Technol*, 98:14–21

Ketchal, J.M. (2012). Preparation and characterization of activated carbons obtained from maize cobs by zinc chloride activation. *Amer Chem Sci J,* 2(4):136-160.

Khan, A.R., Tahir, H., Uddin, F., Hameed, U. (2005). Adsorption of methylene blue from aqueous solution on the surface of Wool fiber and cotton fiber. *J appl sci Environ Manag,* 9(2): 29-35

Klass, D.L. (1998). Biomass for renewable energy, fuels, and chemicals. *Academic Press San Diego, CA.*

Knapp, J.S., Newby, P.S. (1995). The microbiological decolorization of an industrial effluent containing a diazo-linked chromophore. *Water Res,* 7:1807-1809.

Kumar, K.V., Sivanesan, S., Ramamurthi, V. (2004). Adsorption of methylene blue onto pithophorasp, Green pages-The Global Directory for Environmental Technology.

Lorenc-Grabowska, E., Gryglewicz, G. (2007). Adsorption characteristics of congo red on coal-based mesoporous activated carbon. *Dyes Pigments*, 74(1):34-40.

Malik, D.J., Strelko, V.Jr., Streat, M., Puziy, A.M. (2002). Characterization of novel modified active carbons and marine algal biomass for the selective adsorption of lead. *Water Res,* 36:1527-1538.

Manickavasakam, K., Krishnan, S.M., Sameena, Y., Vennilamani, N., Pattabhi, S. (2004). Removal of methylene blue from aqueous solution by adsorption onto activated Carbon. *Indian J Environ Pollut,* 24(7):534-541.

Mehmet, D., Alkan, M., Onganer, Y. (2000). Adsorption of methylene blue from aqueous solution onto Perlite, *Water Air Soil Pollut*, 120:3-4.

Mishra. G., Tripathy, M. (1993). A critical review of treatment for decolourization of textile effluents. *Colourage*, 40:35-38.

Mohammad, M.E., Muttucumlutants, S. (2009). Removal of pollutants removed by Electro coagulation and Electro coagulation/Flotation Processes. *J Environ Manag*, 90(5):1663-1679.

Namasivayam, C., Yamuna, R.T. (1994).Utilizing biogas residual slurry for dye adsorption. American Dyestuff Reporter.

Önal, Y., Akmil-Basar, C., Eren, D., SarIcI-Özdemir, C., Depci, T. (2006). Adsorption kinetics of Malachite green onto malachite green onto activated carbon prepared from Tuncbilek lignite. *J Harz Mater*, 128-150.

Otero, M., Rozada, F., Garcoia, A., Moran. (2003). A kinetic and equilibrium modelling of the methylene blue removal from solution by adsorbent materials produced from sewage sludges. *Eng J,* 15:59-68.

Panday, K.K., Prasad, G., Singh, V.N. (1986). Mixed adsorbent for Cu(II) removal from aqueous solution. *Environ Tech Lett,* 50:547–554.

Pollard, S.J.T., Fowler, G.D., Sollars, C.J., Perry, R. (1992). Low-cost adsorbents for waste and waste-water treatment*:* A Review. *Sci Total Environ*, 116(1-2): 31-52.

Raghuvanshi, S.P., Singh, R., Kaushik, C,P., Raghav, A.K. (2005). Removal of textile basic dye from aqueous solutions using saw dust as bio-sorbent, *Int J Environ Studies*, 62(3):329-339.

Rahman, I.A., Saad, B. (2003). Utilization of guava seeds as a source of activated carbon for removal of methylene blue from aqueous solution. *Malay J Chem*, 5(1):8-14.

Rajeshwarisivaraj, S., Sivakumar, P., Senthilkumar, V., Subburam. (2001). Carbon from cassava peel, an agricultural waste, as an adsorbent in the removal of dyes and metal ions from aqueous solution. *BioresourTechnol*, 80 :233–235.

Salleh, M.A.M., Mahmoud, M.A., Karim, W.A.W.A., Idris. A. (2011). Cationic and anionic dye adsorption by agricultural solid wastes: A comprehensive review. *Desalination,* 280(1):1-13.

Schwarzenbach, R.P., Egli, T., Hofstetter, T.B., Gunten, U.V., Wehrli, B. (2010). Global water pollution and human health. *Annual Review Environ Resourc,* 35:109-136.

Senthilkumaar, S., Varadarajan, P.R., Porkodi, K., Subbhuraam,C.V. (2005a). Adsorption of methylene blue onto jute fiber carbon: kinetics and equilibrium studies. *J Colloid Interf Sci* 284:78–82.

Taicheng, A, Li, G., Xiong, Y., Zhu, X., Xing, H., Liu, G. (2001). Photo electrochemical degradation of methylene blue with nano TiO_2 under high potential bias. *Mater Phys Mech,* 4:101- 106.

Tsai, W.T., Chang, C.Y., Lin, M.C., Chien, S.F., Sun, H.F., Hsieh, M.F. (2001). Adsorption of acid dye onto activated carbons prepared from agricultural waste bagasse by $ZnCl_2$ activation. *Chemosphere,* 45:51–58.

UN. (2016). The world water development report.

Wu, F.C., Tseng, R.L., Juang, R.S. (1999). Pore structure and adsorption performance of the activated carbons from plum kernels. *J Hazard Matter*, B69:287–302.

Wu, F., Tseng R. (2006). Preparation of highly porous carbon from fir- wood by KOH etching and CO_2 gasification for adsorption of dyes and phenols from water. *J Coll Interface Sci,* 294:21-30.

Yalc, N., Sevinc, V. (2000). Studies of the surface area and porosity of activated carbons prepared from rice husks. *Carbon,* 38:1943–1945.

Zahra, D., Mohammad, A. B., Mojdeh, R., Mohammad, F. (2013). Adsorption of methylene blue dye from aqueous solution by modified pumice stone: kinetics and equilibrium studies. *Health scope*, 2(3): 136-144.

Zolllinger, H. (1987). Color chemistry-synthesis, projects and applications of orange dyes and pigments. *VCH publisher, New York*.

CHAPTER-5

REMOVAL OF COLIFORM AND *E.coli* FROM WATER USING SAND SUPPORTED ACTIVATED CARBON

In this chapter study on removal of Escherichia coli from water sample using sand supported carbon column is reported. For this study, different types of carbon column are made with four types of activated carbon. Studies on total bacteria count, coliform bacteria detection, determination of Escherichia coli by serial dilution methods and removal of Escherichia coli are described in details.

5.1. Introduction

The provision of safe drinking water continues to be one of the challenges of 20th century public health. No water is 100% pure; water is contaminated with organic, inorganic and biological contaminants, and therefore water treatment becomes an essential requirement which reduces/removes undesired pollutants that are of concern to human health especially before using it for domestic purposes. Getting access to clean drinking water has become a major problem and it is of great concern especially in developing countries, particularly in rural areas. It is in fact alarming that almost 80% of all diseases in developing countries arise from consumption of polluted drinking water. The influences of agricultural and municipal wastewater, as well as the ageing of water treatment and distribution systems, continue to raise concerns about the microbiological quality of drinking water. Therefore, an amicable approached is required to address such issues by designing appropriate, low-cost and effective methods. In our present study among different water pollutants, *Escherichia coli* (or simply *E.coli*) bacteria was selected as a subject of study because of its adverse affect on human health. *E.coli* is a bacteria that has many strains and used as an indicator for the faecal contamination and other potentially harmful bacteria in a given water sample (Hunter 2003). It is observed that the gram-negative cell wall of *E.coli* is a multiplex system and can stay alive for prolonged periods in natural aqueous system (Jiang et al., 2007). The bacteria is usually transmitted to humans through water which may be contaminated in many different ways (Ashbolt et al., 2004) Although some *E. coli* bacteria that lives in the intestines of healthy humans and most warm-blooded animals helps to maintain the balance of normal intestinal flora (bacteria) against harmful bacteria but many other strains of *E.coli* causes severe illness like diarrhoea, respiratory illnesses, urinary tract infections, pneumonia, etc. especially among children and the elderly (Brenner et al., 1982; Huerata et al., 2000; Goncharuk and Vergolyas, 2014). It is therefore very crucial to remove it from water using suitable techniques. Different processes to reduce/remove *E.coli* bacteria from potable drinking water (Ashbolt et al., 2004) are available, which include techniques such as boiling, distillation, reverse osmosis, water filtration, ozonation, use of fibre filters, ceramic filters, UV irradiation, use of water softeners, activated alumina, sediment filter, etc. (Rivera-Utrilla et al., 2001; Mendez 2009). However, it was observed that removal of pathogens from water is often total; thus reducing the purity

of the water quality, especially for drinking purposes (Davis et al., 2009; Hunt et al., 2008). Moreover, these techniques used has different requirement like high maintenance, continuous power supply, generation of additional waste/ by products, low cost effectiveness etc. which makes their utility somewhat limited in certain cases. Hence an alternative technique is desired for removal of *E.coli* and it was found that this can be achieved by using adsorption technique aided by a low cost adsorbent such as activated carbon. Adsorption is an old process and is one of the preferred technique for the removal of pathogens from water systems (Akhtar 2005**;** Jaguaribe 2005; Kobya 2004). Among the different adsorbent materials available, activated carbon synthesized from various plant materials are of great use (Aji 2015; Ashoka and Inamdar, 2010**;** Cheenmatchaya and Kungwankunakorn, 2014; Chen et al., 2012; Cobb et al., 2012; Junior et al., 2014; Sivakumar et al., 2012; Tsai et al., 2001; Wartelle et al., 2001). It is a well established fact that activated carbon offers an extensive range of applications in separation and purification methods, biomedical development, energy storage and pollution control because of its high porosity and high surface area which is attributed to its high adsorption rate (Buasri et al., 2013; Ilaboya et al., 2013). This bio-adsorbent is usually treated with either acid/base to enhance its surface properties and thus increase its efficiency and selectivity. In this presented work, an attempt has been made to remove *E.coil* from potable water by using carbon based column and to a significant extent the results were satisfactory. The work was planned to utilise the adsorption capacity of activated carbon for adsorption of *E.coil* from water samples. In this chapter, the detail about construction of sand supported carbon column is described and its application in removal of *E.coli* from potable water is discussed. The carbons were synthesized from two kinds of locally available plant residues of *Mucuna pruriens* and *Manihot esculent* and activated by using HNO_3 and H_3PO_4.

5.2. Materials and methods

For this present study the synthesized carbon MPAC-HNO_3, MPAC-H_3PO_4, MEAC-HNO_3, MEAC-H_3PO_4 were used because of their great adsorptive properties. For bacterial study, different reagent like, agar solution, double and single strength lactose broth, brilliant green bile salt media were prepared. For removal of *E.coli* from water samples column was constructed using glass chromatography column. Details about the experimental procedures are discussed below.

Reagents. Peptone, Beef extract, Agar, lactose, bile salt, brilliant green, KBr, Reagent-grade water.

5.2.1. Preparation for different solution for *E.coli* study

To determine the presence of coliform bacteria "multiple fermentation tube" or "most probable number" technique was used. For this nutrient agar and different reagent consisting double and single strength lactose broth and brilliant green bile salt media were prepared as described below

Preparation of Nutrient agar

5.0 g of Peptone, 3.0 g of Beef extract and 15.0 g of agar were added to 1 L of reagent-grade water and the mixture was mixed thoroughly, and heated to dissolve completely. And it was dispensed into a screw-cap tube and autoclaved at 121°C (15 PSI) for 15 minutes. The pH of the final mixture was maintained at 6.8 ± 0.2.

Preparation of double and single strength lactose broth

For preparation of double strength lactose broth, 10 g each of lactose, peptone and beef extract were collected in a 1500 ml glass beaker and 1000 ml of distilled water was added into the mixture and pH 6.7 was maintained by adding small amount of water as per the requirement.

For preparation of single strength lactose broth, 250 ml of the double strength lactose broth solution was transferred into a 500 ml glass beaker and 250 ml of distilled was added to it and then it was autoclaved for 15 minutes at 120^{o}C.

Preparation of brilliant green bile salt media

1 g each of lactose and peptone and 2 g of bile salt along with 1 mg of brilliant green were taken in a 500 ml glass beaker followed by addition of 500 ml distilled water with constant stirring to give brilliant green bile salt media. The pH was maintained at pH 6.7 by adjusting the amount of water in the mixture and the solution was autoclaved for 15 minutes at 120^{0} C.

Column construction

For this *E.coli* removal study, a column was constructed using glass column of 2 cm diameter. The column was packed first with 2 g of sterilized sand, followed by addition of 1 g of *Mucuna pruriens* activated carbon. Thereafter around 2 g of sand was again added so that the carbon could be sandwiched between the two sand layers, thereby preventing the adsorbent from floating (Fig. 5.1)

Fig.5.1. Set up of Sand supported column

Collection of water sample

The water sample was collected from a pond located inside CSIR-NEIST, Jorhat, Assam. To study the presence of *E.coli,* pond water samples contaminated with coliform bacteria were collected in 500 ml sterilised stopper bottle. 100 ml of the sample was first tested to confirm the presence of *E. coli* bacteria. The details experimental are presented below.

5.3. Total bacteria count

The water samples collected were examined for possible bacterial contamination using pour plate method.

Pour plate method

For most potable water samples, plate suitable for containing will be obtained by degree plating 1ml and 0.1ml undiluted sample over media-Nutrient agar medium. Plating of the agar medium was done by melting the sterile solid agar medium in microwave oven. During pouring plates 10-12ml of liquefied medium maintained at 44-46^{o}C were poured into a sterilised petri dish. The plate was then allowed to solidify in a levelled surface. After solidification the plates were inverted and kept in an incubator. Sterility of medium was checked by pouring control plates for each series of sample. 1ml and 0.1 ml of sample were pipette out and slowly released into the medium plate by making to and fro motion. The inoculum was allowed to be absorbed on the surface of the medium before incubation at 37^{o}C for 48 hours.

Counting of the colonies was done after 48 hours using digital colony counter. The result of bacteriological testing were recorded as given below,

Parameter a) Total count/1ml as per 1s 10500

b) MPN coliforms/100ml

c) MPN for *E.coli*/100 ml

Total bacteria colony count

For determination of total bacteria colony count, the experiments were carried out under laminar flow environment (Fig. 5.2), wherein 1 ml of the collected sample was evenly distributed on a petri dish and liquefied readymade agar solution was gently poured into the petri dish followed by incubation for 24 hours at 37^0C. The sample was studied from the agar plate using colony counter-digital (Hi Media laboratory).

Fig.5.2. Experimental set up for bacteria count in the Laminar flow

***E. Coli* study by multiple tube fermentation methods**

In order to study the presence of coliform bacteria present in the water sample, further experiment were carried out using multiple fermentation methods.

Test for confirmation of coliform bacterial activity

After the colony count, 3 sets of 5 sterilised test tubes each were taken for this study and labelled as set 1, set 2 and set 3. Thereafter, 10 ml of water sample was taken in each test tube of set 1 followed by addition of 10 ml of lactose broth double strength solution. In set 2, 1 ml of water sample was taken in each test tube and there after 10 ml of single strength lactose broth solution was added. In set 3, 0.1ml of water sample was taken in each tube followed by addition of 10 ml single strength lactose broth solution.

In the next step, ignition tubes were inverted and gently inserted into each of the test tubes. The bubble formation inside the ignition tubes, when the *E.coli* bacteria oxidized the lactose present in the solution, indicated positive confirmation of bacterial activity. The three sets (i.e. 15 test tubes) as shown in Fig. 5.3, were sealed tightly with non absorbent cotton wool and incubated for 48 hours at 37^0C. After completion of incubation, the bacterial activity was studied using Mc Cardy, MPN Table for five tube dilution. The total coliforms were provisionally identified by the production of acid and gas from the fermentation of lactose.

Fig. 5.3. Multiple tube fermentation methods

Test for E.coli

After the confirmation of coliform bacteria from the water sample, brillant green bile media test was carried out for study of *E.coli*. For this test, 3 sets of test tubes namely sets A, B and C containing 5, 5 and 3 test tubes respectively were taken and 10 ml of brilliant green bile media reagent was added in each of the test tubes of set A, B and C. This was followed by addition of 1 ml of set 1, set 2 and set 3 solution respectively in each test tubes of set A, B and C. These newly prepared solutions were then incubated for 48 hours at 37^0C.

Study on removal of *E.coli* by sand supported carbon column

In a typical procedure, 100 ml of water sample was slowly poured into the carbon column and was allowed to stand for around 30 minutes and the sample was collected in a sterilised bottle. Bacterial activity studies were done following the same experimental procedure that was used for untreated water using double and single strength lactose broth solution. Brilliant green bile media test was also done using the same procedure as that for untreated water wherein 3 sets of test tubes were taken, *viz*., set A, B and C test tubes, set containing 2,1 and 1 test tubes respectively. Then

10 ml of Brilliant green bile media was taken in all the 3 sets followed by addition of 1 ml of set 1, set 2 and set 3 solution respectively in set A, set B and set C and was incubated for 48 hours at 37^0C.

In order to ascertain the removal of *E.coli* by sand only, similar test were conducted by passing the water sample through the column without carbon and then compared with results with carbon column.

5.4. Physical characterization of adsorbent after bacteria adsorption

Pre and post surface morphological analysis of activated carbon was conducted in order to determine the extent of bacterial adsorption onto the different activated carbon samples.

Surface area analysis

The changes in the surface area of the adsorbents were studied to find out the extent of adsorption of *E.coli* along with other bacteria that was present in the water. Thus surface area analysis for different carbon adsorbents were carried out using surface area analyser (Smart instrument, SS93/02).

Zero point charge

In order to find out whether there was any change in the surface charge of the activated carbon after bacteria adsorption, pH_{ZPC} analysis was conducted, since it provides information about the charge density on the surface of the adsorbent.

5.5. Results and discussion

Study on removal of *E.coli* from water samples

To study the removal of *E.coli,* initially total bacteria count was estimated in the water samples to confirm the activity of bacteria in the water sample under investigation. Once the presences of bacteria were confirmed, the presence of coliform bacteria was analysed. From the experiment conducted for total bacteria count of the water sample, total bacteria colony was approximately estimated as 200+ colonies and the results are given in Table 5.1.

Table 5.1. Showing total bacterial count /1ml

No.	Sample	Total count/1ml
1	Untreated water	200+
2.	Treated water with sand	200+
3.	Treated water with sand supported MEAC-HNO_3 and MEAC-H_3PO_4 activated carbon	30+ and 40+ respectively
4.	Treated water with sand supported MPAC-HNO_3 and MPAC-H_3PO_4 activated carbon	20+ and 30+ respectively.

Further when the experiment for presence of coliform bacteria was conducted, it was observed that among the three experimental sets, all t 5 (five) test tube were tested positive for bacterial activity for both set 1 and set 2. Whereas for set 3, only three out of five were found to be positive. The details of the results are given in Table 5.2. Thus, according to the present finding for coliform bacteria analysis of the water sample, the MPN values obtained were (5,5,3) corresponding to 900 bacterial colonies in 100 ml of water sample (Table 5.2). Using similar procedures an experiment was further conducted to study the presence of *E.coli* bacteria using brillant green bile media test where the activity of *E. coli* was determined by Mc Cardy, MPN Table. The results gave MPN/100 ml value of (5,5,1) corresponding to 350 colonies of *E. Coli* as shown in Table 5.3.

Table 5.2. Bacterial colonial studies for untreated water sample

No.	Set	No. of test tube/s	Sample (ml)	Double strength lactose broth (ml)	Single strength lactose broth (ml)	MPN/100ml
1	1	5	10	10	-	(5,5,3) corresponding to 900 bacterial colonies.
2	2	5	1	-	10	
3	3	5	0.1	-	10	

Table 5.3. *E.coli* colonial count of untreated water sample

No.	Set	No. of test tube/s	Sample from set 1,2,3 (ml)	brilliant green bile media	MPN/100 ml value
1	A	5	1	10	(5,5,1) corresponding to 350 colonies of *E.coli*
2	B	5	1	10	
3	C	3	1	10	

In order to study the removal of *E.coli* from water, the collected water samples were passed through the sand supported column made of different carbons. After passing

through the column, the total bacteria/*E.coli* count was conducted as per the procedure given above. It was found that there was a considerable reduction in total bacteria colony in the water samples, and a graphical representation of the removal percentage is shown in Fig. 5.4. In order to confirm the removal of bacteria from water samples by sand samples only, the same experimental procedure using only sand sample was conducted, the results obtained are presented in Table 5.1.

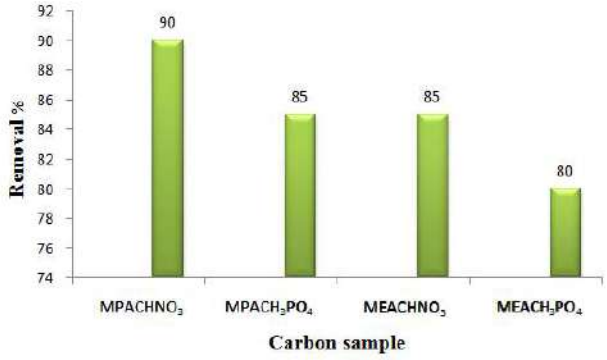

Fig. 5.4. Removal percentage of Total bacteria count after passing the water sample through activated carbon of different sample.

The bacteria counts reduced from 200+ counts/ml to about 20+ and 30+ counts/ml respectively, when the water was allowed to pass through MPAC-HNO_3 and MPAC-H_3PO_4 sand supported activated carbon columns. Similarly it reduced from 200+ counts/ml to 30+ and 40+ counts/ml for MEAC-HNO_3 and MEAC-H_3PO_4 activated carbon samples (Table 5.1).

When the water sample was passed through the MPAC-HNO_3 carbon column, the MPN value, which was (5,5,3) corresponding to 900 bacterial colonies of coliform bacteria was reduced to (2,1,1) corresponding to 9 colonies of bacterial colonies. Similarly for MEAC-HNO_3 carbon, the value reduced to (2,2,1) corresponding to 12 bacterial colonies (Table 4). However when the study of the activity for *E. coli* was estimated by Mc Cardy, MPN Table, after passing through the columns, the activity gave MPN/100 ml value of (0,0,0) signifying 100% removal of *E.coli* by the carbon made of MPAC-HNO_3 activated Carbon (Table 5).

Table 5.4. Bacterial colonial studies of treated water sample with sand supported MPAC-HNO_3 and MEAC-HNO_3

No.	Set	No. of test tube/s	Sample (ml)	Double strength lactose broth (ml)	Single strength lactose broth (ml)	MPN/100ml
1	1	5	10	10	-	(2,1,1) and (2,2,1) for MPAC-HNO_3 and MEAC-HNO_3 carbon corresponding to 9 and 12 bacterial colonies respectively.
2	2	5	1	-	10	
3	3	5	0.1	-	10	

Table 5.5. *E.coli* colonial count of treated water sample with sand supported MPAC-HNO_3 and MEAC-HNO_3.

No.	Set	No. of test tube/s for MPAC-HNO_3 and MEAC-HNO_3 respectively	Sample from set 1,2,3 (ml)	Brilliant green bile media	MPN/100 ml value
1	A	2 2 1	10		(0,0,0) and (0,0,0) for both the carbon indicating 100% removal of *E.coli.*
2	B	1 2 1	10		
3	C	1 1 1	10		

Interestingly the activity of *E.coli* after the water samples passed through MEAC-HNO_3 was also found to be (0,0,0), signifying the fact that total *E. coli* removal was possible by using column method. The same experiment was carried out with MPAC-H_3PO_4 and also MEAC-H_3PO_4 activated carbon. From the experimental results it was obvious that both the carbon sample show good removal percentage. The results and different values obtained from MPN table for MPAC-H_3PO_4 and MEAC-H_3PO_4 carbon sample are shown in Table 5.6 and Table.5.7 respectively.

Table 5.6. Bacterial colonial studies of treated water sample with sand supported MPAC- H_3PO_4 and MEAC-H_3PO_4

No.	Set	No. of test tube/s	Sample (ml)	Double strength lactose broth (ml)	Single strength lactose broth (ml)	MPN/100ml
1	1	5	10	10	-	(2,1,2) and (3,1,2) for MPAC-H_3PO_4 and MEAC-H_3PO_4 carbon corresponding to 12 and 17 bacterial colonies respectively.
2	2	5	1	-	10	
3	3	5	0.1	-	10	

Table 5.7. *E.coli* colonial count of treated water sample with sand supported MPAC-H_3PO_4 and MEAC-H_3PO_4.

No.	Set	No. of test tube/s for MPAC-HNO_3 and MEAC-HNO_3 respectively		Sample from set 1,2,3 (ml)	Brilliant green bile media	MPN/100 ml value
1	A	2	3	1	10	(0,0,0) and (0,0,0) for both the carbon indicating 100% removal of *E.coli.*
2	B	1	1	1	10	
3	C	2	2	1	10	

This result signifies the fact that both the synthesised activated carbons are excellent adsorbent which allow 100% removal of *E.coli* from water sample. This removal/reduction can be attributed to the presence of numerous pores of varying sizes and large surface area of the bio-adsorbent which provides sufficient active sites that could easily trap the bacteria within the activated carbon.

5.5.1. Pre and Post-adsorbent analysis for possible change in surface properties

In order to obtain generalised information about the transformation in the surface properties after adsorption of *E.coli*, surface analysis was done using BET surface area analyser. From the results obtained it was found that there was a considerable reduction in specific surface area as well as the pore volume of the carbon samples (Table 5.8) suggesting that the adsorption onto the carbon surface has occurred to a great extent. The change in the surface area and pore volume may be attributed to the adsorption of suspended particles, impurities or bacteria onto the carbon samples. The change in the surface charge density was found out from the data obtained from pH_{ZPC} values (Table 5.9 –5.12). In all the carbon samples, pH_{ZPC}>pH suggested that the surface is negatively charge, shown in Fig. 5.5. The change in the surface charge density maybe due to bacterial colonisation on the carbon sample (LeChevallier et al., 1978; Weber et al., 1978; Tobin et al., 1979; Steward et al., 1990; Matsunagaet al., 1992; Snyder et al., 1995). This could be because of a combination of factors such as adsorptive properties of carbon sample, which enrich nutrient and oxygen concentration and remove disinfectant compounds; the porous surface of the carbon particles, which provides a protective environment from fluid sheer forces, the presence of various functional groups on carbon surface which enhances microbial attachment and neutralisation of stressor compounds. Consequently the bacteria attached to carbon particles can developed high resistance to disinfectants

((LeChevallier et al., 1984; Steward et al., 1990; Berman et al., 1998) Thus, developing permanent negatively charged onto the surface of the activated carbon and hence, further enhancing the adsorptive properties of the activated carbon.

Table 5. 8. BET surface area pre and post

Sample	Pre-Surface area $m^2 g^{-1}$	Post-Surface area $m^2 g^{-1}$	Pre-Pore volume cc g^{-1}	Post-Pore volume cc g^{-1}
MPAC-HNO_3	931	204.23	0.514	0.087
MPAC-H_3PO_4	883	198.67	0.504	0.073
MEAC-HNO_3	865	194.02	0.508	0.079
MEPA-H_3PO_4	812	183.55	0.498	0.068

Table 5.9. pH_{ZPC} of MPAC- HNO_3

Sl.No.	pH_i	pH_f	pH_f-pH_i
1	6.52	6.36	0.16
2	6.82	6.74	0.08
3	7.09	6.97	-0.12
4	7.25	7.01	-0.24
5	7.47	7.19	-0.28
6	7.58	7.26	-0.32

Table 5.10. pH_{ZPC} of MPAC-H_3PO_4

Sl. No.	pH_i	pH_f	pH_f-pH_i
1	6.42	6.58	0.16
2	6.72	6.76	0.04
3	7.11	7.05	-0.06
4	7.25	7.12	-0.13
5	7.3	7.08	-0.22
6	7.58	7.31	-0.27

Table 5.11. pH_{ZPC} of MEAC-H_3PO_4

Sl. No.	pH_i	pH_f	pH_f-pH_i
1	6.36	6.5	0.14
2	6.67	6.73	0.06
3	6.80	6.78	-0.02
4	7.09	7.01	-0.08
5	7.44	7.26	-0.18
6	7.58	7.37	-0.21

Table 5.12. pH_{ZPC} of MEAC-HNO_3

Sl. No.	pH_i	pH_f	pH_f-pH_i
1	6.33	6.44	0.11
2	6.81	6.85	0.04
3	7.06	7.01	-0.05
4	7.33	7.22	-0.11
5	7.58	7.34	-0.24
6	7.71	7.39	-0.32

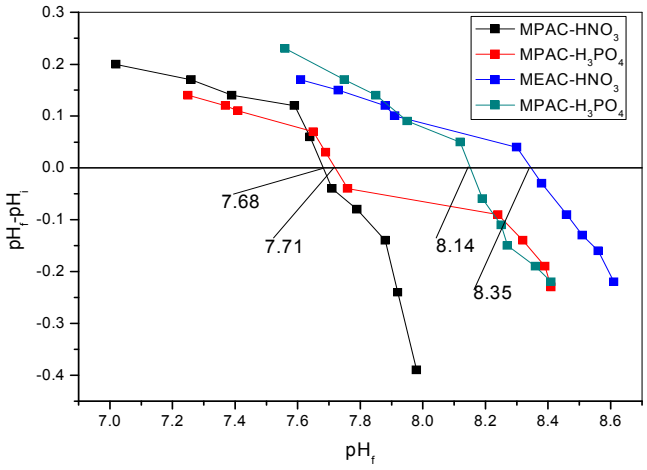

Fig. 5.5. Zero point charge plot against pH_f vs pH_f-pH_i for different adsorbent sample after bacteria adsorption

5.6. Conclusions

A columnar sand supported activated carbon has been successfully used for the removal of *E.coli* from water. The reduction in the bacterial colonies was observed when activated carbon was used as an adsorbent, and there was a considerable decrease in the total bacterial colonies from 200+ to 20+, 30+, 30+, 40+ for MPAC-HNO_3, MPAC-H_3PO_4, MEAC-HNO_3 and MPAC-H_3PO_4 respectively. Further when the test was carried out for particular coliform bacteria (*E.coli*) from the collected water sample, the adsorbents show 100% bacteria removal capacity. Hence, by using columnar sand supported activated carbon it is possible to treat water contaminated with coliform bacteria making the water free from bacteria related diseases, thereby improving the quality of the water. The adsorption of *E.coli* onto activated carbon is attributed to the adsorbents high surface area and presence of numerous pores of different shapes and sizes which trap the *E.coli* within the adsorbent. Further the change in the surface area and pore volume of the adsorbent were observed,

suggesting that the adsorption has occurred to a great extent. The increase in the negative surface charge density was observed from pH_{ZPC}, which indicates that the adsorbent can further be used for removing traces elements such as iron, chromium, and lead etc, which are usually positively charged species. The novelty of these bio-adsorbents is that the raw materials used are readily available almost throughout the year, inexpensive and user friendly. This method can be effectively practiced by using bamboo/hollow tubes of appropriate diameter columns in rural areas where access to treated public water supply is scarce and modern water purification system is limited, thereby reducing the risk of exposure to water borne diseases.

References

Aji, M.M., Gutti, B., Highina, B. K. (2015). Production and characterization of activated carbon from groundnut shell sourced in maiduguri. *Columba J Life Sci,* 17:18-24.

Akhtar, M., Bhanger, M.I., Iqbal, S., Hasany, S.M. (2005). Efficiency of rice bran for theremoval of selected organics from water: kinetic and thermodynamic investigations. *J Agri and Food Chem,* 53:8655-8662.

Ashbolt, N. (2004). Microbial contamination of drinking water and disease outcomes in developing regions. *J Toxicol,* 198:229–238.

Ashoka, H.S., Inamdar, S.S. (2010). Adsorption removal of methyl red from aqueous solution with treated sugarcane bagasse and activated carbon- a comparative study. *Global J of Enviro Lett Res*, 4:175-182.

Berman, D., Rice, EW., Hoff JC. (1998). Inactivation of particle-associated coliforms by chlorine and monochloramine. *Appl Environ Microbiol,* 54:507-512.

Brenner, D.J., Davis, B.R., Steigerwalt, A.G. (1982). Atypical biogroups of *Escherichia coli* found in clinical specimens and description of *Eschericha hermannii* sp. nov. *J Clin Microbiol*, 15: 703.

Buasri, A., Chaiyut, N., Loryuenyong, V., Phakdeepataraphan, E., Watpathomsub, S., Kunakemakorn, V. (2013). Synthesis of Activated Carbon Using Agricultural Wastes from Biodiesel Production. *International J Chem Mol Nuc Mater and Metallurgical Eng,*7:106-110.

Cheenmatchaya, A., Kungwankunakorn, S. (2014). Preparation of activated carbon derivedfrom rice husk by simple carbonization and chemical activation for using as gasoline adsorbent. *Int J Environ Sci and Development,* 5:171-175.

Cobb, A., Warms, M., Maurer, E.P,. Chiesa, S. (2012). Low-tech coconut shell activated charcoal production. *Int J for Service Learning in Eng,* 7:93-104.

Chen, C.X., Huang, B., Li, T., Wu, G.F. (2012). Preparation of phosphoric acid activated carbon from sugarcane bagasse by mechanochemical processing. *Bioresources,*7:5109-5116.

Davis, A.P., Hunt, W.F., Traver, R.G. (2009). Bioretention technology: overview of current practice and future needs. *J Environ Eng ASCE,* 135:109-117.

Goncharuk, V.V., Vergolyas, M.R. (2014). Toxic impact of *Escherichia coli* bacteria depending on their content in water of test organisms. *J Water Chem Techno*, 26:83-91.

Huerta, M., Grotto, I., Gdalevich, M. (2000). A waterborne outbreak of gastroenteritis in the Golan Heights due to enterotoxigenic *Escherichia coli*. *Infection*, 28: 267–271.

Hunter, P.R. (2003). Drinking water and diarrhoeal disease due to *Escherichia coli*. *J Water Health*, 1:65–72.

Hunt, W.F., Smith, J.T., Jadlocki, S.J., Hathaway, J.M., Eubanks, P.R. (2008). Pollutant removal and peak flow mitigation by a bioretention cell in urban Charlotte. NC. *J Environ Eng ASCE,* 134:403-408.

Ilaboya, I.R., Oti, E.O., Ekoh, G.O., Umukoro, L.O. (2013). Performance of activated carbon from cassava peels for the treatment of effluent wastewate. *Iranica J of Ene & Environ*, 4:361-375.

Jaguaribe, E.F., Medeiros, L.L., Barreto, M.C.S., Araujo, L.P. (2005). The performance of activated carbons from sugarcane bagasse, babassu, and coconut shells in removing residual chlorine. *Braz J Chem Eng*, 22:41 – 47.

Jiang, J.Q., Wang, S., Pangoulopouloa, A. (2007). The role of potassium ferrate(VI) in the inactivation of *Escherichia coli* and in the reduction of COD for water remediation. *Desalination*, 210:266-273.

Junior, O.P., Cazetta, A.L., Gomes, R.C., Barizão, É.O., Souza, I.P.AF., Martins, A.C., Asefa, T., Almeida, V.C. (2014). Synthesis of $ZnCl_2$-activated carbon from macadamia nut endocarp (*Macadamia integrifolia*) by microwave-assisted pyrolysis: Optimization using RSM and methylene blue adsorption. *J Anal Appl Pyrol*, 105:166-176.

Kobya, M. (2004). Adsorption, kinetic and equilibrium studies of Cr(VI) by hazelnut shell activated carbon. *Adsorpt Sci Technol,* 22:51-64.

LeChevallier, M.W., Hassenauer, T.S., Camper, A.K., McFeters, G.A. (1984). Disinfection of bacteria attached to granular activated carbon. *Appl Environ Microbiol,* 48:918-923.

Matsunaga, T., Nakasono, S., Masuda, S. (1992). Electrochemical sterilization of bacteria adsorbed on granular activated carbon. *FEMS Microbial letters,* 93:255-260.

Mendez, H., Geary, P.M., Dunstan, R.H. (2009). Surface wetlands for the treatment of pathogens in stormwater: three case studies at Lake Macquarie, NSW, Australia.*Water Sci and Techno*, 60:1257-1263.

Rivera-Utrilla, L., Bautista-Toledo, I., Ferro-Garcia, M.A., Moreno-Castilla, C. (2001). Activated carbon surface modifications by adsorption of bacteria and their effect on aqueous lead adsorption. *J Chem Technol Biotechnol,* 76:1209-1215.

Tsai, W.T., Chang, C.Y., Wang, S.Y., Chang, C.F., Chien, S.F., Sun, H.F. (2001). Preparation of activated carbons from corn cob catalyzed by potassium salts and subsequent gasification with CO_2. *Bioresour Technol,* 78: 203–208.

Tobin, R.S., McElhaney, J., Suffer, I.H. (1979). Pilot plant testing of activated carbon adsorption system. *J Am Water,* 71:660-673.

Sivakumar, B., Kannan, C., Karthikeyan, S. (2012). Preparation and characterization of activated carbon prepared from balsamodendron caudatum wood waste through various activation processes. *Rasãyan J Chem*, 5:321-327.

Snyder, J.W. Jr., Mains, C.N., Anderson, R.E., Bissonnette, G.K. (1995). Effect of point-of-use, activated carbon filter on the bacteriological quality of rural groundwater supplies. *Appl Environ Microbiol,* 61:4291-4295.

Steward, M.H., Woffe, R.L., Means, E.G. (1990). Assestment of the bacteriological activity associated with granular activated carbon treatment of drinking water. *Appl Environ Microbiol,* 56:3822-3829.

Wartelle, L.H., Marshall, W.E. (2001). Nutshells as granular activated carbons: physical, chemical and adsorptive properties. *J Chem Technol Biotechnol,* 76:451-455.

Weber, W.J. Jr., Pirbazari, M., Melson, G.I. (1978). Biological growth on activated carbon: An investigation by scanning electron microscopy. *Environ Sci Technol,* 12:817-819.